Reliability Study under the Smart Grid Paradigm Using Computational Intelligent

Techniques and Renewable Energy Sources

Adeniyi Kehinde Onaolapo

219090348

A thesis submitted to
the University of KwaZulu-Natal,
College of Agriculture, Engineering and Science,
in partial fulfillment of the requirements for the degree of

Doctor of Philosophy

Supervisor: Dr. Rudiren Pillay Carpanen
Co-Supervisor 1: Prof. David G. Dorrell
Co-Supervisor 2: Dr. Evans E. Ojo

School of Engineering, Electricity Engineering

University of KwaZulu-Natal

April 2022

I, Adeniyi Kehinde Onaolapo , declare that:

(i) The research reported in this thesis, except where otherwise indicated, is my original research.

(ii) This thesis has not been submitted for any degree or examination at any other university.

(iii) This thesis does not contain other persons' data, pictures, graphs or other information, unless specifically acknowledged as being sourced from other persons.

(iv) This thesis does not contain other persons' writing, unless specifically acknowledged as being sourced from other researchers. Where other written sources have been quoted, then:

  a) their words have been re-written but the general information attributed to them has been referenced:

  b) where their exact words have been used, their writing has been placed inside quotation marks, and referenced.

(v) This thesis does not contain text, graphics or tables copied and pasted from the Internet, unless specifically acknowledged, and the source being detailed in the dissertation/thesis and in the References sections.

Candidate: Adeniyi Kehinde Onaolapo

Signature: ______________________________

As the candidate's supervisors, we agree to the submission of this thesis for examination.

Supervisor: Dr. Rudiren Pillay Carpanen

Signature: ________________________

Co-Supervisor 1: Prof. David G. Dorrell

Signature: ________________________

Co-Supervisor 2: Dr. Evans E. Ojo

Signature: ________________________

ABSTRACT

Reliability Study under the Smart Grid Paradigm Using Computational Intelligent Techniques and Renewable Energy Sources

Adeniyi Kehinde Onaolapo
School of Engineering
Doctor of Philosophy

The increase in the demand for a reliable electricity supply by the utilities and consumers has necessitated the evaluation of the reliability of power systems. A reliable electricity supply is characterized by no or minimal duration and frequency of supply outages. Current power systems are changing due to increasing power demand and depletion of fossil fuel deposits. These changes are related to smart grids which are intelligent electric networks that are capable of using demand management methods, supporting communication devices and monitoring of consumer energy consumption. They can also integrate renewable energy sources thereby reducing reliance on fossils fuel sources. The main objective of this study is to optimize power systems operations and improve reliability. Different optimization methods are proposed in this study to address the issues of power systems operations. These optimization problems consider different constraints for maximum operations of the power systems. Case studies are used to confirm the proposed methods using the historical and climatic data for the City of Pietermaritzburg (29.37°S and 30.23°E), and Newcastle (27.71°S, 29.99°E) South Africa. Firstly, the implementation of the back-propagation algorithm method of the artificial neural networks (ANNs) for designing a predictive model for power system outage is proposed. The results obtained are found to be satisfactory. In situations where there is the problem of accessibility to large system data and presence of multiple system constraints, another method is proposed. This second technique proposes the application of a maximum entropy function-based multi-constrained event-driven outage prediction model, using the collaborative neural network (CONN) algorithm. The outcome is better than the conventional event-driven methods. Lastly, an adaptive model predictive control (AMPC) method with the integration of renewable energy sources (RESs) and a battery energy storage system (BESS) is proposed to further improve the reliability of the power system. The developed method uses a modified Roy Billinton Test System (RBTS) to implement the reliability improvement of the power system. The proposed computational intelligent techniques fulfil the necessities of operation robustness, implementation simplicity and reliability improvement of the power systems.

Keywords: Artificial neural networks, multiple linear regression, exponential smoothing, predictive model, weather events, collaborative neural network, event-driven forecasting, multiple constraints, maximum entropy function, weather conditions, adaptive model predictive control, battery energy storage system, cost of electricity, financial feasibility, reliability, renewable energy sources, solar PV, wind plant.

PUBLICATIONS ARISING

Reliability Study under the Smart Grid Paradigm Using Computational Intelligent Techniques and Renewable Energy Sources

Adeniyi Kehinde Onaolapo
School of Engineering
Doctor of Philosophy

Journal Papers

1. A.K. Onaolapo, R. Pillay Carpanen, D.G. Dorrell, and E.E. Ojo. A comparative assessment of conventional and artificial neural networks methods for electricity outage forecasting. *Energies*, 15(2):511, 2022
2. A.K. Onaolapo, R. Pillay Carpanen, D.G. Dorrell, and E.E. Ojo. Event-driven power outage prediction using collaborative neural networks. *IEEE Trans. on Industrial Informatics*, pages 1–10, 2022
3. A.K. Onaolapo, R. Pillay Carpanen, D.G. Dorrell, and E.E. Ojo. Reliability evaluation and financial viability of an electricity power micro-grid system with the incorporation of renewable energy sources and energy storage: A case study of KwaZulu-Natal, South Africa. *IEEE Access*, 9:159908 – 159924, 2021

Conference Papers

1. A.K. Onaolapo, R. Pillay Carpanen, D.G. Dorrell, and E.E. Ojo. Forecasting electricity outage in KZN, South Africa using trend projection and artificial neural networks techniques. pages 1–5. IEEE PES/IAS Power Africa, 2021
2. A.K. Onaolapo, R.Pillay Carpanen, D.G. Dorrell, and E.E. Ojo. A comparative evaluation of conventional and computational intelligence techniques for forecasting electricity outage. pages 1–6. Southern African Universities Power Engineering Conference (SAUPEC), 2021
3. A.K. Onaolapo, R.Pillay Carpanen, D.G. Dorrell, and E.E. Ojo. Transmission line fault classification and location using multi-layer perceptron artificial neural network. pages 5182–5187. IEEE Industrial Electronics Society Conference (IECON), 2020
4. A.K. Onaolapo, R.Pillay Carpanen, D.G. Dorrell, and E.E. Ojo. Assessment of sustainable development: A nexus between reliability, greenhouse gas emissions and renewable energy technologies. pages 1–5. Southern African Universities Power Engineering Conference (SAUPEC), 2022

ACKNOWLEDGMENTS

"O give thanks unto the **LORD**; for **HE** is good: for **HIS** mercy endures forever." –Psalm 136:1. My adoration belongs to God for seeing me this far. He alone deserves ALL the glory.

To my supervisors **Dr. Rudiren Pillay Carpanen, Prof. David George Dorrell, and Dr. Evans Eshiemogie Ojo**, I cannot be grateful enough for their constructive criticisms, patience, tutelage, guidance, professionalism, moral and financial supports throughout my PhD. journey.

I hereby acknowledge the supports in the form of grants and bursary awards from the **Council for Scientific and Industrial Research** (CSIR), the **UK Newton Fund scheme**, and the **Eskom Power Plant Engineering Institute** (EPPEI).

My gratitude goes to my colleagues **Anuoluwapo Aluko, Olanrewaju Lasabi, Oladejo Oladayo, Abayomi Adebiyi, Elutunji Buraimoh**, to mention a few; for their solutions to difficult problems in my PhD. journey. Special thanks to my parents **H.R.H. Oba Samson Babatunde Onaolapo and Olori Hannah Bolanle Onaolapo**, my parents-in-love **Elder Samuel Oduola Oladijo and Mrs. Victoria Omosalewa Oladijo**, and my spiritual mentors **Pastor & Pastor (Mrs) G.K. Adejimi** for their moral and spiritual supports. My siblings **Bolaji, Adebowale, Adeleye, Adeola, Adeoye and Aderoju** are all appreciated for standing by me. Finally, my sincere appreciation goes to my wife **Dr. Titilope Funmbi Onaolapo** and children **Kemisola Grace, Doyinsola John and Busolami David** for their tolerance, supports, prayers and encouragements during my doctoral aspiration. You all made it happen.

ACRONYMS

AMPC	Adaptive Model Predictive Control
ANNs	Artificial Neural Networks
ARIR	Annual Real Interest Rate
BESSs	Battery Energy Storage Systems
CC	Capital Cost ($/hr)
CLD	Cloud (%)
CoC	Confidence coefficient
CONN	Collaborative neural network
CRF	Capital Recovery Factor
C_{acc}	Annual Capital Cost ($/yr)
C_{acs}	Annual Cost of System ($/yr)
C_{afc}	Annual Fuel Cost ($/yr)
C_{aec}	Annual Emission Cost ($/yr)
C_{amc}	Annual Maintenance Cost ($/yr)
C_{arc}	Annual Replacement Cost ($/yr)
C_{coe}	Cost of Electricity ($/kWh)
C_{eens}	Expected Energy Not Served Cost ($/yr)

C_{npc}	Net Present Cost ($/yr)
C_{toc}	Total Outage Cost ($/yr)
DoD	Depth of Discharge
DTF	Deployment time factor
EC	Emission Cost ($/hr)
ECOST	Expected Interruption Cost ($/yr)
EENS	Expected Energy Not Served (MWh/yr)
EF	Equipment failure
EMP	Empangeni
ES	Exponential Smoothing
EWE	Extreme weather events
FC	Fuel Cost ($/hr)
FP	Frost point (°C)
FRSD	Number of frost days (days/month)
FSE	Emergency due to fuel supply
GHG	Greenhouse Gas
HTW	Heatwaves
HUR	Hurricanes

IF	Intensity factor
KZN	KwaZulu-Natal
KZNOU	KwaZulu-Natal operating unit
MAD	Mean absolute deviation
MAE	Mean absolute error
MAPE	Mean absolute percent error
MC	Maintenance Cost ($/hr)
MLR	Multiple Linear Regression
MSD	Mean Squared Deviation
MSE	Mean squared error
NN	Neural Network
NOCT	Nominal Cell Operating Temperature (°C)
NWC	Newcastle
OD	Outage Date
OU	Operating unit
PA	Public appeal
PET	Potential evapotranspiration (mm/month)
PMB	Pietermaritzburg

PRE	Precipitation (mm/month)
R^2	Coefficient of determination
RBTS	Roy Billinton Test System
RC	Replacement Cost ($/hr)
RESs	Renewable Energy Sources
RF	Rainfall (mm/month)
RH	Relative humidity (%)
RMSE	Root mean-square error
SAWS	South African Weather Service
SF	System Failure
SFF	Sinking Fund Factor
SI	System islanding
SNW	Snow/winter storms
SoC	State of Charge
SOD	Disruption in the course of system operation
Solar PV	Solar Photovoltaic
SP	Surface pressure (kPa)
SPF	Speed factor

SSV	System sabotage and vandalism
TDS	Thunderstorms
TMN	Minimum temperature (°C)
TMX	Maximum temperature (°C)
VAPD	Vapor pressure (hPa or mb)
WETD	Number of wet days (days/month)
WDR	Wind/rain
WP	Wind Plant
WS	Wind Speed (m/s)

Contents

List of Figures

List of Tables

Chapter 1

Introduction

1.1 Background

Power system reliability is the probability that electric components supply power to the consumers in an acceptable manner and quality [8]. Power system reliability is a germane requirement for electric utility systems as well as to customers. Access to high quality uninterrupted power supply is vital to the economic and industrial development of a nation. The main essence of a power system is to supply electric power that is reasonably reliable and economically acceptable to consumers at all times. An electricity power system is highly integrated and very complex. Faults in any part of the network can lead to outages ranging from minor to major. Such outages could have a serious economic impact on the utility and consumers alike. It could also cause damage to appliances and even loss of lives in critical sectors like the hospitals. The three components of a power system are the generation, transmission and distribution networks. The distribution network components of a power system require more attention in terms of reliability improvements because outages are more common with varying degree of impact on consumers [9]. More than 80% of customer reliability problems are traceable to distribution systems [10]. Reliability improvement of the distribution network is directly proportional to the reliability improvement for the customer. The daily increase in the demand for reliable electricity necessitates the need to exploit computational intelligent techniques to make networks smarter and more reliable [11]. The increasing emission of greenhouse gases, the challenge of fossil fuel depletion and the increase in prolonged outages from traditional power systems has brought about the integration of renewable energy sources (RESs) such as solar photo-voltaic and wind turbine generation, and use of battery energy storage systems (BESSs), to improve system reliability [3]. As of 2020, the global fraction of power generation is 29% renewable energy, this is projected to become 35% in 2030 with solar and wind energies taking a significant portion [12]. This transition comes with its technical challenges which has resulted in unexpected outagesdue to the intermittency nature of the RESs [13, 14, 15, 16]. Hence, the need for new models, algorithms and methods to tackle these challenges in power systems. This thesis proposed different computational intelligent techniques for dealing with renewable energy sources to investigate their reliability impacts in the power systems.

1.2 Motivation

This research was motivated by the experience of load shedding that takes place in South Africa. This is coupled with electrical faults, that are often accompanied by short circuits when restored. These short circuits can damage appliances and create avoidable inconveniences. Two questions can be posed: if load shedding continues every year, i) Could it be related to the weather events? ii) Is there be a deliberate plan, policy or project to prevent repeats of such occurrences? The answer is not far-fetched, the solution is in making the grid smart or smarter. Reliability of the grid cannot be over-emphasized.

The transition of power systems from the traditional to one with substantial renewable energy resource, with intermittent supplies, requires new smart techniques to make them reliable. The contribution of renewable sources such as solar or wind to electricity needs is not accurately predictable. This has resulted in fluctuations in supply and varying disturbances that create serious reliability challenges in the power systems. These challenges, encountered as a result of renewable energy integration into the power systems pose greater challenges for the reliability, stability and safety of the grid. Techniques are required to improve the performance and handle uncertainties in the power systems. Stand-alone micro-grids (made up of renewable sources), with high level of reliability, can be used in remote communities with complex terrains with little or no access to the national grid. Grid-connected micro-grids can complement grid supplies at the distribution network level, and improve the reliability of supplies during load-shedding and outages, thereby providing consumers with environmentally-friendly, renewable and sustainable supplies. Such critical sectors that need uninterrupted supplies, such as, hospitals, laboratories, medical facilities and important academic and economic facilities can be connected to micro-grids for their supplies.

1.3 Aim and Objectives

The aim of this thesis is to investigate the application of computational intelligent techniques to improve the reliability of power systems with integrated renewable energy sources. The proposed intelligent techniques are implemented in the design of different models to improve the reliability. The objectives of this research are:

1. To investigate the reliability of electric power systems using the back-propagation algorithm (BPA) of the artificial neural networks (ANNs) model, designed to predict electricity outages caused by weather events;
2. To design and implement a multi-constraint event-driven outage model that depends on a maximum entropy function for power systems reliability improvement;
3. To optimize micro-grid system operations and solve the optimization problem of disturbance prediction using the adaptive model predictive control (AMPC) algorithm; and
4. To model a modified Roy Billinton Test System (RBTS) in order to improve reliability, reduce emissions, balance the demand and supply of energy through RESs and a battery energy storage system (BESS), and investigate the economic feasibility of the integration of RESs and BESSs into power systems.

1.4 Hypothesis

This thesis formalizes the hypothesis that developing relevant electricity outage forecasting model, using optimization methods (and sometimes with renewable energy sources) can be used to improve the reliability of the power systems.

1.5 Contributions of Thesis

- Assessment of the dynamic and complex inter-relationship between climatic and technological factors of system failure. The application of ANNs to forecast power outages of a South African power system. The study findings are significant in the South African context, as they show that AI methods can be applied to outage forecasting, and weather conditions do impact on the performance of a distribution power system in South Africa. This contribution has been published in [1];

- Development of a useful model for power utilities which will assist maintenance. Development of a model for power outage forecasting using meteorological data and artificial neural networks. This model uses the approach of expressing the outage events per season as the target output. This contribution has been published in [1];

- Adoption of extensive statistical measures in evaluating the developed outage models. To increase the credibility of the results, real-life data are used. The proposed method demonstrates an improved performance, reduced computation time and an ease of implementation when compared to other baseline methods. This contribution has been published in [1];

- Development of a model that will improve decision making by utilities. This can mean that they pre-position materials and crews, and proactively inform consumers of possibilities of outage. Conventionally, restoration plans of utilities are based on management discretion and experience, and not expert outage prediction models. This contribution has been published. in [1];

- Proffering of solution to complex event-driven power outage forecasting problems using neural network methods. The use of event-driven power outage algorithm can be applied using CONN to various application cases to meet different power outage forecasting requirements. This contribution has been published in [2];

- Development of a maximum entropy function model for a multi-constrained event-driven power outage problem which converts the complex problem into two single-objective subproblems. This contribution has been published in [2];

- Development of an event-driven outage model with multiple constraints converting the complex problem into two single-objective sub-problems which are continuously differential, this solves the problem that the objective function of the conventional min-max model is non-differential. This contribution has been published in [2];

- Evaluation of the reliability, financial viability, and ecofriendly impacts of RESs incorporated into a micro-grid system are investigated. This contribution has been published in [3];

- Development of a model used for reliability evaluation of a power system with the integration of RESs. This contribution has been published in [3].

- Development of a model used for reducing C_{acs} and C_{coe} and increasing the use of RESs in a power system. This contribution has been published in [3];

- Integration of a model which will help in estimating the costs of supply interruptions by utilities, thereby improving power system reliability. This contribution has been published in [3];

- Use of a model which will help in monitoring the efficiency of a power system with the integration of RESs. This contribution has been published in [3];

- Implementation of a modified Roy Billinton Test System (RBTS) model which is verified using the adaptive model predictive control (AMPC) method. This contribution has been published in [3];

- Quantification of the emission parameters (oxides) from different case scenarios. This contribution has been published in [3];

- Investigation of the impacts of annual real interest rates on the cost and emission parameters of the micro-grid. This contribution has been published in [3].

1.6 Thesis Structure

The structure of this thesis is organized in a multi-paper format. Three main chapters (Chapters 3 to 5) have been prepared for publications. The entire thesis is made up of six chapters that are organized as follows.

- Chapter 1 is the introduction for the thesis. It contains the general background of power systems reliability, the motivation, the aim and objectives, and the contribution of this thesis.
- Chapter 2 contains the theoretical background of the thesis. It covers the theoretical backgrounds of different but related research work recorded in Chapters 3 to 5 of this thesis. The mathematical modelling of the different methods used is discussed in their respective chapters.
- Chapter 3, which has appeared in [1], provides the design and implementation of an artificial neural networks (ANNs) model, using a back-propagation algorithm (BPA) for predicting electricity outages caused by weather events.
- Chapter 4, which has appeared in [2], provides the design and implementation of a multi-constraint event-driven outage model that depends on maximum entropy function for power systems reliability improvement.
- Chapter 5, which has appeared in [3], presents the model of a modified Roy Billinton Test System (RBTS) designed to improve reliability, reduce emissions, balance the demand and supply of energy through RESs and battery energy storage system (BESS), and investigate the economic feasibility of the integration of RESs and BESS into the power systems. The model was used to optimize micro-grid system operations and solve the optimization prob-

lem of disturbance prediction using the (adaptive model predictive control) AMPC algorithm.

- Chapter 6 summarizes the conclusions, limitations of the work reported in this thesis and future work.

Chapter 2

Theoretical background

2.1 Introduction

This thesis contains theoretical formulations and simulation experiments with their methodologies, results, and conclusions. The work as a whole is based on several related research projects brought together to form a complete study. The overriding theme is the relationship between reliability studies, smart grid paradigm, renewable energy sources and computational intelligent techniques. This chapter summarizes the relationships between the theme aspects.

2.2 System Reliability

The evaluation of power system reliability has typically been done using probabilistic and the deterministic approaches [17]. The deterministic approach considers the characteristics and internal organization of the power system they operate and the previous experience of utilities on the system. Its reliability is determined using a simple heuristics or rules-of-thumb. However, the probabilistic approach considers the operation of the system and the stochastic characteristics or modelling of the components of the system. The probabilistic approach is more intensive and complex because it adopts a more complete depiction of the system. It requires more computational effort to evaluate the reliability of the system. Despite the limitations of the probabilistic method, it is more accurate and effective than the deterministic method. Hence, most literature report on the probabilistic approach.

2.2.1 Fundamental Concepts of Reliability

The reliability of a system is its ability to accomplish its proposed function in a specified period of time under a given operating conditions. There are two fundamental concepts of reliability, namely, system adequacy assessment (SAA) and system security assessment (SSA) [18].

An SAA relies on the sufficiency of resources in meeting the operating requirements and customer demands. The resources include the equipment needed to supply electricity from generation, to transmission, to distribution, and finally to consumers. An SAA associates with static conditions and does not consider the transient perturbation responses and system dynamics. A system state is adjudged successful if all operating constraints are met after evaluation. Such operating requirements include the loading limits, bus voltages, and the load. If one or more of the constraints are not met, corrective actions, such as bus voltage set-points, reactive power adjustments or generating units re-dispatch, are taken. To enforce the operating requirements, loads might be curtailed.

The scope of an SSA covers the ability of a system to return from transient perturbation to stable operating conditions after a disturbance. Hence, the system resilience against possible disturbance that might result in voltage, frequency or transient instabilities or cascading failures of equipment is the concern of an SSA. Solving the time-domain system dynamic behavior differential equations might require numerical methods, such as the Runge-Kutta method, which is necessary to conduct a detailed SSA study. This would include restoration actions, control processes and protection systems representations [19]. SSA studies are highly complex in nature and are typically made for a scheduled number of probable scenarios of disturbances and operations.

This study is concerned with the SAA of power systems.

2.2.2 Hierarchical Levels and Functional Zones

A modern electric power system is very complex and large. An SAA study uses simulation and mathematical methods to solve the models depending on the available computational power and the features needed for the illustration of the system components. For simplicity, power systems are categorized into functional zones in SAA studies. The first SSA category proposed a three functional zone separation of power systems (HL1 – HL3), which are: Generation, Transmission and Distribution (Figure 2.1) [17].

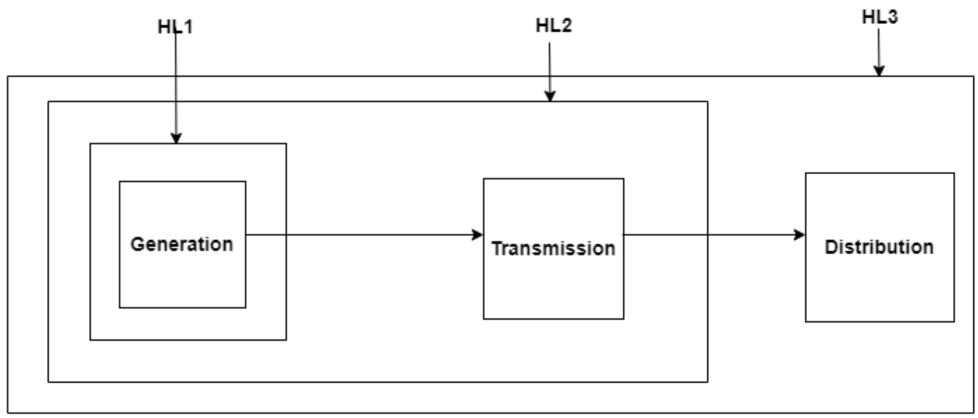

Figure 2.1 Functional zone Category 1 [18].

The second SAA category proposed a four functional zone separation of power systems (HL0 – HL3), which are: Energy, Generation, Transmission and Distribution [20]. The new functional zone added in (Figure 2.2), i.e., Energy, accounts for the intermittent energy sources or intrinsic variables (the renewable energy). HL0 gives a more accurate illustration of the generation sources available in time. A Hierarchical level (HL) is usually a combination of Functional Zones (FZs). The generation components and their ability to supply the system form Hierarchical Level One (HL1). The generation and transmission facilities and their ability to supply the bulk consumption points form Hierarchical Level Two (HL2). Finally, all functional zones and the system's combined ability to supply load continuously to every consumer form Hierarchical Level Three

(HL3). Approximate models are usually used for representing the components of Energy, Generation and Transmission zones to avoid making the scale of the problem cumbersome resulting in a computationally unrealistic adequacy assessment [20].

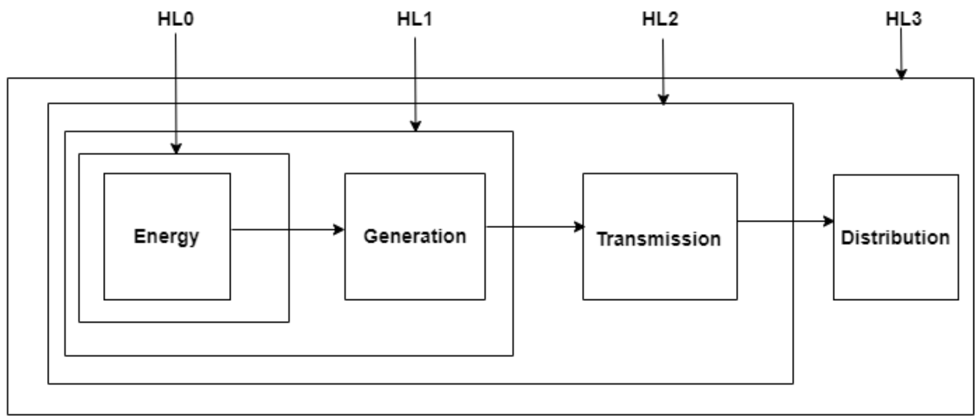

Figure 2.2 Functional zone Category 2 [18].

The restructuring of electric power systems has resulted in privatization, decentralization and unbundling of the generation, transmission and distribution operations. This restructuring in conjunction with the new technology has renewed and strengthened the interest in the distributed generation (DG). Hence, there has been a promotion for massive integration of DG into the distribution network. This has rendered the previous HL concept developed under centralized distribution (CD) paradigm obsolete, and led to a re-organization that takes care of the DG (Figure 2.3) [21]. SAA studies and methods described in this work cover the functional zones Category 3.

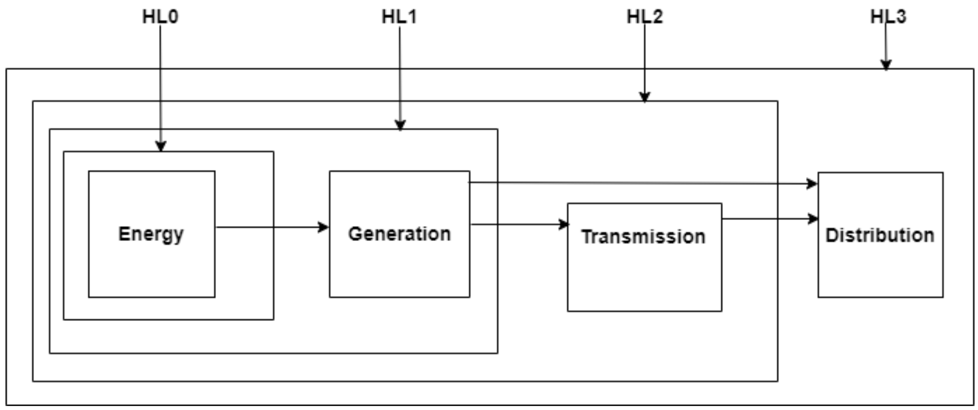

Figure 2.3 Functional zone Category 3 [18].

2.2.3 Reliability Indices

Reliability indices are very important outcome of SAA probabilistic studies. Reliability indices are broadly referred to as past or predictive performance indices [22]. Information on system reliability is provided by predictive indices which helps in the design horizon. Actual reliability of the system and events observed are reported by past performance indices. Only predictive indices are used in this work. The predictive reliability indices (or simply put, reliability indices) are designated differently in accordance with the HL involved in the SAA study. Reliability indices are classified as duration, frequency, energy, economic or probability indices, irrespective of the designations [17]. A few examples of reliability indices are given below.

Duration and frequency indices:

- Loss of Load Duration - LOLD (hour, day or week/occurrence), is a measure of the average duration of an event involving load curtailment; and
- Loss of Load Frequency - LOLF (occurrence/year), is a measure of the average number of load curtailment events in a given assessment period (typically a year).

Energy indices:

- Expected Energy Not Supplied - EENS (MWh/year), is a measure of the average energy curtailed in a given assessment period (typically a year); and
- Expected Power Not Supplied - EPNS (MW), is a measure of the average load curtailed.

Economic Indices:

- Expected Interruption Cost – ECOST (currency or $/year), is a customer damage functions, i.e., a measure of the costs incurred as a result of power supply interruptions in a given assessment period (typically a year); and
- Loss of Load Cost - LOLC (currency or $/year), is a measure of the average cost of load curtailment in a given assessment period (typically a year).

Probability indices:

- Loss of Load Expectation - LOLE (hour, day or week/year), is a measure of the average number of hours, days or weeks in a given assessment period (typically a year) with load curtailment; and
- Loss of Load Probability - LOLP, is a measure of the probability of load curtailment.

In Chapter 5 the reliability indices used are EENS and ECOST.

2.3 Smart Grid

Emerging solutions to address the problems of a modern electricity system that provide high quality of power, reliable electricity supply and integrate RESs such as hydroelectricity, wind and solar into electrical networks are called the Smart Grids. The smart grid concept is distinguished from the traditional passive grid in its ability to control, coordinate and manage connected resources [23]. Controllable loads and small interconnected voltage generators make up the micro-grid. Micro-grid can be grid-connected (i.e., linked to the main grid) or islanded (i.e., stand-alone). Strategies such as centralized/decentralized load dispatching, local decentralized control, and supervisor control are used to control a micro-grid. In application, two or more of these strategies are at times combined resulting in combinations of possible types of control [24].

2.3.1 Smart Grid Concept

The smart grid concept uses a system of upgrading the existing grid infrastructure by integrating multiple technologies such as forecasting systems, advanced automated controls, automated sensors, two-way communication, and two-way power flow. A smart grid enables communication between the utility and the consumers which encourages energy to be used optimally based on technical issues, price and environmental preferences. This improves the security, efficiency and reliability of the grid, and reduces greenhouse gases (GHG). Today, energy generation is heavily dependent on fossil fuels and there is an increasing demand for reliable energy daily; hence, renewable energy needs be adopted to reduce GHG emission and for a sustainable supply [24, 25]. The integration of intermittent renewable sources into the existing electrical grid need serious modifications and improvements for an efficient system. Smart grids, therefore, harness the communication, control, system management and efficient monitoring capability to the existing electrical grid for improved economy and efficiency. A smart energy management system is needed to coordinate the use of time-varying models of energy pricing, smart home technologies, and smart grid [26]. A smart grid system has a cost saving advantage for users and utilities alike by reducing the number of power plants on standby and automatically shedding or reducing the peak demand, thereby responding to varying costs of energy [27]. Table 2.1 shows a comparison between the traditional grid and a smart grid.

The two-way communication in a smart grid facilitates communication between subscribers and the utility which minimizes peak hours, reduces power loss, increases efficiency, increases reliability and minimizes the total cost of subscriber energy. A Demand-Side Management (DSM) program is used on the side of the consumer to manage the consumption patterns in accordance with varying electricity prices. The consumer can use a DSM to move their load demand to off-peak periods, reduce their load demand, and reducing their dependence on grid energy by relying on renewable energy. To design an efficient smart grid system, the expertise and knowledge from many fields need be integrated. One of these fields is computational intelligence or mathematical optimization [24]. It is used to optimize (minimize or maximize) objective function(s), under equality and inequality constraints. In this work, ANN, CONN and AMPC intelligence techniques are used. The canvassing for the incorporation of RESs into smart grid system is gaining momentum. Renewable energy resources, such as, hydro, wind, and PV, are emerging alternatives for electricity generation systems because they are clean and sustainable sources. In Chapter 5, wind plants and solar PV are the RESs used together with a BESS.

Table 2.1 A comparison between the traditional grid and smart grid [28].

S/n	Traditional Grid	Smart Grid
1	Dumb technology, infrastructure is electro-mechanical. Devices do not communicate among each other, and self-regulation is little.	Digital technology, devices communicate among each other, even remotely and self-regulate.
2	Traditional grid separates alternative energy from power plants because of lack of integrating infrastructure, thereby giving consumers no choices.	Smart technologies allow different companies and forms of alternative energies on the grid, thereby giving consumers choices.
3	Power distribution is one-way i.e. from the generating plant down to the distribution system.	Power distribution is two-way i.e. from the generating plant down to the distribution system and vice versa.
4	Limited control, it has to do with physical presence at the power plant or substation.	Unlimited control, which is achieved using smart infrastructures and sensors. Remote monitoring of energy and consumption is prevalent.
5	Centralized energy generation.	Decentralized energy generation which decreases peak time strains, balances the load and reduces the frequency power outages.
6	Prone to failures as a result of limitations and ageing.	Power can be re-routed around any faulty area using smart technologies.
7	Equipped with limited sensors, making location of fault a difficult task.	Equipped with multiple sensors, making location of fault easy, thereby limiting downtime.
8	Fault restoration is manual and has to do with physical presence at the location of fault.	Self-healing and remote restoration is possible.
9	Energy distribution is monitored manually because of the nature of infrastructure.	Digital technology enables smart grid to monitor itself, thereby managing distribution, troubleshoot outages, and balance loads.

2.4 Renewable Energy

As at 2020, the energy mix of South Africa, which is the country of the study areas for this research, is 88.9% fossil fuel, 5.6% nuclear energy, and 5.5% renewable energy. The renewable energy components is made up of 2.0% wind, 2.1% hydro, 0.3% solar thermal, 1.0% solar PV, and 0.1% biofuels [29]. The need for the development of sustainable energy and the design tools for sustainable energy is discussed in this section. Chapters 3 and 4 investigate the reliability of the power system based on the current mix of electricity. A design with greater incorporation of renewable energy sources, integrated with a fossil fuel generator and optimized using an intelligent technique is presented in Chapter 5.

2.4.1 Renewable Energy for Sustainable Living

The design for sustainable living is planning which improves the economic, social and ecological well-being of both the present and the future [30]. The demand for sustainable energy is increasing globally and the trend will continue in the next few decades as the environmental effects of GHG emissions by fossil fuel become obvious. The use of renewable energy technologies in small and large scales is becoming more evident as the prices of the components are becoming attractive and cost-effective.

Mankind has used captured energy in different forms and for diverse purposes since fire was discovered and animal power harnessed. This includes using wastes, biomass and wood for metal melting, heating and cooking; and using animal for transportation, mechanical works, waterwheels and windmills [31]. This leads to the events of the industrial revolution when there became a heavy reliance on energy. The discovery of vast deposits of fossil fuel having higher density than biomass fuel, the rapid development of industrial processes which were energy intensive, and the increase in energy demand in industrialized countries, resulted in the development of electricity. Because fossil fuels were in abundance and inexpensive, machines (Ford Model T cars and Rudolf Diesel's engines) that were initially designed to run on alcohol and biomass fuels were converted to fossil fuel engines. Since then, machines have been developed to rely heavily on fossil fuels; and its demand and use, particularly in the transportation and electricity sectors have become a very significant part of the technological society [32]. But about two centuries down the line, the adverse effects of the fossil fuels in our environment became obvious. This awareness has led to stricter legislation, policies and collaborations at the international level to curb the effects of GHG emissions [7]. Despite this awareness, the transition to sustainable energy has been slow, while energy consumption increases rapidly globally due to increased industrialization and rapid population growth.

2.4.2 Generating Electricity from Renewable Sources

Grid networks are well established in most advanced countries. However, the siting of plants and the generating methods for renewable energy is different from the conventional fossil fuel generating methods. Transition to sustainable energy will have implications on the re-design of these grids. Electricity generators can be classified into three, these are: i) capacity-limited; ii) energy-limited; and iii) intermittent [30]. These are discussed in this section.

Conventional Thermal Generators

The oil-fired, gas-fired, coal-fired and nuclear power plants can be classified as capacity-limited plants. The operation constraints, such as, the unplanned outages and time required for maintenance; and the physical capacity of the plant, determine the quantity of electricity generated in this category [33]. Conventional generators have large generating capacities, supported by a large expanse of expensive conversion equipment and transmission lines. Electricity is transported from the central generating points to the consumers over possibly several hundred kilometers away via many branches of transmission and distribution lines. The long distances of electricity transmission often lead to high line losses. Although nuclear power plants do not generate electricity using fossil fuels, but they have safety and environmental concerns, such as the possibility of accidents, contamination of nearby water and land, and radioactive waste disposal.

Sustainable Energy Generators

Energy generation which depends on seasonal crop yields, waste, rainfall, etc. are classified as energy-limited plants [34]. These energy sources are limited by the quantity of fuel or energy available to them in a particular place, at a particular time; and as such, find it difficult to run at the rated capacity. Plants fueled by waste, landfill gas, biomass, and hydro-electric power with reservoirs, are some of the examples of such generators. Unlike the intermittent sources, energy-limited plants have in-built storage capacities which depend on the size of storage facilities, for instance, the size of reservoir for hydropower plants. The fast response and storage capacity of energy-limited plants help the spinning reserve function, thereby providing energy to networks during peak times, thus matching demand with supply. Energy-limited plants are expensive and difficult to develop, the fuels are of lower energy densities, the local resources are limited, and their rated capacities are much lower than capacity-limited plants.

Intermittent plants are renewable sources such as tidal, solar, wave and wind. These sources of energy (apart from the tidal), vary according to weather, have no storage capacity and are unpredictable [35]. The integration of a large percentage of intermittent sources into the grid can lead to network balancing, control and reliability problems. Although weather prediction of an area may indicate that sufficient electricity will be generated, the availability of that sufficient amount of electricity at the time needed is not guaranteed. Intermittent plants may produce electricity when there is no demand or refuse to generate when it is needed. Demand with the seasons and weather pattern variations need be taken into consideration. Renewable plants (both the energy-limited and intermittent plants) are generally smaller in capacity than the conventional (capacity-limited) plants (except for the tidal plants). They are distributed throughout the network, usually located wherever the energy can be exploited; hence, the name – distributed generation. The generators are usually small in size, many in number, and sited throughout the network particularly in remote locations and difficult terrains where the grid capacity is low.

2.4.3 Increased Incorporation of Renewable Energy Resources into the Grid

Increased incorporation of renewable energy resources into the grid has interesting implications for electricity utilities. An electricity network that is more interconnected is required for a network containing a large number of small generators spreading through the network. Many small areas of the network will be self-sufficient while the rest will be designed for back-ups. The network will be energized with different types of energy mixes depending on the available local resources, suitable locations and the type of area. Incorporation of renewable energy resources into the grid comes with benefits such as reduction in energy losses, elimination of heavy investment on energy transmission over a long distance, reduction in environmental and health concerns, increase in the security of supply, and greater autonomy and energy reliability, particularly in isolated terrains. As fossil fuel generators approach the end of their useful lives, it is expected that they will be replaced with renewable generators. The intermittent features in the readily available renewable sources, such as solar and wind, will cause network reliability problems. This is an envisaged challenge for the transitional period because the demand and supply balance has to be reliably and effectively maintained, with the ultimate goal of 100% renewable energy in mind. There are different opinions on what to expect if intermittent sources are significantly integrated into a conventional electricity networks. Some are of the opinion that a sizeable quantity of spinning reserve should be provided by fossil fuel generators while others opined that energy storage is vital to intermittent energy [36, 37, 38, 39]. To design a sustainable energy system with high degree of reliability, the issue of spinning reserve must be resolved. However, the solution is not provided by one single method and the situation varies with the energy demand patterns, available local resources, weather pattern, location, type and size of the network considered. Decision makers, local authorities and utilities should take up the responsibility of maximizing the energy requirements, potentials, constraints, etc. of intermittent renewable sources for a smooth transition to a grid that is heavily reliant on renewable sources.

2.4.4 High Penetration of Renewable Sources in Small Areas

The grid networks that are currently with high penetration or 100% renewable energy developments are in small scale areas where main grid connection is expensive or difficult particularly in difficult terrains, remote areas or islands [40, 41, 42]. There are the farms, industries and buildings making use of their waste products which are difficult to dispose of, reducing fuel bills and ensuring energy self-sufficiency. These are the autonomous applications where high penetration of renewable energy are currently taking place. The cost competitiveness of renewable energy is increasing due to the increase in the cost of disposing of waste and increase in the comparative cost of conventional energy. Economies of scale, increase production, research and further experience will increase the economic feasibility and reliability of such systems. There is extensive literature on the generation of electricity on a small scale for individual farms, grid-isolated islands, and rural communities using renewable energy [43, 44, 45, 46]. However, few studies have used a grid-backup connection; most have been autonomous systems. Despite the differences in the emphasis of the studies, they have some important points:

- To allow energy supply with high reliability and security using renewable sources, there must be adequate matching of demand and supply, and this is dependent on weather patterns. Therefore, there must be optimal correlation between demand and supply by considering all available supply sources.
- To allow energy supply with high reliability and security using renewable sources, it is necessary to compensate for the unpredictable and variable nature of individual sources by using a mix of available generation methods.
- When demand is not met by an intermittent supply, spinning reserves from energy-limited sources should be used. If energy-limited sources are not available, electricity storage should be considered, particularly in small scale projects. Generation increase during winter months and inter-seasonal fuel storage can be considered in some climates.

2.4.5 System Design Approaches to Renewable Energy

Different models in the form of computer simulation packages have been proposed to help in renewable energy system design. Various programs dealing with optimization and design of renewable energy have been proposed [47, 48, 49, 50]. The proposed systems can be classified into: i) Geographical information-based systems; and ii) The matching system for demand and supply for the assessment of energy from waste and biomass and the temporal analysis of intermittent energy sources. These are further discussed in this section.

Geographical Information-based Systems

A comprehensive map of a particular area is produced by integrating different information sources on a computer database, which is referred to as the geographical information system (GIS). The map may be built up using different layers, representing the wind or solar potential, the three-dimensional relief, meteorological data, land availability, existing electrical network, the topology, etc., to find the optimal solution or economic evaluation for energy supply of the area [51, 52].

Matching System for Demand and Supply

When dealing with energy supplies from renewable sources, the climate, quantitative and temporal natures should be analyzed [53]. For instance, to design such a project as a solar powered streetlight project, first, the photovoltaic arrays need to be correctly sized, then the battery requirement is calculated, taking into consideration the available solar resource in the shortest day and the required energy during the longest night. The cloud cover effects and battery inter-seasonal storage are factored into the equations. The design results for such a system near the south or north poles with six months of light followed by six months of darkness will be different from that of a location near the equator where the day lengths do not vary. The results of such design would be more complicated if it were to be wind power because of its unpredictable nature which makes it vary significantly throughout the day. The intermittent nature of wind and solar sources has made it expedient to consider the variations (both daily and seasonal) in their electricity supplies and compare it with the demand pattern expected from a particular area. This way, the demand can be matched to supply and the type and size of the intermittent sources, the spinning reserve or storage devices needed to ensure security and reliability of supply, can be determined. Grid connection, auxiliary engines and the use of storage devices are few of the ways to evaluate intermittent wind energy and PV supply systems, on an hourly or daily basis, by matching the potential supplies with expected demands temporarily [54].

Optimisation Tools for Renewable Energy Design

There are different tools for the design of renewable energy supply systems for optimum solutions. Optimization tools are known to be very effective and with high degree of accuracy. It is a complex system that performs a detailed analysis of, usually, the economic and technical feasibility. These provide solutions for power quality issues, distances to customers, actual line design, and reliability issues. The operation strategy and design for a demand profile set and a given area can be found using an optimization program. Analysis can be done on systems containing battery storage, diesel generators, wind turbines, and solar PV; taking into consideration the non-linear performance of the components. Optimization is usually achieved through a set of algorithms using relevant data (e.g., demand and climatic data) and economic and technical characteristics and constraints [55, 56, 57].

2.5 Computational Intelligent Techniques

Adaptive systems (both natural and man-made) respond to environmental feedback by modifying internal structures or variables which results in better performance of the system. Such modification is referred to as adaption or learning. Computational intelligent techniques are part of several man-made adaptive systems [58, 59].

2.5.1 Artificial Neural Networks

An ANN is a computer architecture modeled after the working operation patterns of the brain. It is assembled by a sequence of nodes or neurons which are structured in layers [60]. These neurons establish connections between different neural network processing elements and their associated parameters. The neurons are connected in consecutive layers and each layer is weighted. The weight w_{ij} is the connection strength between i^{th} neuron and j^{th} neuron in one layer and the next. A neural network structure is made up of one input layer, one or more hidden layers, and one output layer. The complexity of the neural network system determines the number of hidden layers. The data collected by the neurons of the input layer is transformed for the first hidden layer neurons via the weight connecting them. The data moving from one layer to the next is processed and the outcome transformed to the next layer. The process is further explained in the following steps, using the input data (x_i), processed in the next layer by j^{th} node [61]:

1. The sum of weighted inputs is calculated and bias terms added, which is expressed as:

$$net_j = \sum_{i=1}^{m} x_i \times w_{ij} + \theta_j (j = 1, 2, ..., n) \tag{2.1}$$

2. A transfer function is used to normalize net_j bringing the inputs and outputs to a predetermined range of values. This enhances the training trends and patterns of the neural network. There are many types of transfer functions, but only a sigmoid transfer function is used in Chapter 3 as deemed suitable for use. This is:

$$f(x) = \frac{1}{1 + e^{-x}} \tag{2.2}$$

3. The result is finally transformed to the neurons in the next layer.

ANNs are popular because of their ability to learn and adapt by discovering existing patterns in the input data. Network training can either be supervised or unsupervised. In supervised training, the expected outputs is provided together with the inputs to optimize to minimum error in the output using the best set of weights. Supervised training models are used in areas such as pattern and sequence recognition, time series prediction, regression analysis, and function approximation. In unsupervised training, the model is left to make sense of the patterns of inputs given and determine the outputs by itself, without providing any expected outputs. Unsupervised training models are used in areas such as anomaly detection and clustering. Although Artificial Neural Networks are said to have difficulty of showing the problem to the network and unexplained functioning of the network, but they can implement non-linear tasks, employ parallel features to continue operation whenever an item of the neural network declines, and, handle incomplete data sets in both training and predicting [62].

Multilayer Perceptron Model

This is a form of feedforward artificial neural network (FFANN) containing a minimum of three layers of nodes. It is referred to as a multilayer perceptron model (MLP). The neurons in the hidden layer(s) and output layer of an MLP use non-linear activation functions. The non-linear activation function and multiple layers differentiate MLP from standard linear perceptron and helps the network to differentiate non-linearly separable data [63]. These networks are suitable for modelling applications like function approximation, prediction, and pattern classification. Function approximations are used to model relationships between variables, prediction uses the knowledge of current and previous trends to model forecasted outcomes, while pattern classification puts data into discrete classes.

Feedforward ANN Model

In a FFANN, the data or unit connections of the network move in the forward direction and not in a cycle like recurrent neural network (RNN) models. The direction of movement originates from the input nodes, passes through the hidden node(s) and terminates at the output node. FFANNs find applications in data mining, pattern recognition, time series forecasting, dynamical modeling, and complex pattern classification problems. An ANN is used in Chapter 3.

2.5.2 Collaborative Neural Networks

Collaborative Neural Networks (CONNs) apply the decisions from multiple agents to rethink or improve the outputs given. For instance, using an artificial intelligent (AI) model for Task A, which deals with predicting the future price of an apartment in Location A; and using another AI model for Task B, which deals with predicting the future inflation rates in Location B. Although the tasks use completely different data and arrive at unrelated outputs, it can be easily realized that the objectives of the two tasks are indirectly related and influence each other. The Expert A, handling Tasks A could possibly improve their outcomes by considering the insights of Expert B and vice versa. The re-evaluation of results could be done until an optimal outcome is reached. This idea is translated into neural networks as follows.

Having an n number of networks, and each network comprising [64]:

- I_i, $1 \geq i \geq n$ for the network input layer;
- N_i, $1 \geq i \geq n$ for the network hidden layer;
- O_i, $1 \geq i \geq n$ forthe network output layer.

The output of the ANN, $O_1, O_2, ..., O_n$ represents the input of the CONN, yielding a new and improved output of O'_1 ,O'_2, ...,O'_n. The idea is developed from the fact that, though finding solutions to complex problems may be difficult, the solutions of easier sub-problems might be used to solve a complex problem. The output of the complex system is formed from the predictions of all the sub-systems. Although Collaborative Neural Networks may require higher computational demands than the simple artificial neural networks, but in addition to the advantages of simple artificial neural networks stated in section. . . ., the collaborative neural networks significantly increase the robustness to label noise and reduce the generalization error [65]. A CONN is used in Chapter 4.

Although the works reported in Chapters 3 and 4 use completely different data and arrive at unrelated outputs, it can be easily realized that the objectives of the two works are indirectly related and complement each other. However, the work reported in Chapter 4 super-cedes that of Chapter 3 in that the work in Chapter 4 employs the collaborative neural network model. The model converts the complex event-driven outage forecasting problem into two continuous differential single-objective sub-problems which are then solved by neural networks.

2.5.3 Model Predictive Control

Model Predictive Control (MPC) is dependent on a model to forecast the future state of a system accurately. They are prone to modelling errors or unknown external disturbances. Instability and inefficiency can result if provision is not made for uncertainty. MPCs can be divided into Stochastic MPC (SMPC) or Robust MPC (RMPC) methods. SMPC assumes that the uncertainty is probabilistic while RMPC assumes the uncertainty is bounded [66]. The MPC control scheme is capable of managing operational and physical constraints such as the slew-rate limits of a power generator or storage capacity; integrating demand and supply projections; addressing complex system constraints; and offering a feedback mechanism. These make the system very sensitive to disturbances and uncertainties [67, 68].

Adaptive MPC

Although an MPC is able to control system uncertainties to a certain degree, it has some drawbacks. MPCs dealing with significant systemic uncertainties are inherently inadequate due to their deterministic formulations. Inaccuracy in handling varying dynamics because the internal plant models they use for prediction is constant, and they cannot achieve optimal outcomes because of their constant penalty weights [69]. An adaptive-based MPC (AMPC) is able to overcome the drawbacks mentioned above. They have excellent control performance because they utilize a discrete model for their control operation. They are capable of making accurate forecasting for new operating conditions by taking an updated model for the current operating condition at each time step. Therefore, an AMPC is superior in regulating control and tracking performance as compared to non-adaptive MPCs [70]. Although adaptive model predictive control may have the possibility of costly installation but has the advantage of allowing the optimization of the current timeslot, while keeping future timeslots in account; and gives high degrees of optimality and precision [71]. An AMPC is used in Chapter 5.

Chapter 3

A Comparative Assessment of Conventional and Artificial Neural Networks Methods for Electricity Outage Forecasting

This chapter is based on the work reported in [1].

3.1 Abstract

The reliability of the power supply depends on the reliability of the structure of the grid. Grid networks are exposed to varying weather events, which makes them prone to faults. There is a growing concern that climate change will lead to increasing numbers and severity of weather events, which will adversely affect grid reliability and electricity supply. Predictive models of electricity reliability have been used which utilize computational intelligence techniques. These techniques have not been adequately explored in forecasting problems related to electricity outages due to weather factors. A model for predicting electricity outages caused by weather events is presented in this study. This uses the back-propagation algorithm as related to the concept of artificial neural networks (ANNs). The performance of the ANN model is evaluated using real-life data sets from Pietermaritzburg, South Africa, and compared with some conventional models. These are the exponential smoothing (ES) and multiple linear regression (MLR) models. The results obtained from the ANN model are found to be satisfactory when compared to those obtained from MLR and ES. The results demonstrate that artificial neural networks are robust and can be used to predict electricity outages with regards to faults caused by severe weather conditions.

3.2 Introduction

Reliable electrical power is very important. Plans for economic development in developing countries are incomplete without including planned reliable electricity supply. This is virtually indispensable in modern society and requires dependable generation, transmission and distribution stages. For grid systems, there is an interrelation between weather events and outage events; an increase in weather events leads to an increase in the rate of grid fault occurrence. This makes the supply less reliable with higher maintenance costs. To solve this problem, electricity outage predictive models that are dependent on weather events are important for reliable and efficient electricity supply [72]. In this study, there is a comparative evaluation of the performance of artificial neural networks (ANN), multiple linear regression (MLR), and the exponential smoothing (ES) models.

The authors in [73] successfully modeled failure rates in overhead distribution lines using prediction models. They used Bayesian network and Poisson regression techniques and analyzed them using a Monte Carlo method. Rodriguez and Vargas [74] estimated the restoration time-range to solve the problem of load restoration using a fuzzy-heuristic technique. The proposed technique was tested in a real network consisting of 290 nodes. Zhou *et al*. [75] proposed a method to reduce large cascades of outages using the Markov chain to model historical data. The lines responsible for large cascades were found using the asymptotic characteristic of the Markov model. Kankanala *et al*. [76] estimated weather-induced outages in power systems using an ADABOOST algorithm. They evaluated the performance of the model using real-life weather and historical data of four cities in Kansas.

The authors in [77] investigated a less-researched weakness of a power system through which the system can be attacked, thereby causing damage and outage. The proposed model was capable of identifying the weakness of the system and quantifying the impact of the attacks. Eskandarpour and Khodaei [78] developed a model based on the characteristics of the data used to predict power outage using the support vector machine (SVM) method. The features of the data considered were the seriousness of, and the distance from, the extreme event, together with component deterioration. Eskandarpour and Khodaei [79] proposed a method for predicting the component outage of a power grid in expectation of a looming hurricane. The method used was logistic regression, and the performance was validated using a case study. Jaech *et al*. [80] introduced a method for predicting the duration of an outage using field records. They trained neural networks as models and validated the performance using natural language processing. They were able to establish good correlations between environmental properties used and outage causes. In [81], the use of predictive models that can improve the reliability and availability of electricity supply on a long-term basis was reported. A display system for predictive maintenance purposes was developed. This determined the date for servicing different components of the plant to avoid failure during operation.

The effects of vegetation on the reliability of the distribution system were analyzed in [82]. The researchers used parameters obtained from historical vegetation growth to develop models. It was observed that, to achieve improvement in system reliability, a predictive model is required to calculate the failure rate. In [83], the authors assessed the predictive reliability of a distribution network in the USA. They developed a model with five-year historical fault data and proved, through the results, the prospects and benefits of predictive models. An ANN and logistic regression (LR) were used in [84] to develop a prediction model in the medical field. The ANN performed more favorably than LR, confirming the efficiency of ANN models.

There are many components of distribution and transmission grids which are exposed to unfavorable weather events and susceptible to faults, reviewed in [72]. It was reiterated that, as weather events increase and become more severe due to climate change, electricity supply and grid reliability will be affected. A review was given in [85] on the different factors which are responsible for failures in distribution systems. The factors were categorized into: intrinsic factors (age of equipment,equipment manufacturing defects, conductor sizes, etc.); external factors (ice, lightning, wind, birds/animals, trees, etc.); and human error factors (vandalism, work crew accidents, vehicle accidents, etc.). It was inferred that external factors are predominant in causing faults in distribution systems. Yuan *et al*. [86] developed a prediction outage model for typhoons using historical data and random forest techniques. They were able to estimate the number of damaged poles and customer outages during a storm. Alpay *et al*. [87] developed a prediction model directly from weather forecasts for understanding the hourly dynamics of outages caused by thunderstorms using event-wise outage prediction models (OPMs). The validation work showed that the model is capable of reporting temporary and storm-wide outage characteristics. Pasqualini *et al*. [88] presented a technique for overcoming a lack of data and distribution models in data-poor environments using winter conditions and hurricane-force winds to forecast outage. Nateghi *et al*. [89] identified the main features responsible for forecasting the duration of outages caused by hurricanes. They were able to forecast the post-storm restoration times. In [90], Cerrai *et al*. presented outage predictions for ice and snow related storms using Bayesian regression tree and random forest models. The techniques were able to predict both lower impact events and extreme events. They followed on from this [91] and used the regression tree technique. This utilized weather and soil spatial distribution, together with historical power outage and vegetation data, to predict the spatial distribution and number of outages in a power distribution network. Dokic *et al*. [92] described how a weather-related outage was modeled and assessed in real-time in a transmission network. Wanik *et al*. [93] demonstrated an improvement in outage prediction using land cover and utility-specific infrastructure data. The authors in [94] proposed a method based on the multi-interval parameter estimation to determine outage in a Korea Electric Power Corporation network. The algorithm proved appropriate for power system analysis of low frequency oscillation and efficient in term of reliability and accuracy. An analysis of the resilience of the grid to extreme weather events was conducted by Jufri *et al*. Grid vulnerability, grid exposure, and weather event intensity were used as determinants to evaluate the resilience of the grid. This analysis can be used as a tool to plan, prioritize and manage improvement strategies of grid resilience [95]. Kang and Lee presented the demand response based prediction of load curtailment using historical data and k-nearest neighbor (k-NN) ensemble method to alleviate the problem of scarcity of data and the uniqueness of customer characteristics. The proposed method was compared with support vector regression and a multi-layer perceptron and gave superior results [94]. GIS spatial methods were used to analyze hurricane-induced power outages in Tallahassee, USA, by Ghorbanzadeh *et al.* to understand the difference in the impacts of Hurricane Michael and Hurricane Hermine previously experienced by the city. The study results were able to identify high-risk areas. This will be useful for engineers and planners who can focus on those areas for safety intervention efforts, and accessibility and power restorations [96]. Lo Frano *et al.* investigated the creep phenomena and impact of ageing by subjecting an old reactor pressure vessel to blackout, and analyzed its thermo-mechanical consequences using MARC and MELCOR codes. The results demonstrated a good agreement between the theoretical and experimental results. Such a predictive model will help in the application of operational management programs [97]. Watson *et al.* presented a weather ensemble impact outage model that is able to predict the potential impacts of thunderstorms, such as the location of storm impacts and the total damage by an event using weather variables, WRF (Weather Research and Forecasting Model) simulation and NOAA (National Oceanic and Atmospheric Administration) analysis data sets. This model found applications in preparing for thunderstorms by decision makers [98]. Yang *et al.* used learning curves and evaluation metrics to develop a model to quantify the uncertainty in outage prediction. The overestimation and underestimation biases in low-severity and high-severity events were addressed using the proposed method [99]. In [5], we developed a model using the ANNs method, and historical and meteorological data for outage prediction; but wind speed, which is a significant factor responsible for high percentage of outages was missing in the data. The model developed was also predicated on fault data instead of outage data.

In summary, a review of previous studies shows that substantial work has been carried out on weather-related outage prediction. This has produced a sound platform, but there is still much work that can be done to create a predictive model with accuracy and efficacy that is satisfactory.

The conventional approach, as used by electric utilities, makes the assumption of co-linearity, and is low in accuracy. Computational intelligence methods are currently used to develop robust models to address system failure problems. These methods are robust, economical, efficient and flexible, and can provide solutions to vague, complex, nonlinear and dynamic real-life problems [6]. They are replacing conventional methods.

For a new weather-event outage prediction method, there must be an improvement on current models. Most existing electricity outage models do not take climate change into consideration; hence, there is a need for new models which will handle this factor. The model should reconcile the dynamic and complex inter-relationship between climatic and technological factors of system failure. This is essential to establish a legacy that is secure and reliable for the future, both at the local and global levels. The extent of the effectiveness of the methods used in this study can be highlighted by comparison to other studies. A comprehensive literature review was carried out to assess the work done in those studies, and Table 3.1 illustrates the effectiveness of the work done here.

Table 3.1 Comparison of studies

Study	Prediction model	Historical data	Meteorological data	Simulated data	Low computation time	Ease of implementation
[75]	✓	✓	-	-	-	-
[76]	✓	✓	✓	-	-	-
[77]	✓	-	✓	-	-	-
[79]	✓	-	-	✓	-	-
[80]	✓	✓	✓	-	-	-
[86]	✓	-	✓	-	-	-
[87]	✓	✓	✓	-	-	-
[88]	✓	✓	✓	-	-	-
[90]	✓	✓	✓	-	-	-
[91]	✓	-	✓	-	-	-
[92]	✓	✓	✓	-	-	-
[93]	✓	-	✓	-	-	-
[94]	✓	✓	-	-	-	-
[95]	✓	✓	✓	-	-	-
[100]	✓	✓	-	-	-	-
[96]	✓	✓	-	-	-	-
[97]	✓	✓	-	-	-	-
[98]	✓	✓	✓	✓	-	-
[99]	✓	✓	✓	-	-	-
This study	✓	✓	✓	-	✓	✓

In this study, the main contributions are as follows:

i Assessment of the dynamic and complex inter-relationship between climatic and technological factors of system failure. The application of ANNs to forecast power outages of a South African power system. The study findings are significant in the South African context, as they show that AI methods can be applied to outage forecasting and weather conditions do impact the performance of the distribution power system in South Africa;

ii Development of a useful model for power utilities which will assist maintenance crews. Development of a model for power outage forecasting using meteorological data and artificial neural networks. This model uses the novel approach of expressing the outage events per season as the target output;

iii Adoption of extensive statistical measures in evaluating the developed outage models. To increase the credibility of the results, real life data are used. The proposed method demonstrated an improved performance, reduced computation time and an ease of implementation as compared to other baseline methods; and

iv Development of a model that will improve decision making by utilities. This can mean that they pre-position materials and crews, and proactively inform consumers of possibilities of outage. Conventionally, restoration plans of utilities are based on management discretion and experience, and not expert outage prediction models.

This study uses feed-forward ANNs for predicting electrical system failure problems. The performance of the developed ANN model is compared with conventional MLR and ES models. The ANN model is further compared with recent optimization techniques.

3.3 Materials and Methods

This study uses three methods: the ES; MLR; and ANN. This forecasted weather was related to electricity system failure. This section contains a brief discussion of the methods.

3.3.1 Exponential Smoothing

Exponential smoothing is a prediction method in the moving average category, which predicts dependent factors by using weighted averages of past data. The weights of previous data sets are subjected to exponential decay, while new data sets are subjected to comparatively bigger weights. The prediction of the dependent parameters from the weighted sum of observed variables is illustrated using [101]:

$$Y_{t+1} = \alpha X_t + (1-\alpha)Y_t \text{ and } (0 < \alpha < 1) \tag{3.1}$$

where X_t = target value at time t, Y_t = predicted value at time t, $(1-\alpha)$ = damping factor and α = smoothing value.

This model operates on the basic notion of a regular and stable time series trend, which persists and has its historical trend continue into the future [102]. The values of damping factor $(1-\alpha)$ or smoothing value (α) determine the accuracy of the ES prediction. The value of (α) is determined using trial and error.

3.3.2 Multiple Linear Regression

Multiple linear regression is formed from the interconnection between a response parameter and two or more explanatory parameters, by assigning a linear equation to the observed data. MLR is given by [103]:

$$Y = \beta_0 + \beta_1 X_1 + \beta_2 X_2 + ... + \beta_k X_k + E \tag{3.2}$$

where the coefficients of regression are β_0, β_1, β_2, β_k; E is model deviation or error notation; Y is the dependent parameter; and X_1, X_2,..., X_k are independent variables.

The deviation notation of an MLR model is used to estimate its performance. This is the deviation between the target and the forecasted values. The performances of MLR models are usually analyzed using statistical calculations such as coefficient of determination (R^2) and the correlation coefficient (r).

3.3.3 Artificial Neural Networks

ANNs are computationally intelligent methods inspired by the operation of the neural networks in a biological brain [104]. They are effective data-driven modelling tools which have found wide application with dynamic, non-linear and complex systems. They are made up of different numbers of perceptron which receive, process and transmit signals by the action of weight and bias adjustments. Feed-forward multi-layer perceptron ANNs are widely used in engineering applications. ANNs have interesting properties, such as real-time adaptability, multidirectional implementation and robustness, irrespective of incomplete or damaged data, asynchronous processing possibility, ability to learn, well-grounded mathematical foundation, automatic generalization, and high level of parallelism. The main disadvantage of an ANN is that there is no rule-of-thumb for selecting the appropriate configuration [104]. The typical structure of a feed-forward ANN is shown in Figure 3.1. ANN models learn from their input data sets iteratively by modifying their connecting weights using their error values. They allocate weights to their input data and modify the weights using training algorithms and transfer functions. The sigmoid transfer function s [105] can be illustrated using

$$F = \frac{1}{1+e^s} \tag{3.3}$$

$$s = (a_1 w_1 + a_2 w_2 + ...) + B \tag{3.4}$$

where F = output of each node, s = output of the sigmoid transfer function, a_1 = input value, B = bias and w = weight.

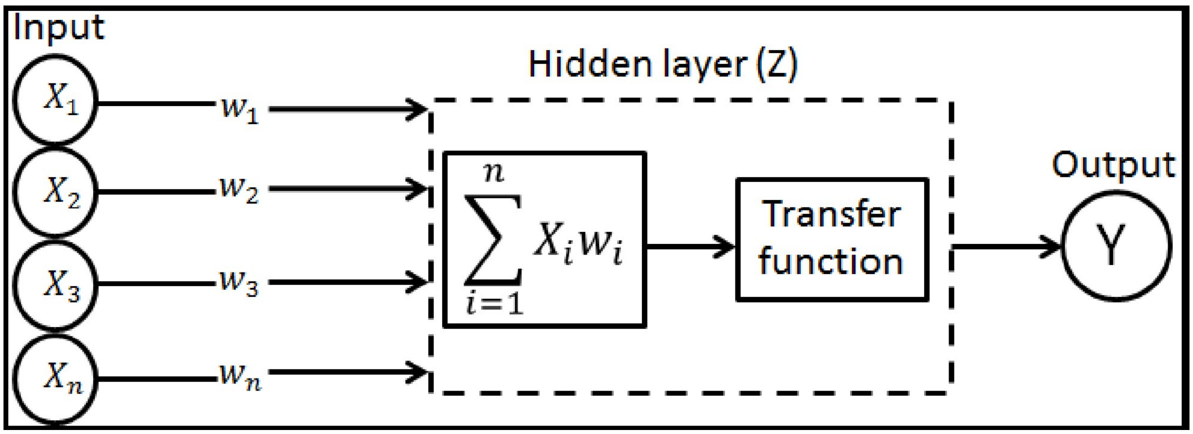

Figure 3.1 A typical structure of an ANN with three layers.

ANNs work iteratively by reducing the overall error E between the target X and the prediction Y. The error is given by [106]:

$$E = \frac{1}{N} \sum_{i=1}^{N} (X_i - Y_i)^2 \tag{3.5}$$

where N represents the total number of actual data, and X_i and Y_i represent the target and the predicted values respectively.

In this study, feed-forward ANNs are created using the ANNs toolbox in the MATLAB environment.

3.4 Description of the Study Area

The case study here is the city of Pietermaritzburg (PMB). The city is the headquarters of the Msunduzi local municipality, the Umgungundlovu district municipality and the KwaZulu-Natal (KZN) province, South Africa. The city was founded in 1838 and is about 70 km from South Africa's tropical East coast and is 676 m above sea level. It often experiences extreme weather. The city population in 2011 was 223,448, and it is growing. The city is the second-largest population in the province with tourism and energy resources [107]. Thus, it is a major South African urban area.

There are three operating units (OUs) in the KZN province; they are PMB, Newcastle (NWC) and Empangeni (EMP) zones. Due to the outage problems associated with the PMB zone (Figure 3.2), and its extreme weather conditions, this network is chosen as representative and suitable for use as a case study. The climatic variables that affect power outage were taken into consideration while applying ANN models. These variables were discussed in [72]. In this work, the variables considered are outage date OD, cloud amount CLD (%), minimum temperature TMN (°C), maximum temperature TMX (°C), number of frost days FRSD (days/month), number of wet days WETD (days/month), potential evapotranspiration PET (mm/month), precipitation PRE (mm/month), vapor pressure VAPD (hPa or mbar), and wind speed WS (m/s). The data sets spanned the period between January 2014 and July 2017 (forty-three months). They were acquired from the South African Weather Service (SAWS) and the electricity public utility Eskom Holdings SOC Ltd., Durban, KZN, South Africa.

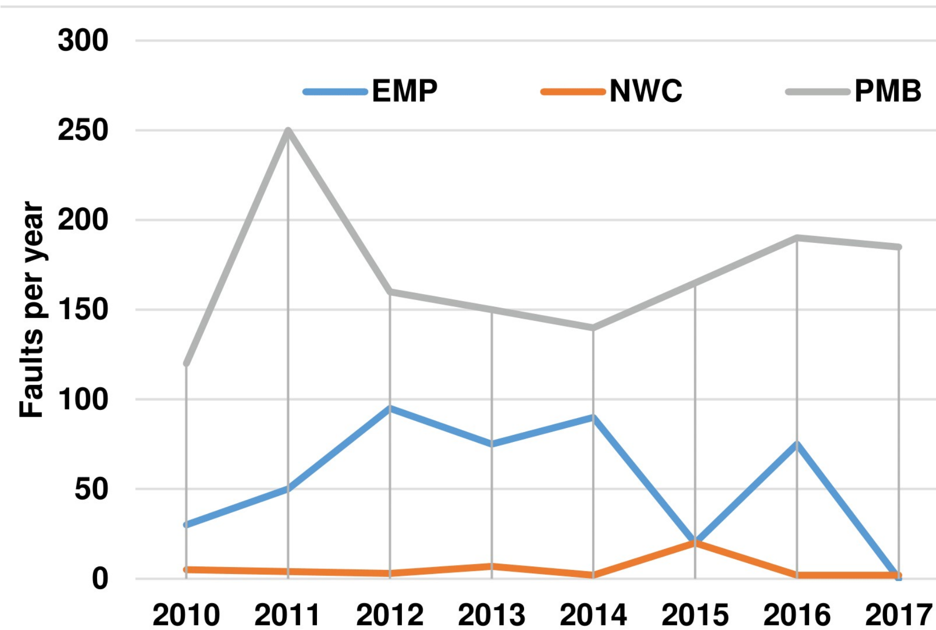

Figure 3.2 Overview of line fault in KZN zones between 2010 and 2017. [Source: Eskom]

The statistical features and historical trends of the acquired data for the case study are shown in Table 3.2 and Figures 3.3–3.8, respectively. Figure 3.3 shows occasional heavy precipitation, which is often accompanied by strong wind, lightning, flooding and landslides (responsible for causing faults). Figure 3.4 shows record high temperatures, which impacts distribution and transmission networks by reducing the maximum power rating of equipment and increasing energy losses. Figure 3.5 shows the numbers of wet days per month. These are very low for several months during the study period. A prolonged drought can result in the drying out of the ground, reducing the thermal conductivity of the soil, and causing the rating of underground cables to reduce. Figure 3.6 shows high maximum wind speed for different months. High wind can cause faults by damaging overhead lines, blowing debris against overhead lines, collapsing trees against overhead lines, and uprooting utility poles in extreme high winds [108].

Table 3.2 Statistics of data used in the research.

Statistical Parameter	PRE	PET	CLD	TMN	TMX	VAPD	WETD	FRSD	WS
Mean	61.51	89.25	45.74	9.97	23.77	13.41	9.57	1.84	2.96
Maximum	146.80	136.90	82.10	16.60	27.80	20.30	18.80	8.27	3.45
Minimum	12.80	57.80	16.50	3.60	20.00	8.30	2.74	0.00	2.08
Standard Deviation	44.22	23.43	17.43	4.17	2.21	3.98	5.73	2.64	0.30
Variance	1.96×10^3	549.0	303.7	17.40	4.88	15.85	32.84	6.96	0.09
Kurtosis coefficient	1.52	1.73	1.98	1.67	1.96	1.73	1.40	2.74	3.15
Skewness coefficient	0.38	0.15	0.24	0.05	-0.12	0.28	0.18	1.11	-0.63

Figure 3.7 shows the fluctuation of the outage events in different months in the city between January 2014 and July 2017. The outage events vary from year to year, but in general, over 50% of the outages have been attributed to weather events. From Table 3.3 and Figure 3.8, it can be observed that 35% of the outages occurred during winter, 27% during autumn, 21% during spring, and 17% during summer within the period covered (note that 2017 did not cover winter in full or cover spring at all).

Table 3.3 Percentage analysis of outages per season

Season	2014	2015	2016	2017	Total
Summer (%)	7	3	4	3	17
Autumn (%)	10	3	4	10	27
Winter (%)	8	14	11	2	35
Spring (%)	8	7	6	0	21

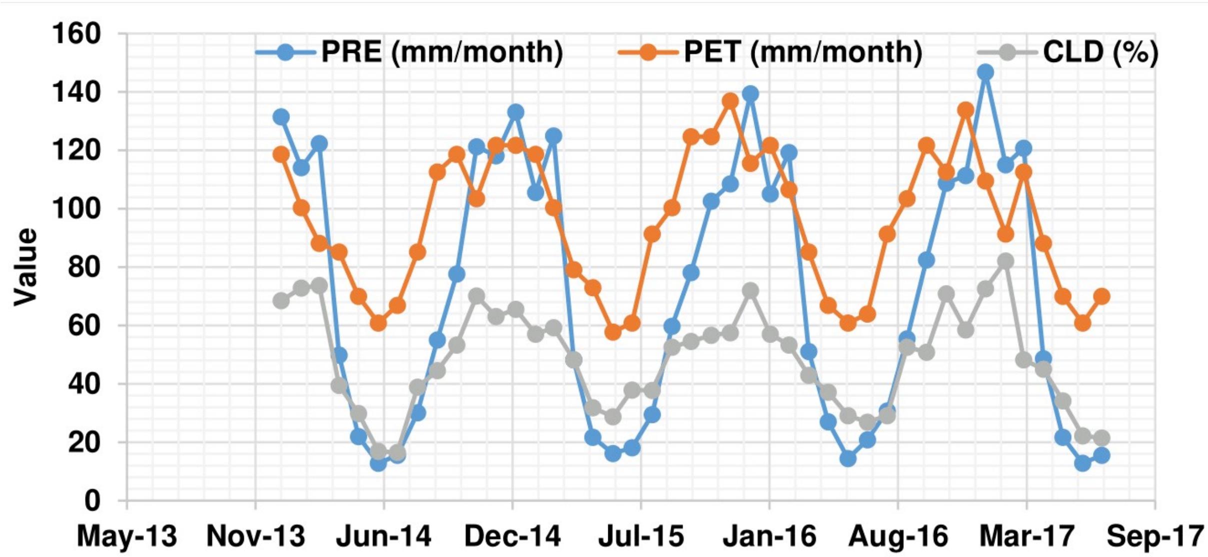

Figure 3.3 Historical trend of PRE, PET and CLD.

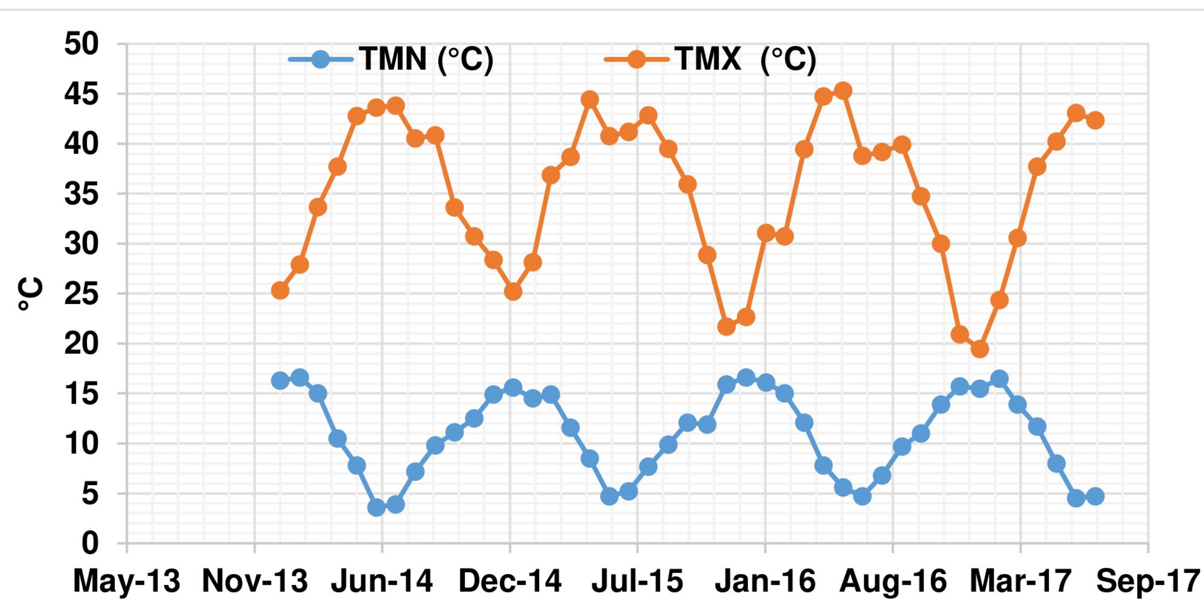

Figure 3.4 Historical trend of TMN and TMX.

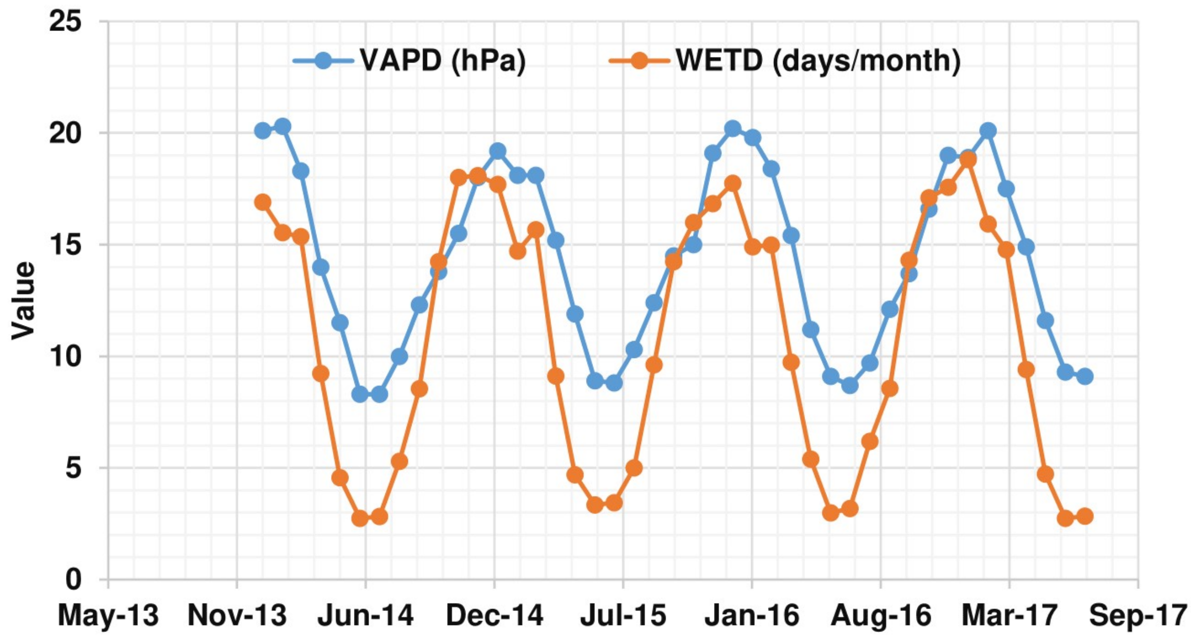

Figure 3.5 Historical trend of WAPD and WETD.

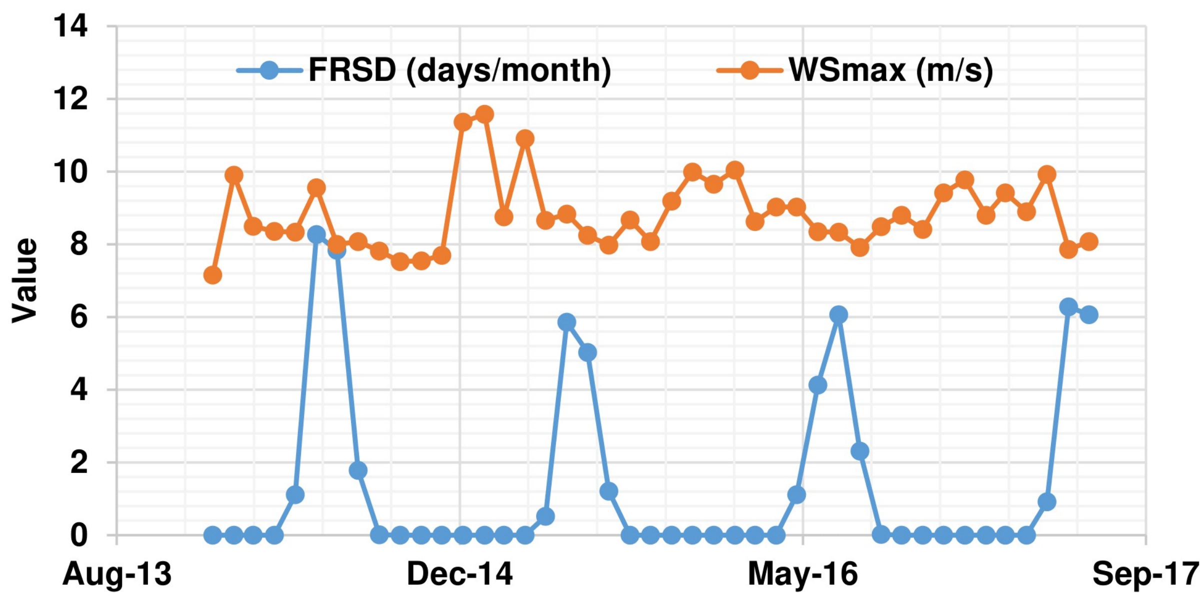

Figure 3.6 Historical trend of FRSD and WS.

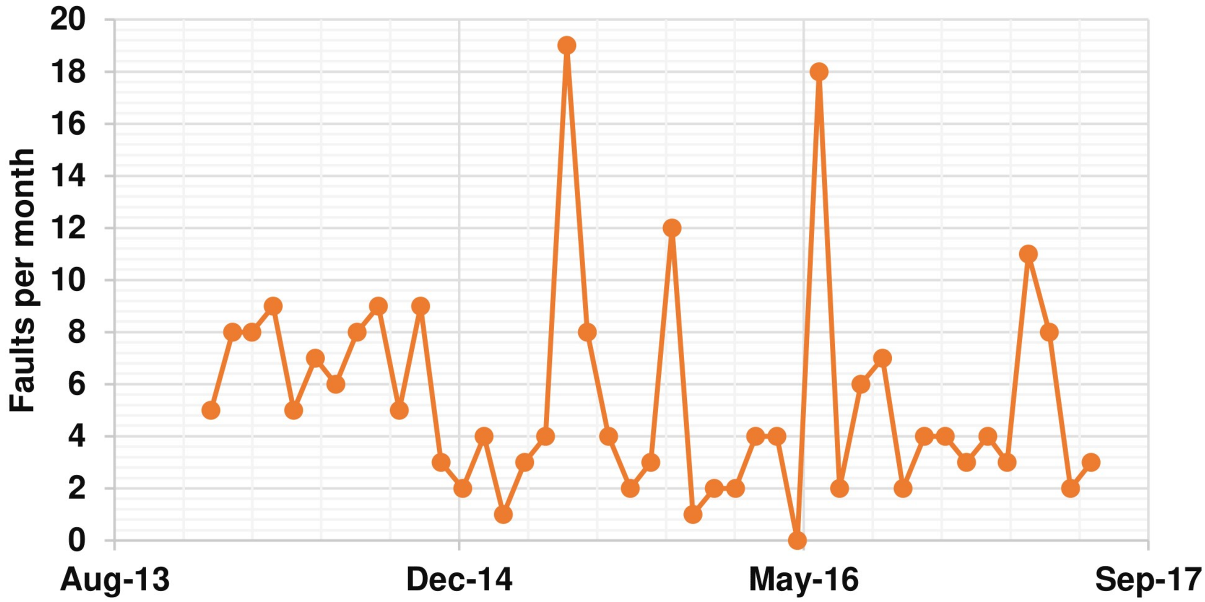

Figure 3.7 Historical trend of faults per month.

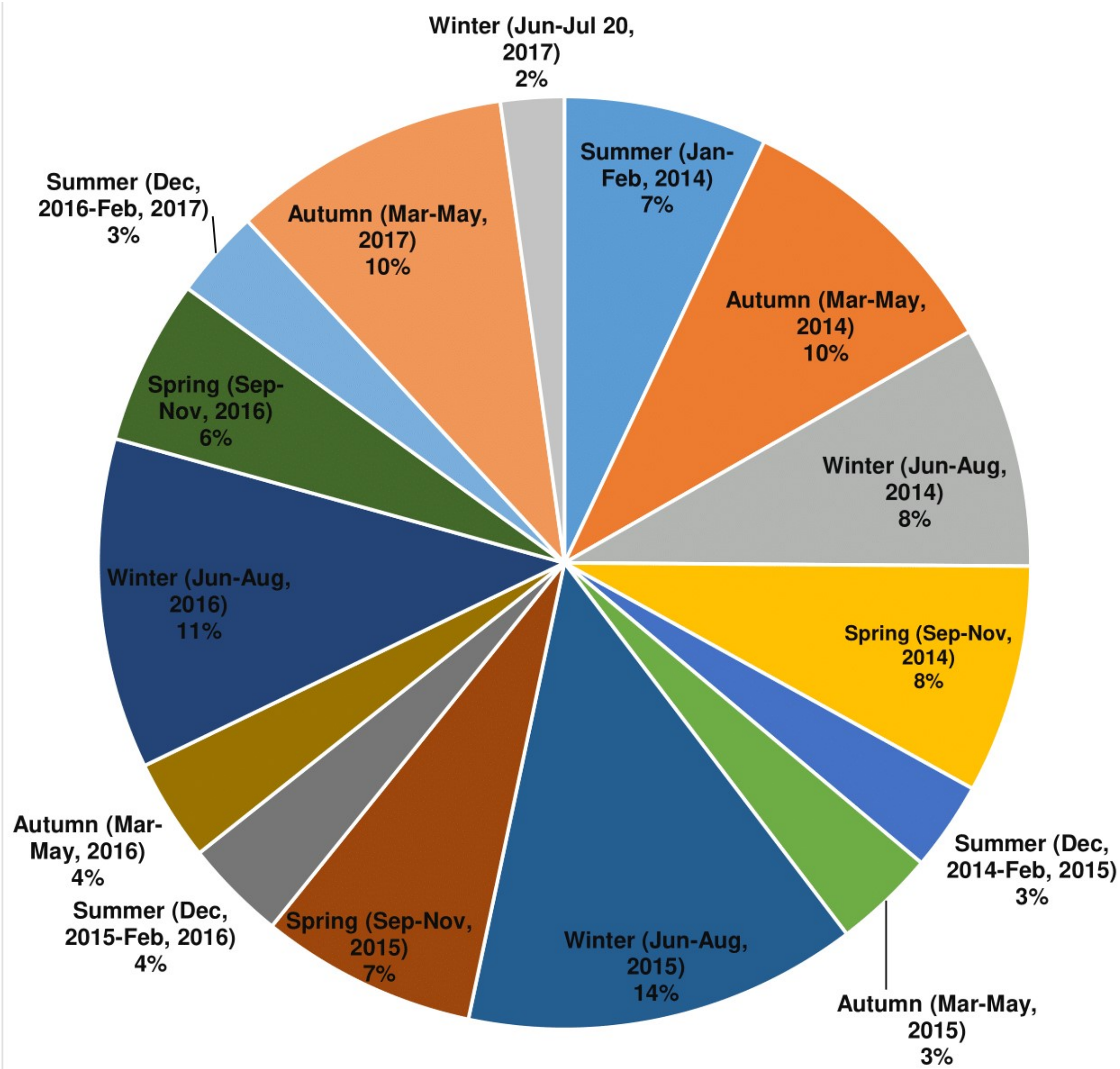

Figure 3.8 Historical trend of outages per season.

3.5 Model Development

The potential explanatory variables were subjected to a screening process to investigate the predictive model for variables with a good description of the system. This is to enhance good generalization from a robust learning process. To implement the ES model, the smoothing factor was varied in steps of 0.1 between 0.1 and 0.9. The best smoothing factor that had the least error estimates was 0.8. In this study, two models were developed for both MLR and ANN. All the historical variables listed under the description of study area were used for Model 1 of both the MLR and ANN methods to determine the weather-related electricity system failure (SF). Model 1, in both cases, is governed mathematically by the expression

$$SF = f(\text{OD, CLD, FRSD, PRE, PET,TMN, TMX, VAPD, WETD, WS}) \quad (3.6)$$

Pearson correlation analysis was used in Model 2 (for both MLR and ANN) to screen the variables to those presumed to be directly related or more appropriate. Table 3.4 presents the results of the correlation analysis. The cut-off mark was chosen by accepting the correlation coefficient in the range $0.5 \leq |x| \leq 1$ and discarding the correlation coefficient in the range $-0.5 < x < 0.5$. The results yield high correlation (0.5 or -0.5) for cloud amount, precipitation, minimum temperature, maximum temperature, vapor pressure, number of wet days and wind speed. The remaining variables with correlation coefficients in the range $-0.5 < x < 0.5$ were discarded.

Table 3.4 Pearson correlation analysis result

S/n	**Variables**	**Correlation coefficients**
1	OD	-0.05051
2	CLD	0.549712
3	FRSD	-0.26586
4	PET	0.471735
5	PRE	0.57765
6	TMN	0.597951
7	TMX	0.520818
8	VAPD	0.638733
9	WETD	0.534573
10	WS	-0.57327

For Model 2, both the MLR and ANN models are governed by the expression:

$$SF = f(\text{CLD, PRE, TMN, TMX, VAPD, WETD, WS}) \tag{3.7}$$

For training and testing purposes, the data sets were split in the ratio 70% to 30%; hence, 159 data sets were used for training, and 68 data sets for testing. For the ANN models, feed-forward ANNs with supervised learning methods were used in this study. Target outputs specified in Table 3.5 were used for the system failure. The two ANN models were implemented in the ANN toolbox in MATLAB, while the MLR and ES models were implemented using Microsoft Excel. The input and output of the outage prediction model are the severity of the weather variables and the number of outages respectively. The number of outages is a useful input to a system operator in that the expected number of outages per season will assist the utility management, system operator and maintenance crews to be proactive and be well prepared for the projection. This will in turn reduce the down time and improve reliability. The two ANN models were subjected to the expressions in (3.6) and (3.7) respectively; as were the two MLR models. The model performances and the performance of the ES models can be compared. For ANN Models 1 and 2, the configurations used were 10-60-1 (10, 60 and 1 neurons in the input, hidden and output layers) and 7-60-1 (7, 60 and 1 neurons in the input, hidden and output layers), respectively. Linear and sigmoid transfer functions combined with a back propagation algorithm (BPA) were used for the ANN models. The ability of an ANN to approximate functions is expressed through transfer functions. The common types of transfer functions are piece-wise linear, sigmoid, unit step (threshold), and Gaussian. The type of transfer function used is determined by the application requirements. Transfer functions for the binary and bipolar sigmoid can be expressed, respectively, as [109]:

$$F = \frac{1}{1+e^{-\sigma x}} \tag{3.8}$$

$$F = \frac{1-e^{-\sigma x}}{1+e^{-\sigma x}} \tag{3.9}$$

where x = sum of weighted inputs and σ = steepness parameter.

Table 3.5 System failure target outputs

S/n	Year	Time of the year	Season	Outage events
1	2014	1 January – 28 February	Summer	16.0
2	2014	1 March – 31 May	Autumn	22.0
3	2014	1 June – 31 August	Winter	19.0
4	2014	1 September – 30 November	Spring	18.0
5	2014/2015	1 December – 28 February	Summer	7.0
6	2014/2015	1 March – 31 May	Autumn	8.0
7	2014/2015	1 June – 31 August	Winter	31.0
8	2014/2015	1 September – 30 November	Spring	17.0
9	2015/2016	1 December – 28 February	Summer	8.0
10	2015/2016	1 March – 31 May	Autumn	8.0
11	2015/2016	1 June – 31 August	Winter	26.0
12	2015/2016	1 September – 30 November	Spring	13.0
13	2016/2017	1 December – 28 February	Summer	7.0
14	2016/2017	1 March – 31 May	Autumn	22.0
15	2016/2017	1 June – 31 July	Winter	5.0

3.6 Model Evaluation

In this study, the performance of the predictive models was evaluated using six statistical measures. The measures are R^2, RMSE, MAPE, MAD, MSE and MAE. R^2 measures the degree of variance between the predicted and target values. RMSE is a measure of the error variance of the prediction model. MAPE calculates the absolute differences between the predicted and target values. MAD measures the variability of a dataset by defining the deviation between each data point and its mean. MSE (or MSD) is a measure of the average of the squares of the deviations—that is, the average squared error between the predicted values and the target value. MAE measures the errors between paired observations denoting the same phenomenon [110].

The closer that RMSE, MAPE, MAD, MSE and MAE are to zero, the better the model. For R^2, the closer it is to 1, the better the model; this can be obtained from

$$R^2 = \left(\frac{\sum_{i=1}^{N} (Y_i - \bar{Y})(X_i - \bar{X})}{\sqrt{\sum_{i=1}^{N} (Y_i - \bar{Y})^2 \sum_{i=1}^{N} (X_i - \bar{X})^2}} \right)^2 \tag{3.10}$$

The following equations are for the other statistical measures [101, 111, 112, 113].

The error variance of the prediction model can be calculated using

$$\text{RMSE} = \sqrt{\left(\frac{\sum_{i=1}^{N} (Y_i - X_i)^2}{N} \right)} \tag{3.11}$$

The absolute differences between the predicted and target values are

$$\text{MAPE} = \frac{100}{N} \sum_{i=1}^{N} \frac{|Y_i - X_i|}{Y_i} \tag{3.12}$$

while the deviation between each data point and its mean is obtained from

$$\text{MAD} = \frac{1}{N} \sum_{i=1}^{N} |X_i - X| \tag{3.13}$$

and the average of the squares of the deviation is

$$\text{MSE} = \frac{1}{N} \sum_{i=1}^{N} (Y_i - \bar{Y})^2 \tag{3.14}$$

The errors between paired observations can be obtained from

$$\text{MAE} = \frac{1}{N}\sum_{i=1}^{N}|Y_i - X_i| \tag{3.15}$$

where, in these equations, N = number of occurrences in the set; and X_i, Y_i, $\bar{X}$ and $\bar{Y}$ = target, predicted and their respective mean values.

3.7 Results and Discussion

Table 3.6 presents the performance of the predictive models. The results of ANN Models 1 and 2 were satisfactory for both training and testing operations, but the performance of ANN Model 1 is better than all the other models. The performances of the models were compared and the R^2 of ANN Model 1 for training and testing are the highest; they are 0.9982 and 0.9999, respectively. ANN Model 1 also recorded the lowest values for other measures during both training and testing, such as RMSE (0.3156 and 0.0035), MAPE (0.0009% and 0.0001%), MAD (0.0293 and 0.0017), MSE (0.0996 and 0.00001), and MAE (0.0293 and 0.0017). Ranking the models in order of performance based on their statistical measures: ANN Model 1 > ANN Model 2 > ES Model > MLR Model 1 > MLR Model 2). The results indicate that all or most of the considered variables were significant, directly or indirectly, in determining weather-related electricity system failures for PMB.

Table 3.6 Statistics of data used in the research.

	Train	**Test**	**Train**	**Test**	**Train**	**Test**	**Train**	**Test**	**Train**	**Test**	**Train**	**Test**
Technique	R^2	R^2	RMSE	RMSE	MAPE	MAPE	MAD	MAD	MSE	MSE	MAE	MAE
ES	0.77	0.47	3.82	3.83	0.04	0.09	1.18	2.29	14.63	14.67	1.18	2.67
MLR Model 1	0.51	0.56	5.22	3.13	0.14	0.12	4.09	3.13	27.24	9.80	4.09	3.66
MLR Model 2	0.46	0.55	5.51	3.14	0.15	0.12	4.43	3.08	30.31	9.89	4.43	3.60
ANN Model 1	0.99	0.99	0.32	0.01	0.01	0.01	0.03	0.01	0.09	0.01	0.03	0.01
ANN Model 2	0.95	0.99	1.61	0.87	0.01	0.01	0.13	0.15	2.60	0.76	0.13	0.15

A careful analysis of the results shows that the accuracy of the prediction of the power system outages depends on the ten variables considered in ANN Model 1 and MLR Model 1. A reduction in the number of input variables in ANN Model 2 and MLR Model 2 reduced the accuracy of the forecasted values for the models. Therefore, the ten variables make up the best subset of the model that is sufficient to represent the weather related electricity system failure of the city, as opposed to the scaled down number of variables of seven.

For both the training and testing of the five models, Figures 3.9–3.18 show how the data points deviated from the line of equality.

The performance of the ES method is presented in Table 3.6, and in Figures 3.9 and 3.10. This was implemented by incrementing the damping factor by 0.1 between 0.1 and 0.9. It was observed that the damping factor with the highest error estimate was 0.1, while the damping factor with the least error estimate was 0.8. Therefore, the best damping factor (with least error estimate) was taken as 0.8. From Figures 3.9 and 3.10, which show the system failure plots of target vs. predicted value for the ES Model training and testing, it can be observed that the deviations of the data points from the line of equality are high. The percentage overfit suffered by the ES model is between 5.5

and 39.9%, thereby showing unsatisfactory performance.

Figures 3.11–3.14 show the system failure plots of target vs. predicted values for MLR Models 1 and 2 training and testing. It can be seen that the deviation of the data points from the line of equality is high, in a similar manner to the ES model. The percentage overfit of Models 1 and 2 varies between 4.7 and 43.8%, again showing unsatisfactory performance.

Figures 3.15–3.18 show minimal deviations confirming the satisfactory performance of the ANN models and their efficiency when compared to conventional models. The figures show the system failure plots of target vs. predicted value for ANN Models 1 and 2 training and testing. This time, the deviation of the data points from the line of equality are very small. The percentage overfit suffered by ANN models 1 and 2 is generally below 1%. This illustrates that the performance is very satisfactory.

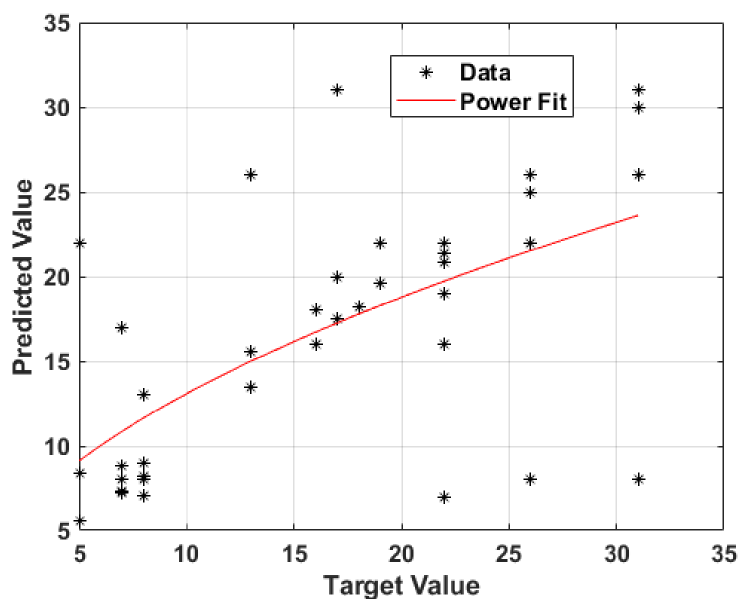

Figure 3.9 System failure plot of target vs. predicted value for ES Model training.

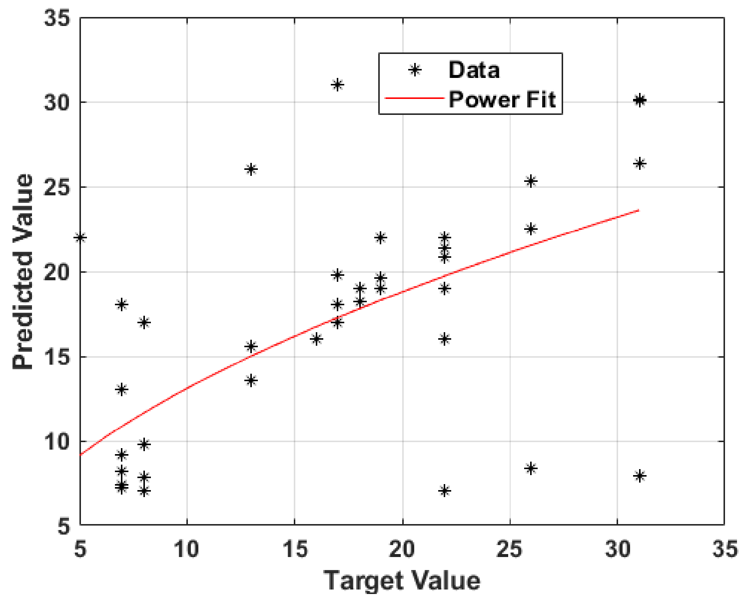

Figure 3.10 System failure plot of target vs. predicted value for ES Model testing.

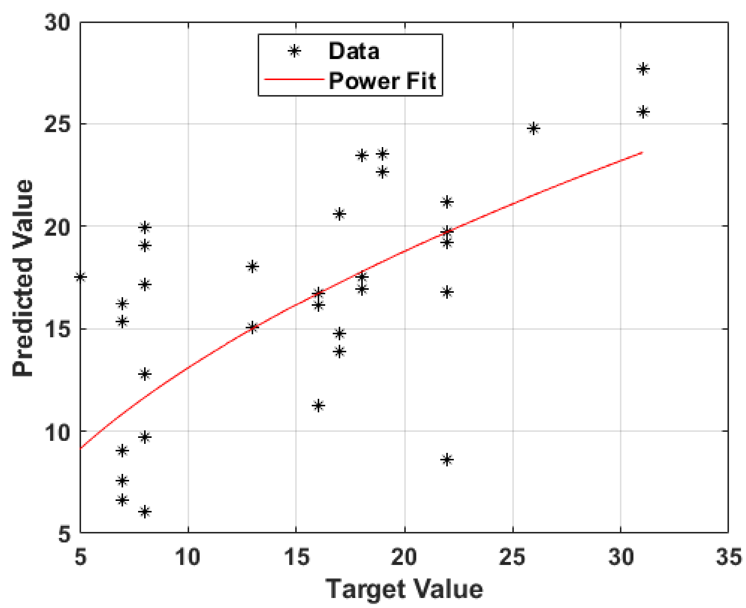

Figure 3.11 System failure plot of target vs. predicted value for MLR Model 1 training.

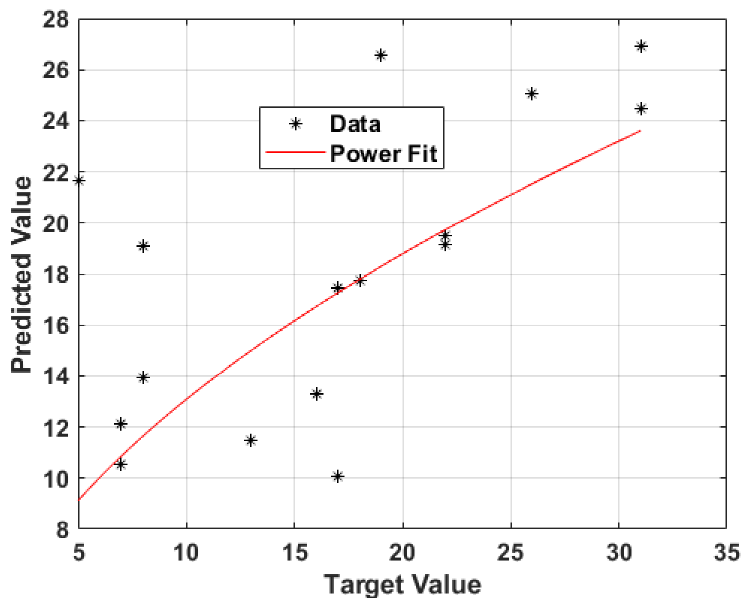

Figure 3.12 System failure plot of target vs. predicted value for MLR Model 1 testing.

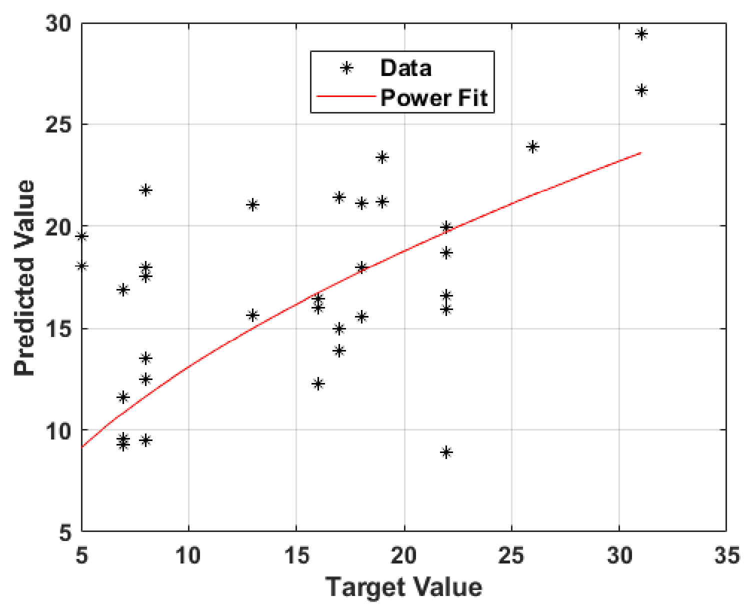

Figure 3.13 System failure plot of target vs. predicted value for MLR Model 2 training.

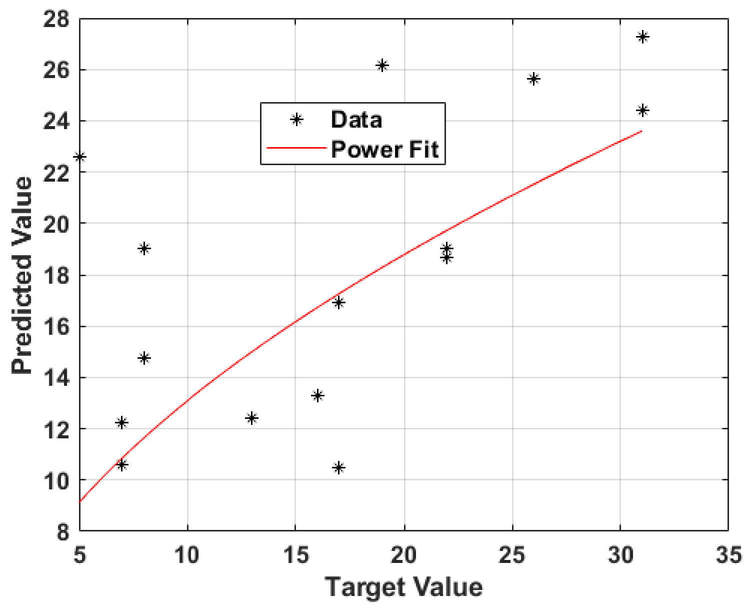

Figure 3.14 System failure plot of target vs. predicted value for MLR Model 2 testing.

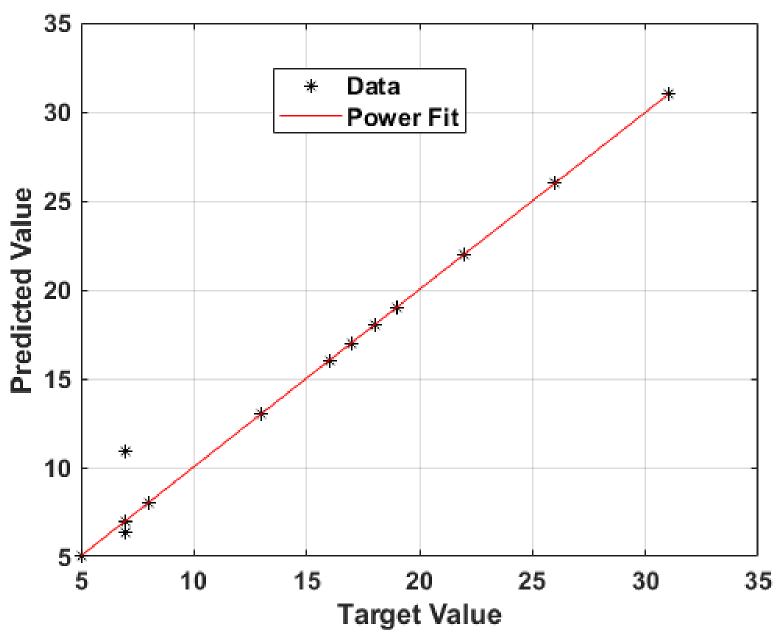

Figure 3.15 System failure plot of target vs. predicted value for ANN Model 1 training.

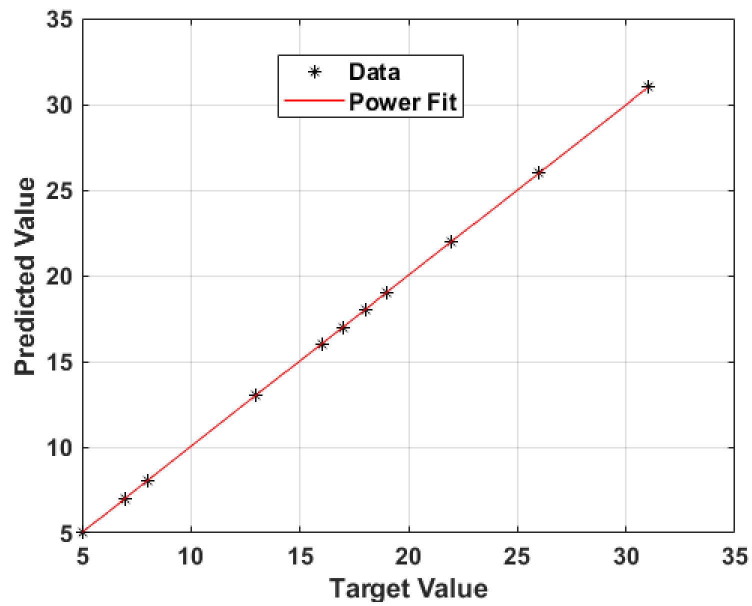

Figure 3.16 System failure plot of target vs. predicted value for ANN Model 1 testing.

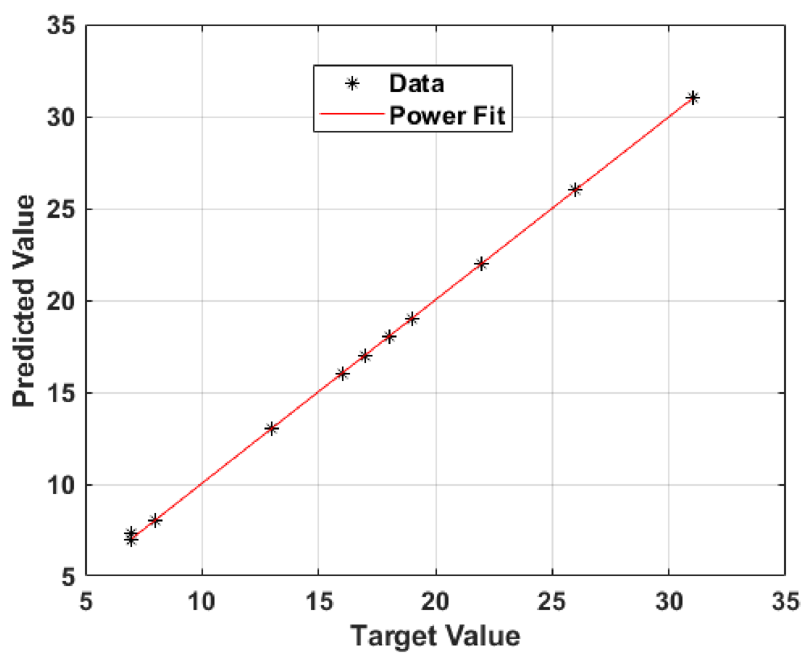

Figure 3.17 System failure plot of target vs. predicted value for ANN Model 2 training.

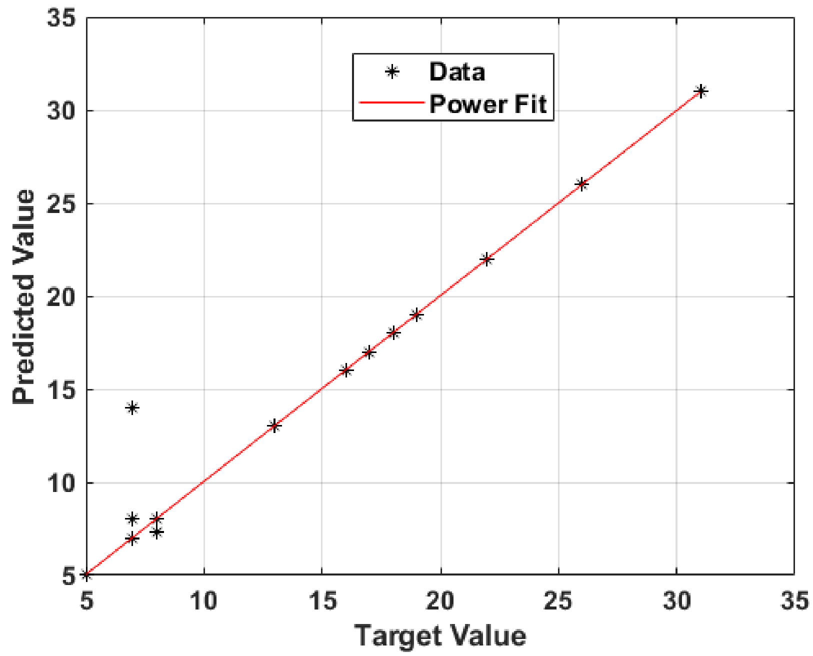

Figure 3.18 System failure plot of target vs. predicted value for ANN Model 2 testing.

The number of input neurons of ANN model 1 was 10 by virtue of the number of input variables. Different configurations consisting of different numbers of hidden layers with different numbers of neurons were trained and the configuration, with one hidden layer containing sixty neurons giving the best results. The methods used in this study further illustrate that ANNs are robust and applicable to weather related power system failure, and that they are able to account for complex relationships between power system failure and climatic parameters. It can be inferred that ANN-based models have potential in terms of managing weather-related power system failure prediction effectively.

3.8 Comparison with some Optimization Techniques

The results of the comparison of the proposed method with some optimization techniques are presented in Table 3.7. The data used for ANN Model 1 training were implemented using a differential search (DS), differential evolutionary algorithm (DE), genetic algorithm (GA) and ant colony optimization (ACO) methods. The results were evaluated using the RMSE statistical measure. Although the RMSE values for all the methods are very close, the ANN Model 1 method excelled by its ease of implementation, its superior computation time, and having the least computation complexity with respect to the other compared optimization methods.

Table 3.7 Comparison with some optimization techniques.

Method	**Computation Time (s)**	**RMSE**
ACO	52.32	0.3222
GA	54.35	0.3417
DE	51.29	0.3365
DS	45.06	0.3323
ANN model 1	25.14	0.3156

3.9 Conclusions

The performance of ANN-based and conventional predictive methods (MLR and ES) was compared for weather related electricity system failure. Statistical measures serve as the basis for the model performance using real-life data sets from PMB, South Africa. Two models were generated for both ANN and MLR. In both cases, ten potential explanatory variables were used for Model 1, while seven potential explanatory variables were used for Model 2 after careful screening using correlation analysis. An analysis showed that ANN Model 1 was better than the other models in terms of performance. The order of performance of the models is ANN Model 1 > ANN Model 2 > ES Model > MLR Model 1 > MLR Model 2. The results are further confirmation of the appropriateness and robustness of ANNs in predicting weather related electricity system failure. The complex relationship between weather events and electricity system failure is demonstrated in this study. Future research could investigate the use of larger data sets, investigate similar ANN models when forecasting outages for multiple power systems, use metaheuristic optimization methods, and compare the accuracy of the developed ANN model 1 against other artificial intelligent methods.

Chapter 4

Event-Driven Power Outage Prediction using Collaborative Neural Networks

This chapter is based on the work reported in [2].

4.1 Abstract

Distribution networks are often exposed to many complex and unfavorable weather conditions that are subject to many constraints and thereby susceptible to outages. Weather events are responsible for several faults on the grid networks. Increase in the weather events can result in increase in the frequency of grid faults thereby leading to increase in the maintenance cost of the grid system and decrease in electricity supply's reliability. Weather events based forecasting models are necessary to overcome these problems. It is necessary to consider intelligent outage models to realize effective weather-based outage forecasting. To develop a better performance model for outage forecasting, it is essential to consider various types of events for different complex weather conditions and constraints. The conventional event-driven forecasting algorithm is only appropriate for a single type of event scenario and unable to adapt effectively to multiple types of event scenarios concurrently. A multiple-constraints event-driven outage model that depends on maximum entropy function is proposed in this paper. The model transforms the complex event-driven outage problem into two continuous differential single-objective sub-problems. An optimal outage forecasting solution for various difficult weather conditions is provided using the collaborative neural network (CONN) algorithm. The CONN event-driven forecasting algorithm successfully resolves the problem of the difficulty in obtaining very large complex weather events and outages data. Unlike the conventional forecasting methods, the CONN algorithm provides an adaptive optimal forecasting solutions for different complex events. This significantly decreases the constraints required in adapting to different weather events. The CONN algorithm's performance was validated by many experiments; which was applied to complex, multi-constrained weather conditions.

4.2 Introduction

Event-driven power outage forecasting is a new research focus in electrical power systems [114, 115, 116]. Event-driven forecasting is a novel forecasting problem that takes into consideration the complex weather events that are responsible for power outages. Event-driven forecasting uses multiple climatic constraints and different outage events to provide the optimal outage forecasting solution in complex scenarios. The conventional outage forecasting methods only address single outage events and are unable to effectively address multiple outage event scenarios simultaneously [86, 87, 117, 90]. However, because electric power networks are subject to different complex environmental events, it is essential to propose an outage forecasting method that is able to provide an optimal forecasting solution for different complex events with multiple constraints such as speed, deployment time, intensity factors, and confidence coefficient. In this study, the event-driven algorithm based on collaborative neural network (CONN) methods was proposed. The problem was effectively solved by the even-driven algorithm based on CONN using historical and meteorological data. An optimal outage forecasting solution can be adaptively provided by the CONN algorithm for different complex outage events such as storm, tornado, hurricane, flood, and earthquake. The use of this method significantly reduces the cost and time involved in adapting to diverse complex application scenarios. Authors in [118] investigated the severity of outages caused by tree in Connecticut under heavy rain and winds events using Hurricane Sandy simulations and machine-learning models. In [119], an algorithm was developed to simulate power outages using the fragility functions under hazard loading. The algorithm works by estimating the probability of experiencing outages due to a natural hazard. The model was validated with accurate predictions despite the use of less input data from Ohio power station. As documented in reference [120] a synthetic open-source extendable electric grid model was developed. The model design was a data-driven, cross-domain, open-source technique for assessing a real-life power system during extreme weather events. In [121], the authors proposed a Support Vector Machine (SVM) based outage model in response to an anticipated hurricane. The effectiveness of the model was evaluated using the IEEE 118-bus test system. Authors in [122] proposed an artificial intelligence (AI) model for improving network resilience in extreme weather events which was validated using standard IEEE 118-bus test system. Reference [116] proposed a computing framework based on Spiking Neural Network (SNN) for accurate classification of outage events in power networks. The proposed method was validated using 16-machine, 5-area New England-New York system. In [123], a multi-hazard method for characterizing the major predictors of sustained power outages due to severe weather was proposed. The authors in [124] designed an approach to monitor the recovery status and spatial extent of power outages using the black marble nighttime light (BMNTL). The design serves as a good source of data for locating the areas where disaster relief are required. In [125], a support vector machine (SVM) model, subjected to the data of heavy-rain hazards was used in making cost-sensitive prediction and the model evaluated using G-mean values. Authors in [114] proposed an optimization technique to coordinate event-driven load shedding (LS) and corrective line switching (CLS) and designed a two-loop algorithm to solve the optimization problem, and its effectiveness was validated using an industrial power system and a standard IEEE 39 bus test system. Reference [127] introduced the conditioned outage prediction models (OPM) to 102 storm events between 2005 and 2020 over the service territory of Eversource Energy, Connecticut, USA. The study [128] proposed a wavelet based method that models the precise behavior of device which eradicates some unrealistic assumptions. The research work as documented in [129] proposed a ramp prediction technique based on event detection context and modified swinging door algorithm and compared with conventional models. Authors in [130] explored a spatial power-outage model and a geographic information systems (GIS) to investigate power failure events and causes. The research in [131] proposed a machine learning method to overcome the challenge of identifying the characteristics of lightning-based outages. Authors in [117] proposed an outage risk models that addressed the epistemic probabilities in physics-based hurricane predictions under climate change.

In view of the reviewed literature, it can be observed that more research is needed to assess the reliability of power systems considering weather events. The reviewed literature did not carry out a concurrent assessment of multiple and complex constraints. The work done in this study is compared with the literature as illustrated in Table 4.1 to assess the effectiveness of the proposed method. The following acronyms were used for the extreme weather events (EWEs) discussed in the table: (i) wind/rain (WDR); (ii) snow/winter storms (SNW); (iii) Heatwaves (HTW); (iv) hurricanes (HUR) and (v) thunderstorms (TDS).

Table 4.1 Comparison of studies

Study	**HTW**	**HUR**	**SNW**	**TDS**	**WDR**	**Complex constraints**	**Multiple constraints**
[86]	-	✓	-	-	✓	-	-
[87]	-	-	-	✓	-	-	-
[90]	-	-	✓	-	-	-	-
[117]	-	✓	-	-	-	-	-
[118]	-	✓	-	-	✓	-	-
[120]	-	-	✓	-	-	-	-
[121]	-	-	-	-	✓	✓	✓
[122]	-	✓	-	-	✓	✓	✓
[124]	-	✓	-	-	-	-	-
[125]	-	-	-	-	✓	-	-
[127]	-	✓	-	-	-	-	-
[129]	-	-	-	-	✓	-	-
[130]	-	-	✓	✓	✓	-	-
[131]	-	-	-	✓	-	-	-
This study	✓	✓	✓	✓	✓	✓	✓

The studies reviewed show that more research is needed to find solutions to power outage forecasting problems due to multiple types of weather events. The contributions in this study are summarized as follows:

1. Solution to complex event-driven power outage forecasting problems was proffered using neural network methods. The use of event-driven power outage algorithm can be applied using CONN to various application cases to meet different power outage forecasting requirements;
2. A maximum entropy function model is proposed for a multi-constrained event-driven power outage problem which converts the complex problem into two single-objective sub-problems;
3. An event-driven outage model with multiple constraints converting the complex problem into two single-objective sub-problems which are continuously differential, this solves the problem that the objective function of the conventional min-max model is non-differential;
4. The problem of non-availability of large amount of outage events and weather data in complex environment is successfully overcome.

Unlike the conventional outage methods, the CONN algorithm can iteratively provide an optimal forecasting solution for different complex events and environments.

4.3 Description of the Study Case

This study chose the city of Newcastle (NWC), Latitude: 27.71° S, and Longitude: 29.99° E, as the study area. NWC with a 2021 population projection of 396 240 is the third and tenth largest city in the province (KwaZulu-Natal) and country (South Africa) respectively [126]. NWC is headquarter to both Newcastle Local and Amajuba District municipalities and one of South Africa's industrial hubs. It is the home of the largest producer of chrome chemicals in Africa and a coal mining site. The municipality is currently executing an aggressive year 2030 city sustainability project [132]. The city is a temperate region and classified as 'cold interior' in South Africa. NWC's temperature often drops below the freezing point during winter season with occasional snowfalls. During summer season, NWC's temperature is often extreme, and sometimes above 40 °C because of the El Nino weather phenomenon and therefore prone to drought [4]. NWC is chosen as the suitable and demonstrative case study for this research out of the three (i.e. the Pietermaritzburg, PMB, Empangeni, EMP, and Newcastle, NWC) operating units (OUs) in Kwazulu-Natal (KZN) province because of its drought-prone feature, extreme weather events and temperate climate.

4.4 Description of Data

This research model was developed using the data discussed in this section. Data sources and analysis are described respectively.

4.4.1 Data Sources

The under-explored, yet valuable outage data repository from the public utility company in South Africa, Eskom Holdings SOC Ltd., serves as an assessment resource for outage events risks in South Africa. The data collected for this study spanned the period of fifteen months (between October 2018 and December 2019) and a total of 323 observations was recorded during the period. Whenever there is any disturbance incidence in the electricity sector, some entities are to file the reports. Such entities include the local, generating and electric utilities, reliability coordinators, balancing authorities, and security, telecommunication and computer offices. The criteria in the database reported information such as (i) date and time when the incidence starts; (ii) date and time when the incidence ends/restored (iii) alert status; (iv) the event type i.e., cause of the outage; (v) estimated peak demand involved; and (vi) estimated number of customers affected during the event. However, under-reporting was observed because there is no enforcements to inadequate reporting [123]. Notwithstanding, the data obtained is an invaluable resource for assessing the power outage patterns and the related hazards to the electricity utilities in South Africa. Besides electricity outage data, climate data of the study area was also collected from the South African Weather Service (SAWS). The data information includes: (i) wind speed (WS in m/s), (ii) surface pressure (SP, in kPa), (iii) rainfall (RF, in mm/month), (iv) frost point (FP, in °C), (v) relative humidity (RH, in %), (vi) minimum temperature (Tmin, in °C) and (vii) maximum temperature (Tmax in °C).

4.4.2 Data Analysis

Exploratory analysis of the power outage data was conducted and the incidents categorized as: (i) equipment failure (EF); (ii) disruption in the course of system operation (SOD); (iii) system sabotage and vandalism (SSV); (iv) public appeal (PA); (v) emergency due to fuel supply (FSE); (vi) system islanding (SI); and (vii) extreme weather events (EWE, including climatic shocks and severe tropical weather). It is observed that 55.2% of the electricity outages recorded in the data occurred as a result of EWE; SSV accounts for about 20.8%; SOD 11.7%; PA 2.9%; EF 3.7%; FSE 3.4%; and SI 2.3%. The impact and frequency trends of electricity outages are shown in Figures 4.1-4.7. It is discovered that EWE was the most often cause of outages (Figure 4.1) while the SSV followed by a distant frequency figure (Figure 4.2). The outage duration as a result of EWE is about 53,281 hours (Figure 4.3) out of the cumulative total outages of 75,925 hours. EWE outage affected about 113,580 customers out of the cumulative total of 208,238 customers.

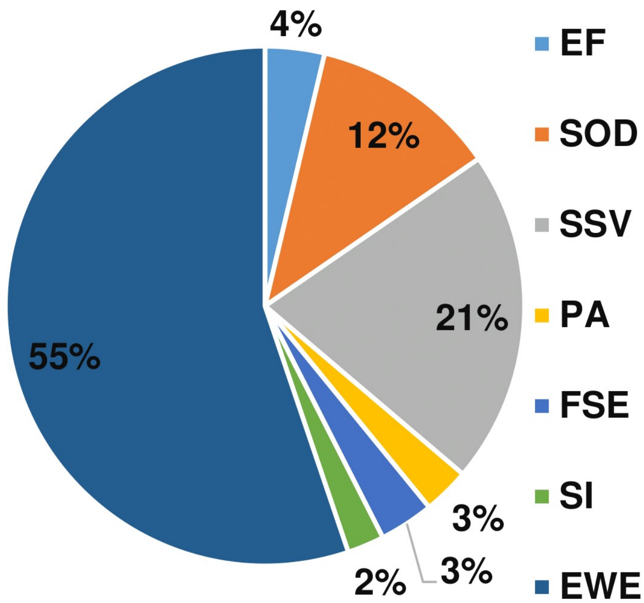

Figure 4.1 Power outage distribution in Newcastle.

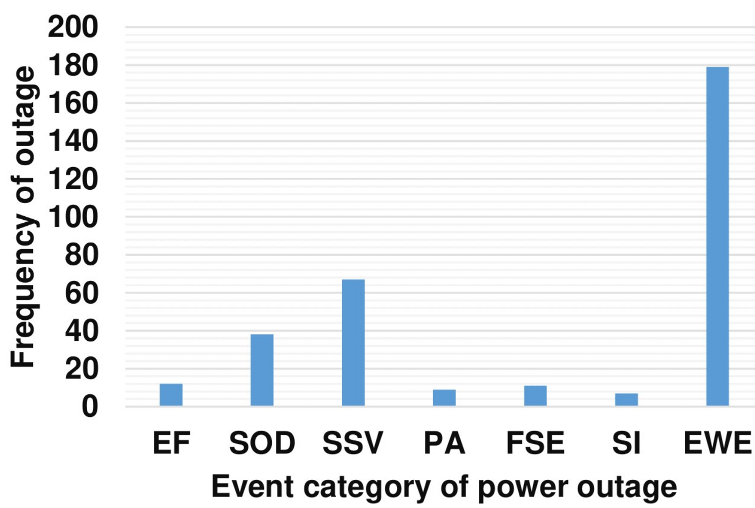

Figure 4.2 Frequency of power outages in Newcastle.

Based on the analyzed data, this study categorized the extreme weather events as: (i) wind/rain (WDR); (ii) snow/winter storms (SNW); (iii) Heatwaves (HTW); (iv) hurricanes (HUR) and (v) thunderstorms (TDS). The duration, frequency and customer affected during climatic shocks are shown in Figure 4.5 – Figure 4.7 respectively. It is observed from the EWE distribution that the

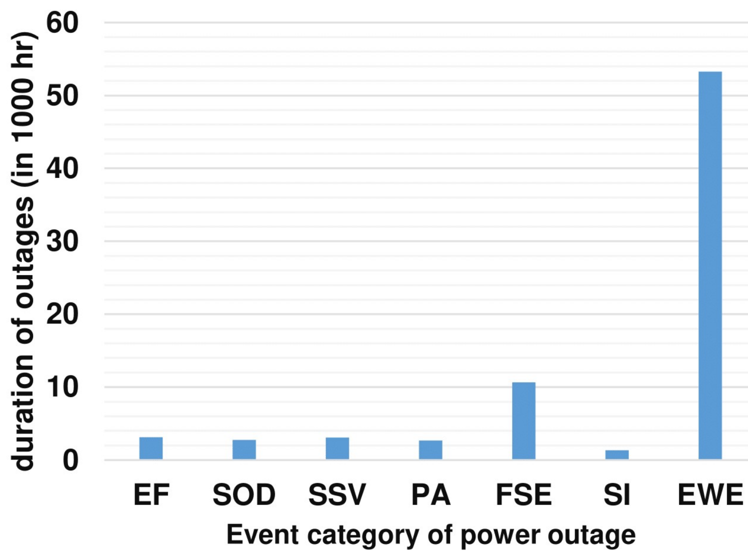

Figure 4.3 Duration of power outages in Newcastle.

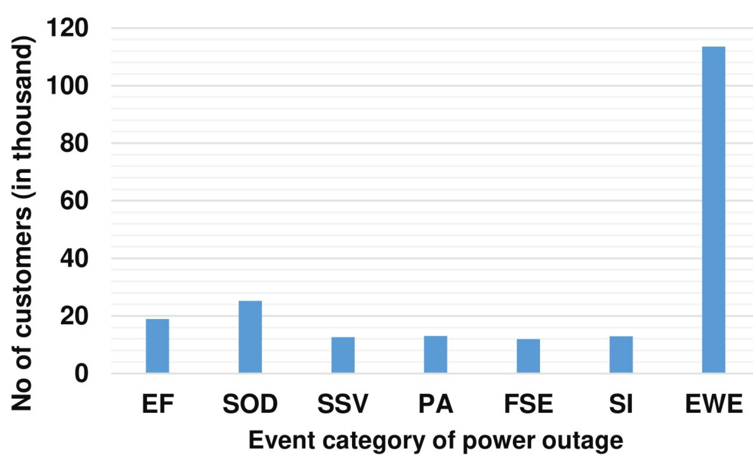

Figure 4.4 Number of customers affected by power outages in Newcastle.

TDS, HUR, SNW, and WDR are the most occurring events with varying impacts.

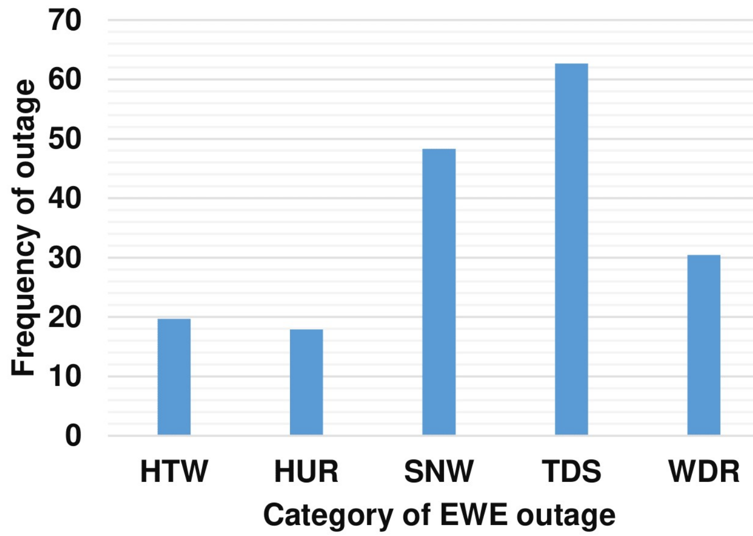

Figure 4.5 Frequency of EWE outages in NWC.

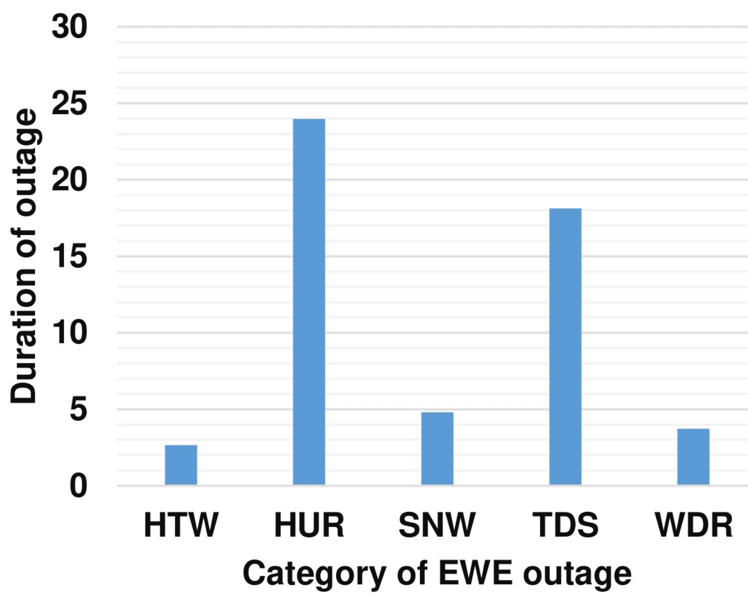

Figure 4.6 Duration of EWE outages in NWC.

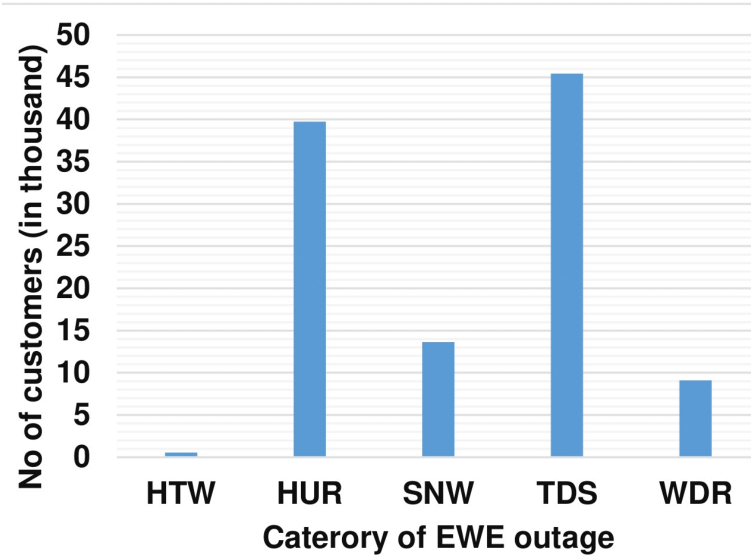

Figure 4.7 Customers affected by EWE outage in NWC.

4.5 Modelling of Compound Event-Driven Power Outage Forecasting using Maximum Entropy Function

A model using maximum entropy function for compound event-driven power outage forecasting problem is proposed in this section. This model converts the complex event-driven outage forecasting problem into two continuous differential single-objective sub-problems. The problem of compound event-driven outage forecasting with multiple constraints can be expressed as [133]:

$$\begin{aligned} maxF(\alpha) &= c_i f_i(\alpha_1, \alpha_1, ..., \alpha_n)(i = 1, 2, ..., p), \\ s.t. f_j(\alpha) &= g_j(\alpha_1, \alpha_1, ..., \alpha_n) \leq 0 (j = 1, 2, ..., p) \end{aligned} \tag{4.1}$$

where $F(\alpha)$ is the event-driven power outage forecasting function, c_i is the confidence coefficient, $c_i \geq 0$, and mirrors the forecasting accuracy of different power outage events; i and j are the numbers of objective and constraint functions respectively; $\alpha = (\alpha_1, \alpha_2, ..., \alpha_n)$ are the different extreme weather outage events, and $\alpha = (\alpha_1, \alpha_2, ..., \alpha_n) \in T \subset R^n$ is an n-dimensional decision vector; $T = \{\alpha \in R^n | d_i \leq \alpha \leq u_i, i = 1, 2, ..., p\}$ is the target space, $d_i \in R$ and $u_i \in R$ are the lower and upper bound of α_i respectively; $f_j(\alpha)$ is the inequality constraints; and $g_j(\alpha)$ represents the inequality constraint function. The $g(\alpha)$ functions, in real-life application, denote different constraints such as speed, deployment time, intensity factors, and confidence coefficient, etc. constraints and they are all positive values. $\Omega = \{\alpha | \alpha \in T, g_i \alpha \leq 0, i = 1, 2, ..., p\}$ is the feasible domain with feasible solutions.

and the maximum entropy function of (4.1) is expressed as:

$$F_e(\alpha) = \frac{1}{e} ln \sum_{i=1}^{p} exp(e f_i(\alpha)), e > 0. \tag{4.2}$$

where $F_e(\alpha)$ denotes a uniform approximation of the problem functions in the limit of e approaching infinity. When $e \to \infty$, for any $\alpha \in R^n$, the compound event-driven power outage forecasting problem with multiple constraints in (1) can be solved using the following multi-constrained single-objective event-driven power outage forecasting sub-problem:

$$\begin{gathered} maxF_e(\alpha, c) = \frac{1}{e} ln \sum_{i=1}^{p} exp(ec_i(f_i(\alpha) - f_i^*)), (i = 1, 2, ..., p), \\ s.t.\ f_j(\alpha) = g_j(\alpha_1, \alpha_2, ..., \alpha_n) \leq 0, (j = 1, 2, ..., q) \end{gathered} \tag{4.3}$$

where f_i^* is the reference points introduced to improve the accuracy of the calculation of the compound event-driven power outage forecasting model.

Equation (4.3) is a function maximization problem with respect to the independent variables α and c. This method converts the complex compound event-driven power outage forecasting problem into a single-objective sub-problem which is continuously differentiable and does neither increase the number of constraints nor introduce new variables. The single-objective event-driven power outage forecasting equation is used to calculate the optimal confidence coefficient as:

$$\begin{aligned} maxF_e(\alpha, c) = \frac{1}{e} ln \sum_{i=1}^{p} exp(ec_i(f_i(\alpha) - f_i^*)) \\ s.t.\ c \geq 0 \end{aligned} \tag{4.4}$$

Therefore, two sub-problems of (4.3) and (4.4) are formed from the multi-constrained compound event-driven power outage forecasting problem. Neural networks are then used to solve the two sub-problems iteratively in order to obtain the Pareto optimal solution for the multi-constrained compound event-driven power outage forecasting problem, as expressed in the next section.

4.6 Compound Event-Driven Power Outage Forecasting Algorithm Based on the Collaborative Neural Network Strategy

The CONN is a form of artificial neural network comprising more than one neural networks. The strength of CONN is in its benefits; it is appropriate for application in complex and large-scale scenarios and it adaptively assigns different neural network modules to different sub-problems. Therefore, the complex and large-scale multi-constraint compound event-driven power outage forecasting problem can be solved using the CONN. The CONN functions mainly by forming a continuous path for the optimization process to begin from the starting point and converge at the optimal solution. The CONN state equation is expressed as [133]:

$$\frac{d}{ds}\begin{pmatrix}\alpha\\ \beta\end{pmatrix} = \xi\begin{pmatrix}-\nabla_\alpha f(\alpha) - \nabla_\alpha(\alpha)^T\beta\\ -\beta + (\beta + g(\alpha))^+\end{pmatrix} \tag{4.5}$$

where the gradient of g_j is $\nabla_\alpha g_j(\alpha)$ for $(i = 1, ..., q)$ and $\nabla_\alpha g(\alpha)^T$=$\nabla_\alpha g_1(\alpha), ..., \nabla_\alpha g_q(\alpha)^T$, ξ represents a positive constant, and $\alpha \in R^n, \beta \in R^q, (\beta)^+ = [(\beta)_1^+, ..., (\beta)_q^+]^T, and (\beta)_j^+ = max\{0, \alpha\}$.

the neural network used in solving sub-problem (3) is expressed as:

$$\frac{d}{ds}\begin{pmatrix}\alpha\\ \beta\end{pmatrix} = \xi\begin{pmatrix}-\nabla_\alpha F_e(\alpha, c) - \nabla_\alpha g(\alpha)^T\beta\\ -\beta + (\beta + g(\alpha))^+\end{pmatrix} \tag{4.6}$$

and another neural network used in solving sub-problem (4) is expressed as:

$$\frac{dc(s)}{ds} = \xi(c - \nabla_c F_e(\alpha, c)) - c \tag{4.7}$$

where $c \in R^p$

$$F = \frac{1}{1 + e^s} \tag{4.8}$$

With respect to the maximum entropy function, the compound event-driven power outage forecasting problem with multiple constraints is broken down into two sub-problems of equations (4.3) and (4.4). The outage forecasting problem is solved by the mutual interaction of these two neural networks, forming a CONN.

4.7 Collaborative Neural Network Approach for Compound Event-Driven Power Outage Forecasting Algorithm

A compound event-driven power outage forecasting algorithm which centers on the collaborative neural network approach is proposed in this section. The compound event-driven power outage forecasting problem with multiple constraints is first transformed into two single-objective sub-problems using the maximum entropy function, the collaborative neural networks are then applied to the two single-objective sub-problems, the initial confidence coefficient is assumed. If the result of either of these sub-problems lead to the Pareto optimal solution of the compound event-driven power outage forecasting problem, then the algorithm produces its output and stops; otherwise, the confidence coefficient sub-problem is updated using another neural network. Until the process leads to the Pareto optimal solution of the event-driven power outage forecasting problem, the process is repeated. The two single-objective sub-problems are continuous convex, hence the application of two neural networks to solve them. The collaborative neural network is constituted by these two neural networks. The sequence of the compound event-driven power outage forecasting algorithm established on the collaborative neural network approach is highlighted as follows. Figure 4.8 shows the collaborative neural network algorithm [133].

1. Select an initial confidence coefficient c^1 and set the number of initial iterations $s = 1$;

2. Use the Neural Network (4.6) for the confidence coefficient c^s, to obtain the optimal solution α^s of the Lagrange multiplier vector $beta^s$ and the single-objective sub-problem (4.3). If α^s is the Pareto optimal solution of the compound event-driven power outage forecasting problem, then the algorithm produces its output and stops; otherwise, the process proceeds to step 3;

3. With the α^s and β^s obtained in step 2 above, a new optimal confidence coefficient is obtained by solving (4.4) using (4.7);

4. The process proceeds to 2 after the number of iterations is set.

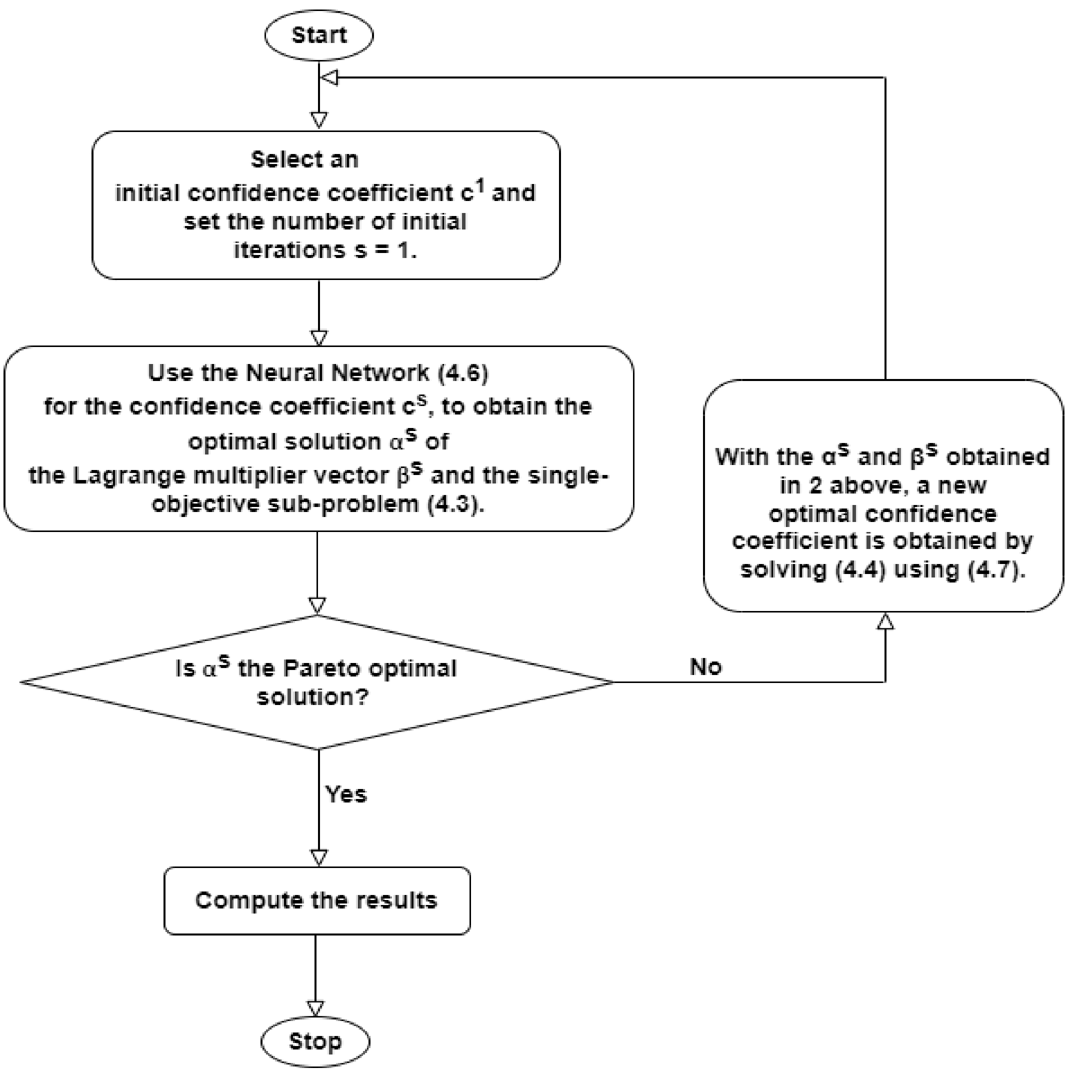

Figure 4.8 The CONN algorithm flow chart.

4.8 Performance Evaluation

The CONN algorithm was assessed in different outage event scenarios. The multi-constrained event-driven outage prediction in power systems was completed using the CONN algorithm. Five types of EWEs with diverse constraints such as speed, deployment time, intensity factors, and confidence coefficient were used. Both the constraints and quality of prediction are required to be met in event-driven outage prediction.

4.8.1 Environment Settings

The program was implemented in Matlab2019b environment. There are five types of EWEs in the experiments. The confidence coefficients of power outage for the five types of events, HTW, HUR, SNW, TDS and WDR are 0.11, 0.10, 0.27, 0.35 and 0.17, respectively. Each types of event had a different perceived speed factor (SPF), deployment time factor (DTF), intensity factor (IF), and confidence coefficient (CoC), according to its own property. Table 4.2 and Table 4.3 presents the parameters of the climatic seasons and that of the power outage events respectively. Four case studies were explored to evaluate the performance of the proposed method.

4.9 Experimental Evaluation

The effectiveness of CONN algorithm was analyzed in multi-constrained power network through simulation experiment. Four diverse case studies were used considering the SPF, DTF, IF, and CoC constraints as shown in Table 4.4. The results and analysis of the experiment are presented in this section.

Table 4.2 The parameters of the climatic seasons [4].

S/N	YEAR	PERIOD	CLIMATE	FAULTS PER CLIMATE
1	2018	1 Oct – 30 Nov	Spring	47
2	2018/2019	1 Dec – 28 Feb	Summer	91
3	2018/2019	1 Mar – 31 May	Autumn	59
4	2018/2019	1 Jun – 31 Aug	Winter	29
5	2018/2019	1 Sep – 30 Nov	Spring	78
6	2018/2019	1 - 31 Dec	Summer	19

Table 4.3 The parameters of the outage events.

SYMBOL	EVENT	SPF	DTF	IF	CoC
α_1	HTW	0.10	0.3	0.25	0.11
α_2	HUR	0.35	0.4	0.40	0.10
α_3	SNW	0.05	0.2	0.20	0.27
α_4	TDS	0.40	0.1	0.15	0.35
α_5	WDR	0.15	0.5	0.30	0.17

In Table 4.4, MIN, Ratio and Time stand for minimum confidence constraints, coverage ratio and computation time respectively. In Figure 4.9- 4.12, the chosen five EWEs were implemented in four case studies using CONN algorithm. The minimum confidence constraint and the network's monitoring requirements were continuously increased from case 1 to case 4. Hence, there is room for additional EWEs in the networks as the necessity arises.

Table 4.4 The parameters of the experiments.

Case	SPF	DTF	IF	MIN	Ratio (%)	Time (s)
1	695	90	815	0.77	41.2	3.024
2	860	126	1230	0.84	63.6	3.407
3	1625	260	2180	0.92	87.9	4.735
4	2080	300	2675	0.99	97.1	5.128

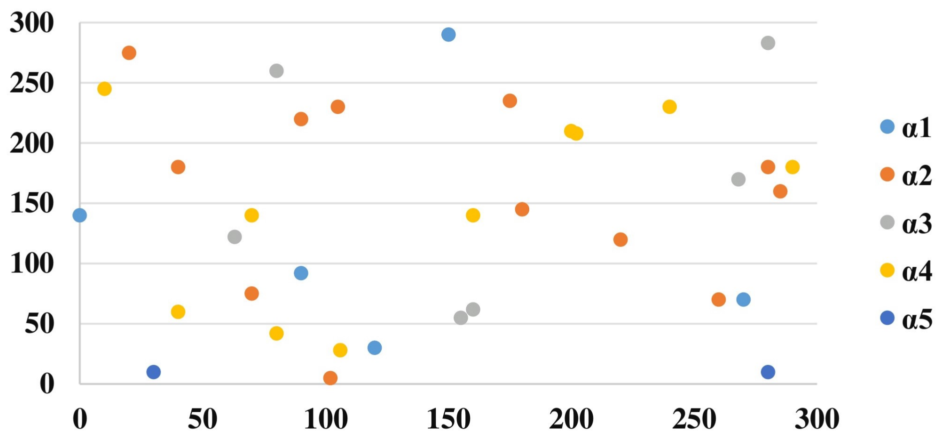

Figure 4.9 Scatter diagram for case 1.

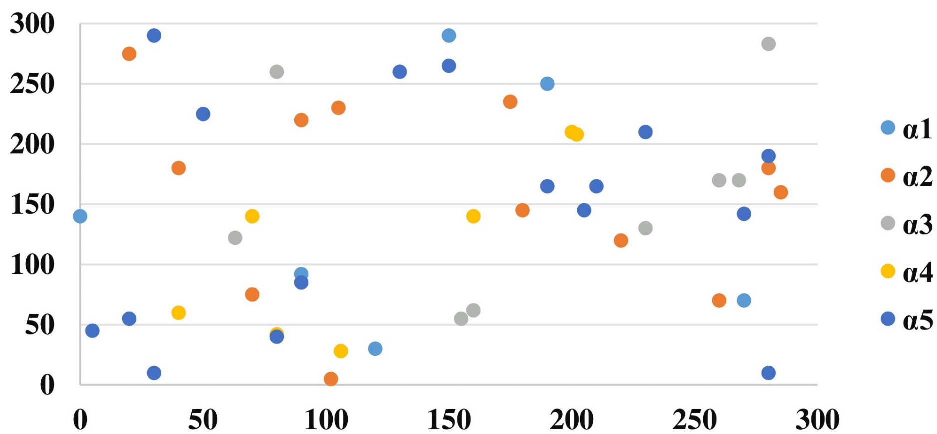

Figure 4.10 Scatter diagram for case 2.

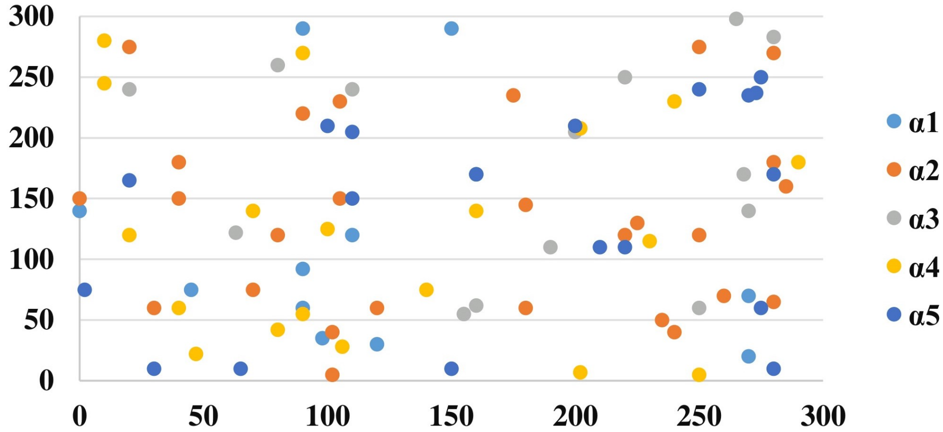

Figure 4.11 Scatter diagram for case 3.

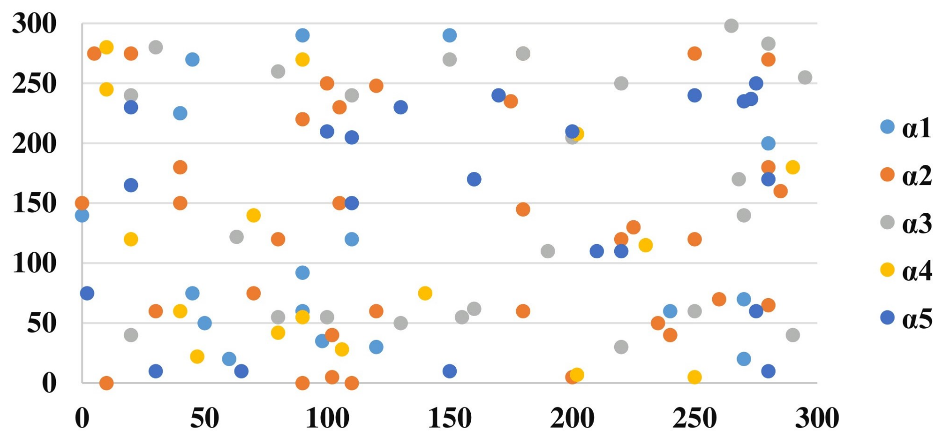

Figure 4.12 Scatter diagram for case 4.

The SPF, DTF, IF and CoC constraints were applied to each case. Each case study depict a particular network constraint as shown in Table 4.3.. The four case studies were chosen carefully for a more instinctive impact. The increase in the number of weather events leads to increase in the probability of outage forecasting and decrease in the coverage holes. In the CONN algorithm, two NNs interacted and modified each other. There is a continuous optimization of the event-driven outage forecasting in the network. In case study 1, the network was made to undergo strict SPF, DTF, IF and CoC constraints. The number of EWEs permitted for the network's use is limited. Therefore, the network's outage prediction outcome (which is 41.2%) is unsatisfactory. The constraints in case study 2 network increases with respect to case 1, the number of EWEs in the network also increases leading to an improvement in the performance (63.6%) of the network. As the number of EWEs in case study 3 network increases the more, the coverage holes reduces considerably in the network and the network forecasting tends to be uniform (87.9%). As the number of EWEs in case study 4 network increases further, the network forecasting tends towards saturation reaching 97.1% coverage ratio. Under the present condition of the network, the CONN algorithm continues its convergence towards the optimal solution, indicating a reasonable network prediction. It is observed here that the CONN algorithm can effectively forecast multiple types of events irrespective of multiple network constraints.

Figure 4.13 shows the event-driven outage performance and the resource allocation for the extreme weather events in the four case studies. The four scenarios has different SPF, DTF, IF and CoC constraints. It can be observed that the MIN requirements kept rising constantly from case 1 to 4. The network's prediction requirements kept improving constantly also. Therefore, to meet the demand of diverse complex constraints, lots of EWEs are to be applied in the network's outage forecasting. The outcomes of the experiment show that the CONN algorithm is efficient in allocating extreme weather resources in multi-constrained networks.

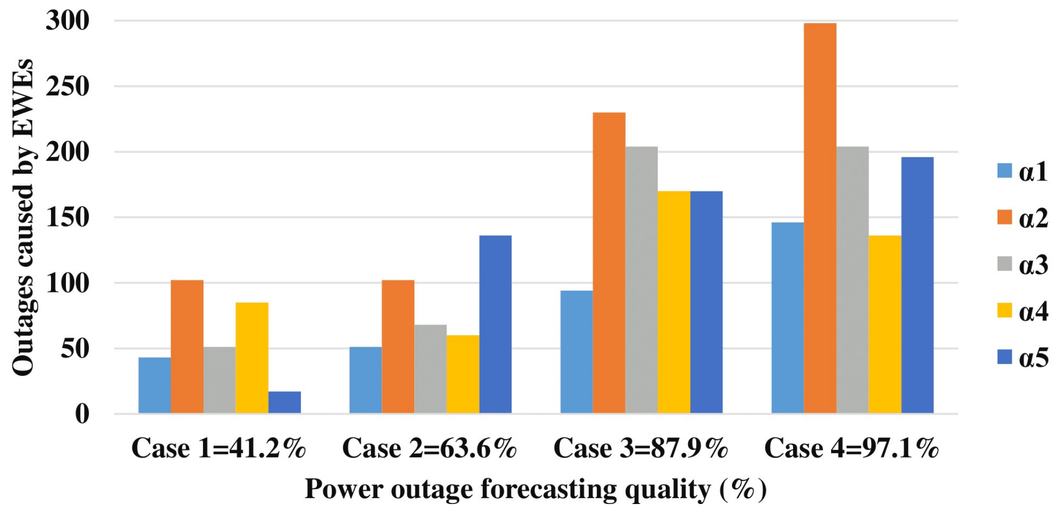

Figure 4.13 The event-driven quality performance of the four cases.

Figure 4.14 shows the forecasting error due to different constraints. It could be seen that the error in MIN is lower than that in IF followed by case DTF and lastly SPF. It is also observed that the percentage error is less in forecasting greater numbers of extreme weather events and vice versa.

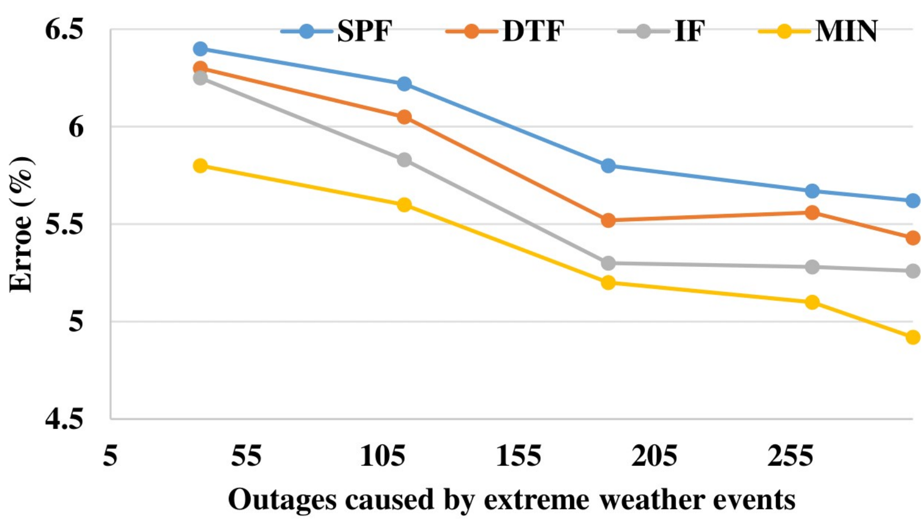

Figure 4.14 Forecasting error due to different constraints.

Figure 4.15 shows the forecasting error of the extreme weather events. The α_2 exhibits the lowest percentage error followed by α_3, then α_5, α_4 and lastly α_1. It is also observed, just like in the case of the percentage error due to different constraints, that the percentage error is less in forecasting greater numbers of extreme weather events and vice versa.

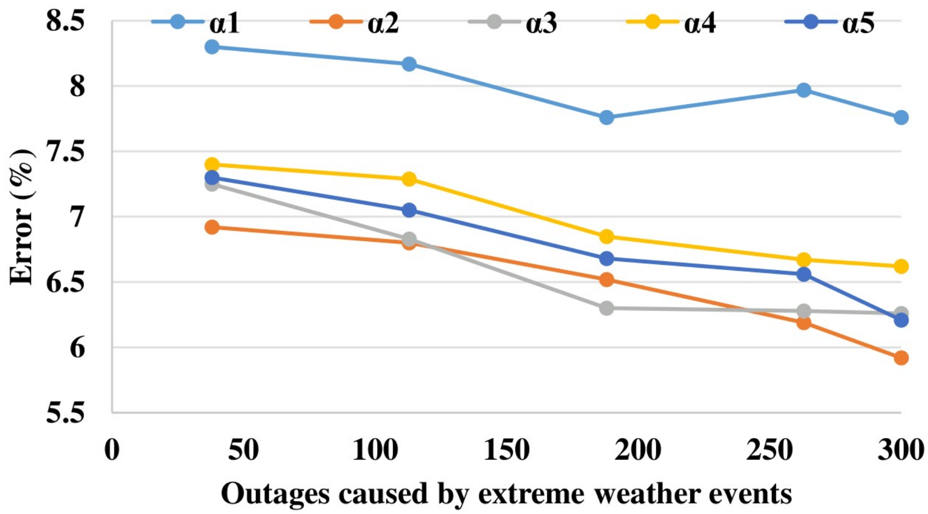

Figure 4.15 Forecasting error for different extreme weather events.

4.10 Comparison with single artificial neural network method

The comparison between solution proffered by a single ANN and that of the CONN is presented in Table 4.5. The results show that, although the computation time (s) for ANN is smaller than that of CONN (which is to be expected because of the workload involved in CONN), the forecasting quality (%), average forecasting error for EWE events at 300 outages (%), and average forecasting error due to different constraints at 300 outages (%) in CONN give improvements over those of the single ANN. The results show that the CONN algorithm is smoother in characteristic and superior in computational efficiency as compared to the ANN algorithm.

Table 4.5 Comparison with Single Artificial Neural Network Method

Parameter	**ANN**	**CONN**
Computation time (s)	27.25	30.57
Forecasting quality (%)	78.62	97.14.
Average forecasting error for EWE events at 300 outages (%)	9.14	6.55
Average forecasting error due to different constraints at 300 outages (%)	7.29	5.31

4.11 Conclusions

In this research, the model using CONN methods and maximum entropy function for multi-constrained event-driven power outage forecasting algorithm was developed for the solution of complex power outage forecasting scenarios. The developed model used solutions of easier sub-problems to solve the complex multi-constrained event driven problem. Five types of power outage events, HTW, HUR, SNW, TDS and WDR with different constraints, SPF, DTF, IF, and CoC, were considered in four different scenarios. An effective optimal power outage forecasting solution was provided by the collaborative neural network algorithm according to the various outage events and network constraints. Moreover, the problem of acquiring a large amount of weather data in a complex environment is overcome by CONN algorithm effectively. Based on the results obtained, it was established that CONN algorithm is effective in providing power outage forecasting solutions to multi-constrained and complex problems as compared to single artificial neural networks method

Chapter 5

Reliability evaluation and financial viability of an electricity power micro-grid system with the incorporation of renewable energy sources and energy storage: Case study of KwaZulu-Natal, South Africa

This chapter is based on the work reported in [3].

5.1 Abstract

The increase in the demand for a reliable electricity supply by the utilities and consumers has necessitated the evaluation of the reliability of power systems. A reliable electricity supply is characterized by no or minimal duration and frequency of supply outages. This has triggered the necessity of using renewable energy sources (RESs) with optimization methods for reliability improvement of electricity systems and reduction of greenhouse gas (GHG) emissions. The main objective of this study is to optimize micro-grid systems operations, improve reliability, reduce emissions and balance the demand and supply of energy through RESs and battery energy storage system (BESS). The adaptive model predictive control (AMPC) method is used to address the issues of micro-grid operation. The AMPC algorithm solves the optimization problem of disturbance prediction in a micro-grid with different types of RESs and BESS integration. This optimization problem considers different constraints for minimum operating costs in different case scenarios. The financial viability of the proposed method is investigated. Solar photovoltaic (Solar PV), wind plant (WP) and BESSs are used with the AMPC method to investigate the impacts of annual real interest rates on cost and emission parameters, quantification of the emission oxides from different case scenarios, reduction of the cost of electricity (Ccoe), and power system reliability improvement. A modified Roy Billinton Test System (RBTS) is used to confirm the reliability enhancement and financial feasibility of the system. Case studies are used to confirm the proposed methods using climatic data for the city of Pietermaritzburg (29.37°S and 30.23°E), South Africa. The results obtained establish that the incorporation of RESs and BESSs using the AMPC method gives satisfactory outcomes.

5.2 Introduction

The ever-increasing demand for electricity due to world population growth and economic expansion has placed a massive demand on a reliable power supply. There are challenges due to the fast depleting global deposits of fossil fuels. Environmental pollution and climate change due to greenhouse gas emission coupled with unpredictable fuel pricing have given rise to the exploitation of renewable energy sources (RESs) as reliable, sustainable, and non-polluting alternatives [134]. The provision of quality and reliable power supplies to the consumers at a reasonable cost is the expectation of every utility [135]. Hence, global utilities have identified the incorporation of RESs as a reasonable option for making such provisions. It has been projected that RES penetration into power systems will increase from 25 % in 2017 to 85 % in 2050. This is mostly through the use of solar photovoltaic (solar PV) and wind plants (WP) [136]. A reliable electricity supply is a booster to the social development, economic growth, health, and physical well-being of a nation. Reliability plays a crucial role in the design, implementation, and operation of an electrical system [137]. The performance of the electrical system can be measured by utilities using reliability indices. 80% of load point outages are caused by distribution system failures rather than transmission and generation failures [138]. The effect of outages can be severe to both the utilities and the consumers. Utilities suffer economic loss and reputational damage while the consumers can suffer damage to their equipment, can experience raw materials spoilage, and suffer from loss of revenue and work. As a result, distribution system reliability deserves attention in the electrical system. Further work on improvements in the reliability of the distribution system is necessary.

Reliability serves as a benchmark for providing the regulatory bodies with necessary information in the deregulated environment. Conventional radial distribution systems can be less reliable because of its single source. A fault on any part of the network can lead to an outage of the entire system because of lack of alternative generation. Hence, the duration of outage is often longer in a single-source conventional distribution system.

When there is a fault on a lateral feeder, consumers on other lateral feeders experience voltage fluctuations due to load changes. The incorporation of a multiple-source micro-grid system has influenced the power system positively in a number of ways. The links between renewable energy sources and consumers do not require investment of hundreds of kilometers of a transmission line; hence, reducing maintenance costs, C_{amc}, system costs C_{acs}, and costs of energy, C_{coe} as well as the installation time. The multiple-source nature of the microgrid system helps to ensure an uninterrupted supply of electricity whenever there is a fault from the main source, thereby enhancing the reliability of the system. Consideration has to be given to RESs as the most cost-effective electrification solutions for the load requirements of remote areas. These are characterized by complex terrains which require high cost installations with long installation times and safety concerns for transmission and distribution lines [139]. As of 2016, 13% of the world population is said to be without access to electricity. About one-fifth of these are said to be living in remote areas with complex and difficult terrains and unable to connect to the national grid due to many constraints [140]. RESs can be integrated into the power system to bring electricity to consumers in such remote and rural settlements. For sustainable growth, microgrid systems can be used to integrate RESs. RESs have many advantages such as low cost of emission, low maintenance and operation cost, low fuel cost, and enhancement of power system reliability [141]. Many utilities have proved their benefits and embraced the integration of RESs to meet global demand for energy and allay public fear of the environmental impacts of using fossil fuels. Wind and solar energy are now widely accepted due to their benefits both technically and economically [142].

The benefits of reducing the emission of greenhouse gases has encouraged utilities to harness the wind and solar potential. The use of more than one RES in a system enables the weakness of one source to be overcome by the strength of other and the disadvantage of intermittent supply is overcome by the use of a battery system. A battery energy storage system (BESS) can store energy during normal operation which is used to supplement the supply during deficit or peak period. Many studies have explored the methodologies and impacts of BESSs and RESs on the reliability and financial viability of electrical systems.

Keshavarzi and Ali presented a control strategy under different operating conditions for BESSs for minimization of power fluctuations due to intermittent supplies from RESs [143]. Hidalgo-Leon *et al*. made a holistic review of the BESS, encompassing its technology, practical implementation, financial viability, and environmental effects [144]. They inferred that integration of a BESS into a RES could effectively mitigate major RES issues. Graditi *et al*. proposed a model for regulating and controlling a BESS in a RES micro-grid to avoid frequency instability and ensure energy restoration in the network [145]. Farias and Canha analyzed the US Department of Energy (DOE) database to provide cases of battery technologies, including their services, applications, and benefits with respect to RES [146]. They explored the technical characteristics of different battery types to provide insights into their energy flexibility, life cycle, and energy-storing capacity. Hassanzadeh *et al*. proposed a multi-term signal feedback technique for regulating constant power and frequency deviation of RESs and BESSs, thereby improving microgrid performance [147]. Montoya *et al*. addressed the problem of optimal dispatch of DC micro-grids with penetration of RESs and BESSs using an exponential load model [148]. Gil-González *et al*. developed a mathematical model for the optimal operation of dc micro-grids. Second-order cone programming was used to convert non-convex into a convex model of economic dispatch and applied it to a system with high penetration of BESSs and RESs to realize their objectives [149]. Brogan *et al*. used the ramp time and delayed time of a BESS to improve the inertial and frequency of a power micro-grid system [150]. Reihani *et al*. proposed optimization techniques for the control of how a BESS charges and discharges in a micro-grid system [151]. Effective voltage regulation, power curve smoothing, and peak load shaving were achieved. Kiptoo *et al*. considered a cost-benefit analysis in harnessing the benefits of the demand-side in optimal capacity sizing of micro-grid components [152].

Ganesan *et al*. proposed a hybrid power controller to manage the intermittent nature of the power supply in a RES by sharing power between diesel generators, solar PV, and BESS [153]. To realize the power flow control, active power from the diesel generator and solar PV were managed with respect to the system frequency. Alhejaj and Gonzalez-Longatt demonstrated that the response from BESS inertia can cause a variation in the degree of change of frequency; thereby, enhancing frequency response and offer frequency support to the system [154]. Ganesan *et al*. discussed an analytical method for identifying suitable rating of voltage source that can act as frequency and voltage references for a BESS [155]. This voltage source-based BESS was found to be suitable in supplying reactive and real power to the load during grid outage. Marchi *et al*. proposed a model covering the life cycle cost analysis of a BESS considering the operation cost components of the system, such as cost of maintenance, decommissioning, and disposal [156].

Badal *et al*. presented the benefits of RESs, integration complexities, and control problems [157]. They investigated different control methods in different scenarios. Adefarati *et al*. proposed a cost-effective, optimized micro-grid system using solar PV, diesel generator, methanol generator and BESS; implemented by the HOMER application tool [137]. The performance of the system was investigated using fuel cost, inflation rate, load demand and solar radiation. Çelikbilek and Tüysüz presented a model for RES evaluation using Multi-criteria Optimization, Analytic Network Process, Decision Making Trial and Evaluation Laboratory [158]. Ranking of RESs was further performed using the proposed method. Kasturi and Nayak proposed a model for optimally allocating RESs using mathematical methods in distribution systems [159]. The optimal allocation problem formulated was solved using a multi-objective optimization approach. Karanki and Xu presented an optimal location and sizing for BESSs to achieve loss reduction in distribution system using the particle swarm optimization method [160]. Tan *et al*. presented a risk and cost model for optimal scheduling of a hybrid energy system using Latin hypercube optimization technique [161]. The results not only reduced the intermittency of RESs, but also smoothed the tie-line power. Ovaskainen *et al*. explored the simultaneous use of a BESS as an active harmonic filter for improving power quality and voltage stability of a micro-grid [162]. Hussain *et al*. developed a coordinated control strategy in a hybrid power system for maintaining system frequency thereby ensuring satisfactory power system stability [163]. It was proved from the simulation results that the load demands can be met by power generated from the RES and stored in the BESS. Khalili *et al*. [164] investigated how voltage reduction (VR) and a demand response program (DRP) affects the operation of a distribution system (DS). The reliability of the network was evaluated using the energy not supplied (ENS) index. The ENS was minimized by reducing the voltage level of the network using the load. The DS reliability was effectively improved through the combination of DRP and VR methods. [165] explored the optimal scheduling of microgrids (MGs) containing a fossil fuel generator and RESs with a DRP. A multi-objective model using a weighted sum technique was used to obtain Pareto optimal solutions which minimized the unused energy of the implemented scenarios. The costs of electricity and generators were minimized, and the MG DRP profit was maximized to achieve an optimal economic status.

In view of the studies reviewed, it can be seen that more work is needed to incorporate RESs into power systems in order to realize the objectives of reliability improvement and cost reduction. The studies reviewed did not carry out a simultaneous evaluation of system reliability, i.e., the system costs C_{acs}, energy costs C_{coe} and net present cost C_{npc}. This was carried out in this study. The impacts of the annual real interest rate (ARIR) on the cost and emission parameters are also investigated. This gap is identified in Table 5.1 which compares the studies reviewed. The models proposed in past studies did not consider the stochastic features of the vital components of the micro-grid system. These are essential for evaluating the reliability of a power system. This study has the goal of exploring the stochastic features of vital components of the micro-grid system to evaluate the reliability of the power system with respect to cost analysis considering C_{acs}, C_{npc} and C_{coe}. Case studies for the reliability evaluation of the micro-grid system are explored. These estimate the expected energy not served $(EENS)$ and expected interruption cost $(ECOST)$ using the proposed model. The contributions from this work are:

i. Evaluation of the reliability, financial viability, and eco-friendly impacts of RESs incorporated into a micro-grid system;

ii. Development of a model used for reliability evaluation of a power system with the integration of RESs;

iii. Development of a model used for reducing C_{acs} and C_{coe} and increasing the use of RESs in a power system;

iv. Integration of a model which will help in estimating the costs of supply interruptions by utilities, thereby improving power system reliability;

v. Use of a model which will help in monitoring the efficiency of a power system with the integration of RESs.

vi. Implementation of a modified Roy Billinton Test System (RBTS) model which is verified using the adaptive model predictive control (AMPC) method;

vii. Quantification of the emission parameters (oxides) from different case scenarios;

viii. Investigation of the impacts of annual real interest rate on the cost and emission parameters of the micro-grid.

To the best of the authors' knowledge, the reliability problems in micro-grid systems with integrated RESs, and the investigation of the impacts of ARIR on the cost and emission parameters, have not been previously addressed using an AMPC optimization algorithm. This work proves, through its results, that the reliability of a power system can be improved by the incorporation of RESs using the proposed method, and C_{acs} and C_{coe} can simultaneously be reduced. This outcome can serve as a measure for making investment decisions by utilities and the governments with respect to renewable energy policies.

Table 5.1 Comparison of studies

Study	**Component sizing**	**Cost optimization**	**Reliability optimization**	**Emission parameter quantification**	**Impact of ARIR on cost parameters**	**Impact of ARIR on emission parameters**
[135][137][138][142][148][149][150] [158][159][163][164][165][166]	✓	✓	✓	-	-	-
[139][154][156]	✓	✓	-	-	-	-
[160][162][167][168][169]	✓	-	✓	-	-	-
This study	✓	✓	✓	✓	✓	✓

5.3 Background

In this study, RESs (in the form of a micro-grid) using AMPC method are adopted for reliability and economic improvements. The micro-grid is described as a small entity of an electricity network with a local supply that can function independently (islanded mode) or in conjunction with the central grid. This can also be stand-alone which is useful for use in remote areas which are isolated from the central grid due to operational barriers such as distance and cost of linking [170]. Islanded operation saves utilities from economic loss as well as improving system reliability and environmental perspective. Economic advantages of the micro-grid are that they do not require long transmission line investment if stand-alone and its operation and maintenance costs are low; in addition and there is emission reduction. A micro-grid network comprises of the loads, control units, sources (in the form of wind plant, mini gas turbine, solar PV, hydropower, diesel generator or other generator), and BESSs. The micro-grid system proposed in this study is made up of diesel generators, solar PV, wind plant, and a BESS. They are designed with system constraints and load requirements arranged to reduce costs (total outage cost, C_{toc}, C_{acs}, and, C_{coe}) and improve reliability. Case studies are used to confirm the proposed methods using climatic data of the city of Pietermaritzburg, PMB (29.37°S and 30.23°E), South Africa. The climatic data is obtained from the South African Weather Services (SAWS) and consists of the wind speed, solar irradiance, and average daily ambient temperature. The proposed micro-grid system is presented in Figure 5.1. The expression for total power generated P_T by the proposed microgrid is obtained using [171]:

$$P_T(i,t) = P_{SPV}(i,t) + P_{WP}(i,t) + P_{GEN}(i,t) \tag{5.1}$$

and power demand by consumers is expressed as:

$$P_D(i,t) = P_{GEN}(i,t) \pm P_{BESS}(i,t) \tag{5.2}$$

where P_{SPV}, P_{WP}, P_{GEN}, and P_{BESS} are the power from solar PV, wind plant, diesel generator, and BESS, respectively; t and i are the time period and node under analysis.

5.4 Modeling of the System Under Study

The system dynamics of a micro-grid network, using a diesel generator with RESs and a BESS, are modeled in the MATLAB/Simulink environment in this work. The reliability of the energy system is investigated in the micro-grid network using the proposed technique. The performance of four case studies are investigated: the diesel generator and BESS; the diesel generator, solar PV and BESS; the diesel generator, wind plant and BESS; and the diesel generator, solar PV, wind plant, and BESS. It can be noted that the RES-generated energy during the normal operation of the micro-grid does not meet demand; hence, the inclusion of a diesel generator in all cases. This serves as back-up to the BESS. The BESS stores excess energy which is used during a generation deficit. The units are connected to the DC buses using power electronic components. The diesel generator, RESs and the BESS have their respective local controllers. These controllers carry out the power conversion commands. Therefore the BESS absorbs any network unbalance, thereby improving reliability and minimizing costs [172], [173].

5.5 Power Scheduling of the Adaptive Model Predictive Controller

AMPC uses common ideas in addressing complex micro-grid problems and utilizes comprehensive structures in organized forms. This work adopts the technique of controlling the micro-grid

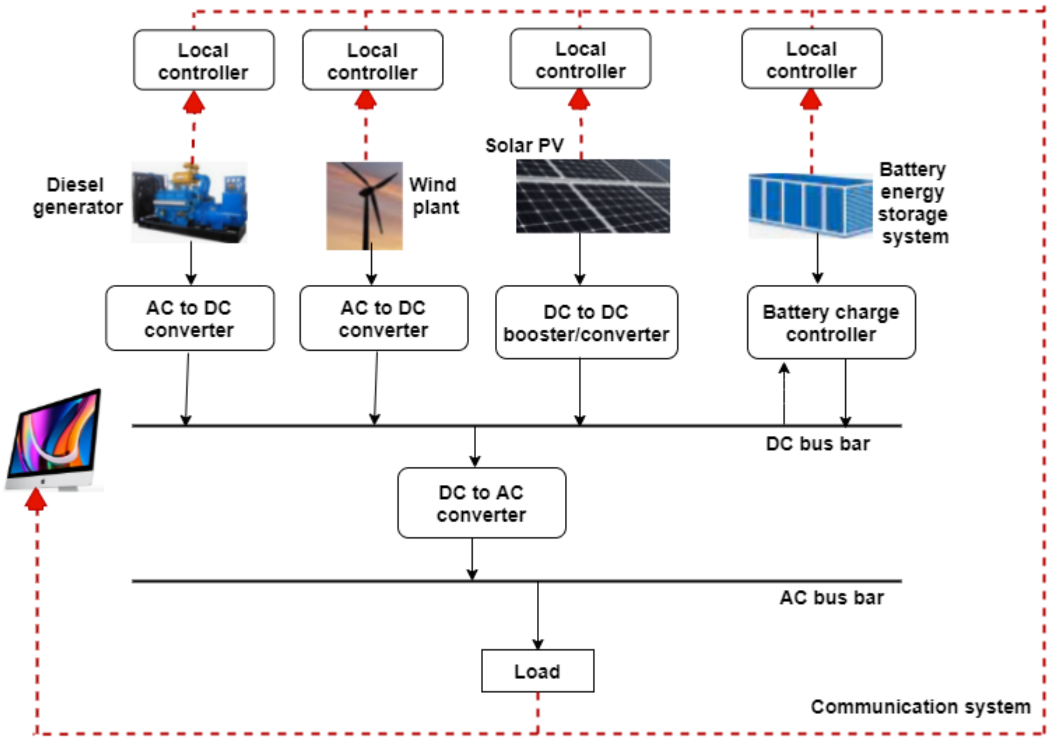

Figure 5.1 Configuration of the micro-grid network under study.

adaptively in order to guarantee an improvement in the reliability of consumer power supply. The adaptive controller harmonizes the power in the network, thereby allowing the optimal generation of power supply from each micro-grid unit. AMPC offers a solution by forming an optimal design of generation, demand, and energy storage for every optimization sample instance. The next sample instance offers a new optimization solution using the output from the previous solution as the new input. In theory, the feedback mechanism generates an optimal design that takes care of the disturbances acting on the micro-grid. The main sources of uncertainty or disturbances in the micro-grid system are the RES-generated energy (caused by wind speed and solar irradiation) and energy demanded. The conventional model predictive controller (MPC) is unable to manage the variations in RESs; hence, the AMPC is more suitable. This operates by updating the system with changes to its internal operating conditions. The AMPC architecture and algorithm flowchart are shown in Figures 5.2 and 5.3. The state-space expressions often used for AMPC modeling is given by [174]:

$$x(t+1) = Ax(t) + Bu(t) \tag{5.3}$$

$$y(t) = Cx(t) \tag{5.4}$$

where $x(t)$, $u(t)$ and $y(t)$ are the BESS charging state, generating units vector variables and the output vector of the system state, respectively.

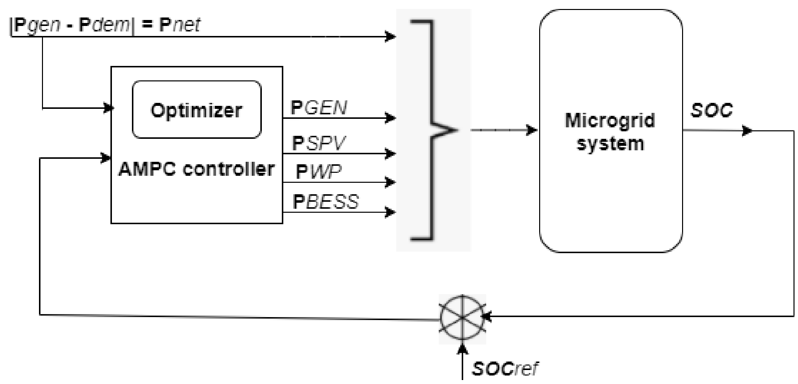

Figure 5.2 Control architecture of the study. (*Pgen*, *Pdem*, and *Pnet* are the generated, demanded, and net power, respectively).

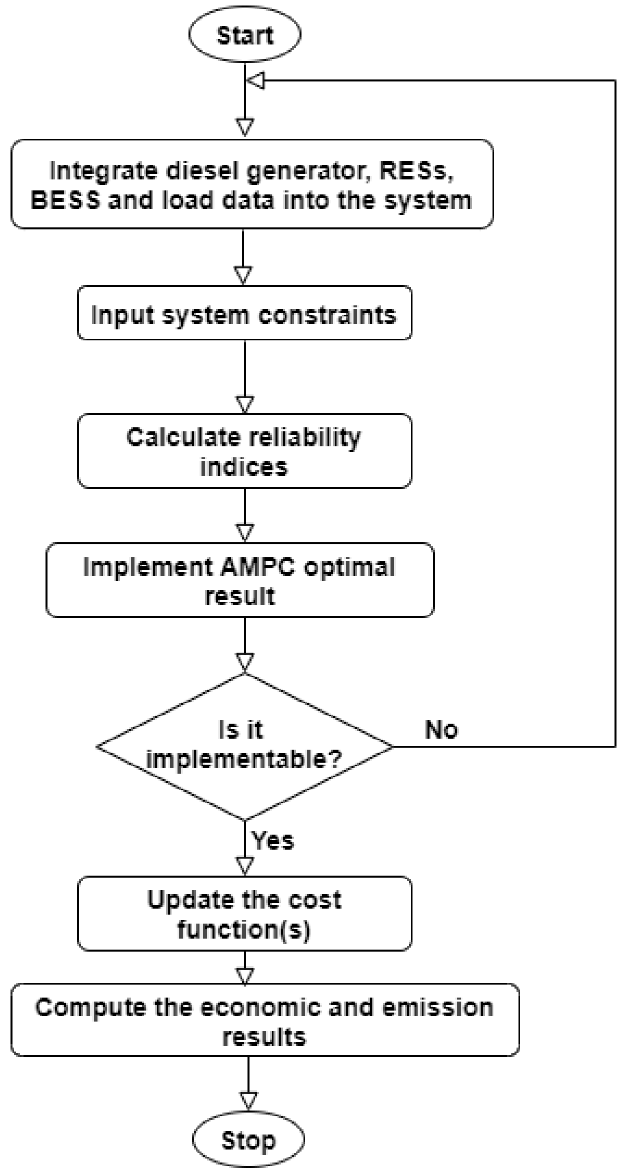

Figure 5.3 AMPC algorithm flowchart.

The generated and demanded powers that are causes of disturbance in micro-grids during normal operations are difficult to predict, vary with time, and cannot be manipulated by the controller because they are external inputs into the system. Hence, the disturbance is a problem that the controller has to overcome. The effects of disturbances on the output can be incorporated into the dynamic model to allow the controller to predict their impact on the performance of the system. The effect of the disturbance, $d(t)$, can be factored into the AMPC state-space design. The dynamic system equation can be expressed as [172]:

$$x(t+1) = Ax(t) + Bu(t) + E_d d(t) \tag{5.5}$$

$$y(t) = Cx(t) \tag{5.6}$$

where E_d is the matrix that computes the impact of disturbances on the states. By discretizing (5.5) and (5.6) with a sample time T_s, the discrete-time space model is:

$$x(t+1) = A_d x(t) + Bu(t) + E_d d(t) \tag{5.7}$$

$$y(t) = Cx(t) \tag{5.8}$$

where the discrete-time expressions are $x(t+1)$, $x(t)$, $d(t)$, $u(t)$, and $y(t)$. Also, A_d, B_d and E_d are e^{AT_s}, $\int_0^{T_s} e^{AT_s} Bdt$ and $\int_0^{T_s} e^{AT_s} Edt$ respectively. Since (5.7) and (5.8) increment, they become:

$$\triangle x(t+1) = A_d \triangle x(t) + B\triangle u(t) + E_d \triangle d(t) \tag{5.9}$$

$$\triangle y(t) = C\triangle x(t) \tag{5.10}$$

where the incremental expressions are $\triangle x(t+1)$, $\triangle x(t)$, $\triangle d(t)$, $\triangle u(t)$, and $\triangle y(t)$. Since existing plant data is required when moving horizon control for control and prediction purposes, $u(t)$ is assumed to be implicitly unable to affect output y(t); but at the t^{th} instant, $u(t-1)$ can affect the output $y(t)$. So (5.9) and (5.10) can be re-arranged to [175]:

$$\begin{bmatrix} \triangle x(t+1) \\ y(t+1) \end{bmatrix} = A \begin{bmatrix} \triangle x(t) \\ y(t) \end{bmatrix} + Bu(t) + Ed(t) \tag{5.11}$$

$$y(t) = C \begin{bmatrix} \triangle x(t) \\ y(t) \end{bmatrix} \tag{5.12}$$

where $A = \begin{bmatrix} A_d & 0_d^T \\ C_d A_d & 1 \end{bmatrix}$; $B = \begin{bmatrix} B_d \\ C_d B_d \end{bmatrix}$; $E = \begin{bmatrix} E_d \\ C_d E_d \end{bmatrix}$; $C = \begin{bmatrix} 0_d^T & 1 \end{bmatrix}$; $0_d = \begin{bmatrix} 0 & 0 & 0 & 0 \end{bmatrix}$

and the augmented state space model matrices A, B and C are used for the predictive control design.

5.6 Modeling of the Renewable Energy Sources, Diesel Generator, and Load

The RESs, the BESS, the diesel generator, and the load used in this study are modeled in this section.

5.6.1 Modelling of the Solar Photovoltaic

Solar PV has good qualities such as no fuel cost, no carbon emission cost, and low O & M cost. The energy generated by solar PV depends on the ambient temperature, solar irradiance, and the sun's position in the sky. The power outputs of the MonoXTH PV module can be expressed using [176]:

$$P_{SPV}(s(t)) = n_{cells} \times FF \times V \times I \tag{5.13}$$

where $s(t)$ is the random irradiance, n_{cells} is the number of functioning photovoltaic cells, and FF is the fill factor:

$$FF = \frac{V_{mp} \times I_{mp}}{V_{oc} \times I_{sc}} \tag{5.14}$$

where V_{mp}, V_{oc}, I_{mp}, and I_{sc} are the voltage at maximum power [V], open-circuit voltage [V], current at maximum power [A], and short circuit current [A], respectively.

$$V = (V_{oc} + K_{vt} \times T_{cell}) \tag{5.15}$$

where V_{oc}, K_{vt}, and T_{cell} are the open-circuit voltage [V], the voltage temperature coefficient [mV/°C], and the cell temperature [°C], respectively.

$$I = s(t) \times [I_{sc} + K_{ct} \times (T_{cell} - 25)] \tag{5.16}$$

where K_{ct} is the current temperature coefficient [mA/°C].

$$T_{cell} = T_{amp} + s(t) \times \left(\frac{NOCT - 20}{0.8} \right) \tag{5.17}$$

where T_{cell}, T_{amp}, and $NOCT$ are the cell temperature [°C], ambient temperature [°C], and nominal cell operating temperature [°C], respectively.

5.6.2 Modelling of the Wind Energy

Wind energy, which is a clean and environmentally friendly RES, has many advantages such as relatively low cost of production, low cost of O & M, free from Greenhouse gas (GHG) emission, sustainable energy source, no fossil fuel costs, and advanced technologies [177, 142]. The power generated by a wind plant can be represented by [178], [176]:

$$P_{WP}(v_i) = \begin{cases} 0 & v_i < v_{ci} \\ P_r^W \times \dfrac{v_i - v_{ci}}{v_r - v_{ci}} & v_{ci} \leq v_i < v_r \\ P_r^W & v_r \leq v_i < v_{co} \\ 0 & v_{co} \leq v_i \end{cases} \tag{5.18}$$

where P_r^W is the rated power output; and v_i, v_{ci}, v_{co} and v_r stand for the actual, cut-in, cut-out, and the rated wind speeds respectively.

5.6.3 Network modelling

The network was modelled out of the set of available routes for optimal configuration. The network was modelled as defined by the matrix [NC] as [179]:

$$[NC] = \sum_{k=1}^{m-1} [AD]^k \tag{5.19}$$

where $[AD]^k$ represents the network's m by m adjacency matrix, at network nodes in iteration k, with elements $[AD]_{i,j}$ which equals 0 if no branch is connecting nodes i and j and equal to 1 if otherwise. If all [NC]'s off-diagonal elements are non-zero, then the network is connected.

5.6.4 Uncertainty modeling

The design is done with consideration on forecasts based on a degree of uncertainty. Factors considered as inputs in uncertainty modeling are distributed generators parameters, failure rates of lines, and peak loads of the customers. The loads uncertainty is modelled as [179]:

$$[S_U] = f_1 . S_L \tag{5.20}$$

where $[S_L]$ is the vector of the network's peak loads, f_1 is the assumed scaling random function with standard deviation $_1$ and mean 1. The uncertainties arising because of failure rates of lines are obtained as the product of the failure rate per unit of line length, adopted standard deviation $_2$ and random function f_2 with mean 1. The mean operating power expected from the generators (i.e., the GEN, SPV, WP, and BESS) is scaled by adopted standard deviation $_3$ and random function f_3 with mean 1.

5.6.5 Modelling of the Battery Energy Storage System

RESs are characterized by an intermittent generation. This problem is solved using a BESS. Excess energy is stored in the BESS, which is used when the RESs experience intermittency, thereby avoiding power fluctuation and enhancing the reliability of the system [144]. The durability and performance of the battery depend on its rate of charge, rate of discharge, state of charge, voltage effect, and ambient temperature. The state of charge (SoC) of the battery, whose operation capacity must be between the minimum and maximum allowable, is [171]:

$$SoC^{min} \leq SoC(t) + \eta_c \sum_{t=1}^{k} P_i(t) \tag{5.21}$$

$$-\eta_d \textstyle\sum_{t=1}^{k} P_i(t) \leq SoC^{max}, for 1 \leq t \leq k$$

and

$$SoC^{min} = (1 - DoD) SoC^{max} \tag{5.22}$$

where SoC^{min} and SoC^{max} are the minimum and maximum allowable states of charge, η_c and η_d are the battery charging and discharging efficiencies, and DoD is the depth of discharge.

5.6.6 Modelling of the Diesel Generator

The operation of a diesel generator can be as the prime source, as standby, as a stand-alone system, or connected to the grid. They can be reliable, mobile, fuel-flexible, easy, and quick to start but have high O & M costs and GHG emissions. The operating parameters of the CAT 3512B diesel generator, such as power output, fuel consumption, and fuel cost, are used in modeling the generator in this study. The power output of the diesel generator P_{GEN} can be represented by [171]:

$$P_{GEN} = P_n \times N_{GEN} \times \eta_{GEN} \tag{5.23}$$

where P_n, η_{GEN} and N_{GEN} are the nominal power generated, efficiency, and number of the diesel generators, respectively.

A diesel generator operates within power constraints which are:

$$P_{GEN}^{min}(i,t) \leq P_{GEN}(i,t) \leq P_{GEN}^{max}(i,t) \tag{5.24}$$

The generator fuel cost FC is

$$FC_i = a_i P_{GEN}^2(i,t) + b_i P_{GEN}(i,t) + c_i \tag{5.25}$$

where a, b and c are the respective coefficients of the fuel cost for the i^{th} diesel generator.

A conventional power generator produces emissions. Emission Cost (EC) is introduced as a penalty for GHG emissions. The EC is an economic benchmark used by the environmental regulators to control the emission of GHG pollutants. It is applied as taxes to discourage the generation of GHGs. The GHG Emission factor and costs for diesel generation is shown in Table 5.2.

5.6.7 Comparison of Microgrid Component Costs and Characteristics

The Cost and technical characteristics of micro-grid system components are shown in Table 5.3. This is important for the design of a system so that they can be built within budget constraints.

Table 5.2 GHG Emission factor and costs for diesel generation [171].

Emission types	Emission cost ($/kg)	Emission factor (kg/kWh)
NOx	1.086	0.00669
SOx	1.800	0.00036
COx	0.017	0.65700

5.6.8 Modelling of the Load

Some loads are critical while others are curtailable. Critical loads are classified as essential and have to be met. The AMPC controller makes necessary load forecasting decisions. The load is predicted at time-steps using the preceding data for future projections. The process continuously estimates and updates the model parameters to minimize errors. The load demand for the micro-grid is [174]:

$$P_{load}(i,t) = P_{load-curt}(i,t)(1-\theta(i,t)) + P_{load-crit}(i,t) \tag{5.26}$$

where $\theta(i,t)$ is the curtailment ratio of the curtailable load; the $P_{load-curt}(i,t)$ and $P_{load-crit}(i,t)$ are the curtailable and the critical loads, respectively.

5.7 Economic Modeling of the Renewable Energy sources

The economic model of the micro-grid under study is made up of the cost of energy C_{coe}, the annual cost of the system C_{acs}, the net present cost C_{npc}, and the total outage cost C_{toc} [180, 171]. The cost of energy is:

$$C_{coe} = \frac{C_{acs}}{P_i} \text{ \$/yr} \tag{5.27}$$

Table 5.3 Cost and technical characteristics of the micro-grid system [171].

Parameter	Value/Description	Parameter	Value/Description
Estimated parameters of the diesel generator			
Installed capacity	4MW	Lifetime	25000 h
Nominal rating	1280 kW	Model	CAT 3512B
Capital cost	1521 \$/kW	Coefficients of the fuel cost	a = 2.4438, b = 208.21, c = 35.968
Replacement cost	1521 \$/kW	Efficiency	80%
Maintenance cost	0.01258 \$/kW h	Diesel fuel price	0.91 \$/L
Estimated parameters of the solar PV			
Installed capacity	2MW	Voltage temperature coefficient	0.325 %/°C
Nominal rating	250 W	Current temperature coefficient	0.050%/°C
Capital cost	550 \$/kW	Short circuit current	8.62 A
Replacement cost	550 \$/kW	Open circuit voltage	38.3 V
Maintenance cost	10 \$/kW/year	Dimension	mm^3
Lifetime	25 yr	Weight	16.8 ± 0.5 kg
Model number	LG250SIK-G3	Cells	6× 10
Maximum power point voltage	30.8 V	Cells type	Monocrystalline
Maximum power point current	8.13 A	Frame	Anodized aluminum
Nominal cell operating temperature (NCOT)	45 ± 2°C		
Estimated parameters of the wind plant			
Installed capacity	2MW	Swept area	5027 m^2
Nominal rating	2MW	Rotor diameter	80 m
Capital cost	651 \$/kW	Nominal revolutions	16.7 rpm
Replacement cost	651 \$/kW	Frequency	50/60 Hz
Maintenance cost	20 \$/kW/year	Generator type	4 pole doubly-fed generator
Lifetime	25 yr	slip ring and Blade dimension:	Length = 39 m, Max. chord = 3.5 m
Model number	V80-2.0MW	Wind speed	v_{ci} = 4 m/s, v_r = 16 m/s and $v_c o$ = 25 m/s
Estimated parameters of the battery energy storage system			
Installed capacity	0.3MW	Lifetime	5 yr
Nominal rating	200 Ah	Battery max SoC	95%
Capital cost	300 \$/battery	Battery min SoC	40%
Replacement cost	300 \$/battery	Battery discharge efficiency	100%
Maintenance cost	10 \$/battery/year	Battery charge efficiency	85%

where C_{acs} is the annual cost of the system in (\$/kWh) and P_i is the annual energy production of the generating units in (kWh).

The annual cost can be represented by

$$C_{coe} = (C_{amc} + C_{aec} + C_{acc} + C_{arc} + C_{afc}) \text{ \$/yr} \tag{5.28}$$

where C_{acc} is the annual capital cost, C_{arc} is the annual replacement cost, C_{amc} is the annual maintenance cost, C_{afc} is the annual fuel cost and C_{aec} is the annual emission cost. The annual capital cost for a micro-grid system consisting of the diesel generator, solar PV, wind plant, and BESS is a simple summation:

$$\begin{aligned} C_{acc} = C_{acc,i} \sum_{i=1}^{n} (P_{GEN} + P_{SPV} \\ + P_{WP} + P_{BESS}) \text{ \$/yr} \end{aligned} \tag{5.29}$$

where $C_{acc,i}$ is the annual capital cost of each component of the micro-grid system. These can be obtained from:

$$C_{acc,i} = CC + CRF(i,n) \tag{5.30}$$

$$C_{arc,i} = RC + SFF(i,n) \tag{5.31}$$

$$C_{amc,i} = MC + (1+f)^n \tag{5.32}$$

$$C_{afc,i} = FC + (1+f)^n \tag{5.33}$$

$$C_{aec,i} = EC + (1+f)^n \tag{5.34}$$

where CC, RC, MC, FC and EC are the capital, replacement, maintenance, fuel and emission costs respectively. The SFF, f and n are the sinking fund factor, annual inflation rate and lifetime of each micro-grid system component.

The sinking fund factor is:

$$SFF(i,n) = \left(\frac{i}{(1+i)^n - 1} \right) \tag{5.35}$$

The maintenance cost for generating unit i is:

$$MC_i = \sum_{i=1}^{n} (C_i P_i + CR_i \times FCR_i) \text{ \$/hr} \tag{5.36}$$

where C_i, CR_i, FCR_i and P_i are the proportionality factor, the capacity rating, the fixed charge rate, and the generating unit output power, respectively.

The fuel cost is:

$$FC_i = \sum_{i=1}^{n} (a_i + b_i P_i + c_i P_i^2) \text{ \$/hr} \tag{5.37}$$

where a, b and c are the diesel generator cost coefficients.

The emission cost is:

$$\begin{aligned} EC_i = \sum_{i=1}^{n} (&\alpha_i P_i EF_{COx} + \alpha_j P_i EF_{SOx} \\ &+ \alpha_k P_i EF_{NOx}) \text{ \$/hr} \end{aligned} \tag{5.38}$$

where $\alpha_i P_i$, $\alpha_i P_j$, $\alpha_i P_k$ and EF_{COx}, EF_{SOx}, EF_{NOx} are the externality emission costs (in \$/kg) and the emission factors for COx, SOx, and NOx gases respectively.

The net present cost C_{npc} can be expressed as:

$$C_{npc} = \left(\frac{C_{acs}}{CRF(i,n)} \right) \text{ \$/yr} \tag{5.39}$$

$$i = \left(\frac{i' - f}{1 + f} \right) \tag{5.40}$$

$$CRF(i,n) = \left(\frac{i(1+i)^n}{(1+i)^n - 1} \right) \tag{5.41}$$

where i, i', f, n and CRF represent the real interest rate, the nominal interest rate, the annual inflation rate, the number of years (i.e., the lifetime of each micro-grid system component) and the capital recovery factor respectively.

The expected energy not served cost (C_{eens}) and expected interruption cost ($ECOST$) are used to obtain the total outage cost:

$$C_{toc} = (C_{eens} + ECOST) \text{ \$/yr} \tag{5.42}$$

$$C_{eens} = (k_e \times EENS) \text{ \$/yr} \tag{5.43}$$

where $EENS$ is the total annual energy not served (kWh) and the lost load value (k_e) is in (\$/kWh).

5.8 Modeling of the Adaptive MPC Optimization Problem

The focus of the proposed method is the economic feasibility of integrating RESs into the power system while taking into consideration the relevant operational constraints. In this section, the cost function formulation is discussed, i.e., the operational and functional constraints.

5.8.1 Formulation of the Cost Function

The proposed method is designed to achieve the objectives of improving the reliability of electricity supply, reducing the operating cost of energy, preventing the battery from deep overcharge and discharge, and guaranteeing energy efficiency by balancing supplies from the diesel generator, RESs, and the BESS. Variables such as the power rates and values, which relate to lifespan and utility cost of the generating units, are incorporated into the cost function. Quadratic cost functions related to different generating units in the micro-grid are harnessed to minimize the total cost of the system and solved by the AMPC algorithm. The cost function can be expressed as [181]:

$$
\begin{aligned}
\min J = \sum_{k=1}^{N_c} \Big[& \alpha_1 P^2_{GEN(t+k)} + \alpha_2 P^2_{SPV(t+k)} \\
& + \alpha_3 P^2_{WP(t+k)} + \alpha_4 P^2_{BESS(t+k)} \\
& + \beta_1 \triangle P^2_{GEN(t+k)} + \beta_2 \triangle P^2_{SPV(t+k)} \\
& + \beta_3 \triangle P^2_{WP(t+k)} + \beta_4 \triangle P^2_{BESS(t+k)} \Big] \\
& + \sum_{k=1}^{N_p} \Big[\gamma_1 (SoC_{t+k} - SoC_{ref})^2 \Big]
\end{aligned}
\tag{5.44}
$$

where N_c is the control horizon, N_p is the prediction horizon, and α_i, β_i and γ_i are the respective weights of the variables. In the first four terms of the cost function, the weight of the manipulated variables is used; hence, the optimal solution will apply weighted means in satisfying the objectives. The subsequent four and one terms penalize the rate and confine the stored energy within an operating point respectively.

5.8.2 Power Balance Constraints

It is necessary to include the energy balance constraints to achieve stability of the power system. The energy demand and production balance for a reliable and effective operation of the micro-grid network need to be met. The equality constraint is:

$$
\begin{aligned}
& \sum_{i=1}^{n} P_{GEN}(i,t) + \sum_{g=1}^{n} P_{WP}(g,t) \\
& + \sum_{h=1}^{n} P_{SPV}(h,t) + \sum_{j=1}^{n} P_{BESS}(j,t) \\
& - \sum_{k=1}^{n} P_{BESS}(k,t) = \sum_{l=1}^{n} P_D(l,t)
\end{aligned}
\tag{5.45}
$$

where $P_{GEN}(i,t)$, $P_{WP}(g,t)$ and $P_{SPV}(h,t)$ are the power output of the diesel generator, wind plant, and solar PV. $P_{BESS}(j,t)$ and $P_{BESS}(k,t)$ are the charge and discharge power of the battery while

$P_D(l,t)$ is the consumer load point power demand. n denotes the number of occurrences in time t in the respective instances.

5.8.3 Inequality Constraints

The inequality constraints are the generating limits of each source as specified by the OEM. To prevent overcharging and undercharging, the SoC of the battery bank is operated within the minimum and maximum limits. This will improve the lifespan of the battery. The constraints are:

$$\begin{cases} P_{GEN}^{min}(i,t) \le P_{GEN}(i,t) \le P_{GEN}^{max}(i,t) \\ P_{WP}^{min}(g,t) \le P_{WP}(g,t) \le P_{WP}^{max}(g,t) \\ P_{SPV}^{min}(h,t) \le P_{SPV}(h,t) \le P_{SPV}^{max}(h,t) \\ P_{BESS}^{min}(j,t) \le P_{BESS}(j,t) \le P_{BESS}^{max}(j,t) \\ P_{BESS}^{min}(k,t) \le P_{BESS}(k,t) \le P_{BESS}^{max}(k,t) \\ SoC^{min}(m,t) \le SoC(m,t) \le SoC^{max}(m,t) \end{cases} \tag{5.46}$$

Variation in power can lead to energy losses. Therefore power rates constraints are formulated. The micro-grid units and BESS are assumed to be electrically strong in responding to fast power rates so that:

$$\begin{cases} \triangle P_{GEN}^{min}(i,t) \le \triangle P_{GEN}(i,t) \le \triangle P_{GEN}^{max}(i,t) \\ \triangle P_{WP}^{min}(g,t) \le \triangle P_{WP}(g,t) \le \triangle P_{WP}^{max}(g,t) \\ \triangle P_{SPV}^{min}(h,t) \le \triangle P_{SPV}(h,t) \le \triangle P_{SPV}^{max}(h,t) \\ \triangle P_{BESS}^{min}(j,t) \le \triangle P_{BESS}(j,t) \le \triangle P_{BESS}^{max}(j,t) \\ \triangle P_{BESS}^{min}(k,t) \le \triangle P_{BESS}(k,t) \le \triangle P_{BESS}^{max}(k,t) \\ \triangle SoC^{min}(m,t) \le \triangle SoC(m,t) \le \triangle SoC^{max}(m,t) \end{cases} \tag{5.47}$$

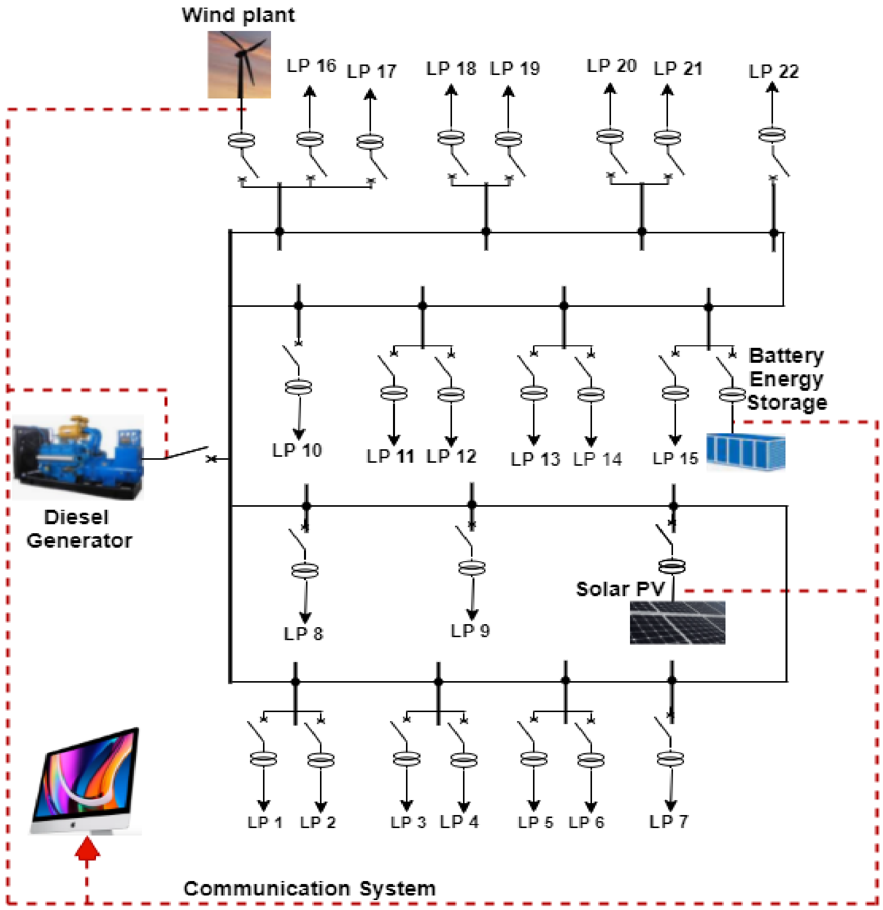

Figure 5.4 Modified Distribution System for RBTS Bus.

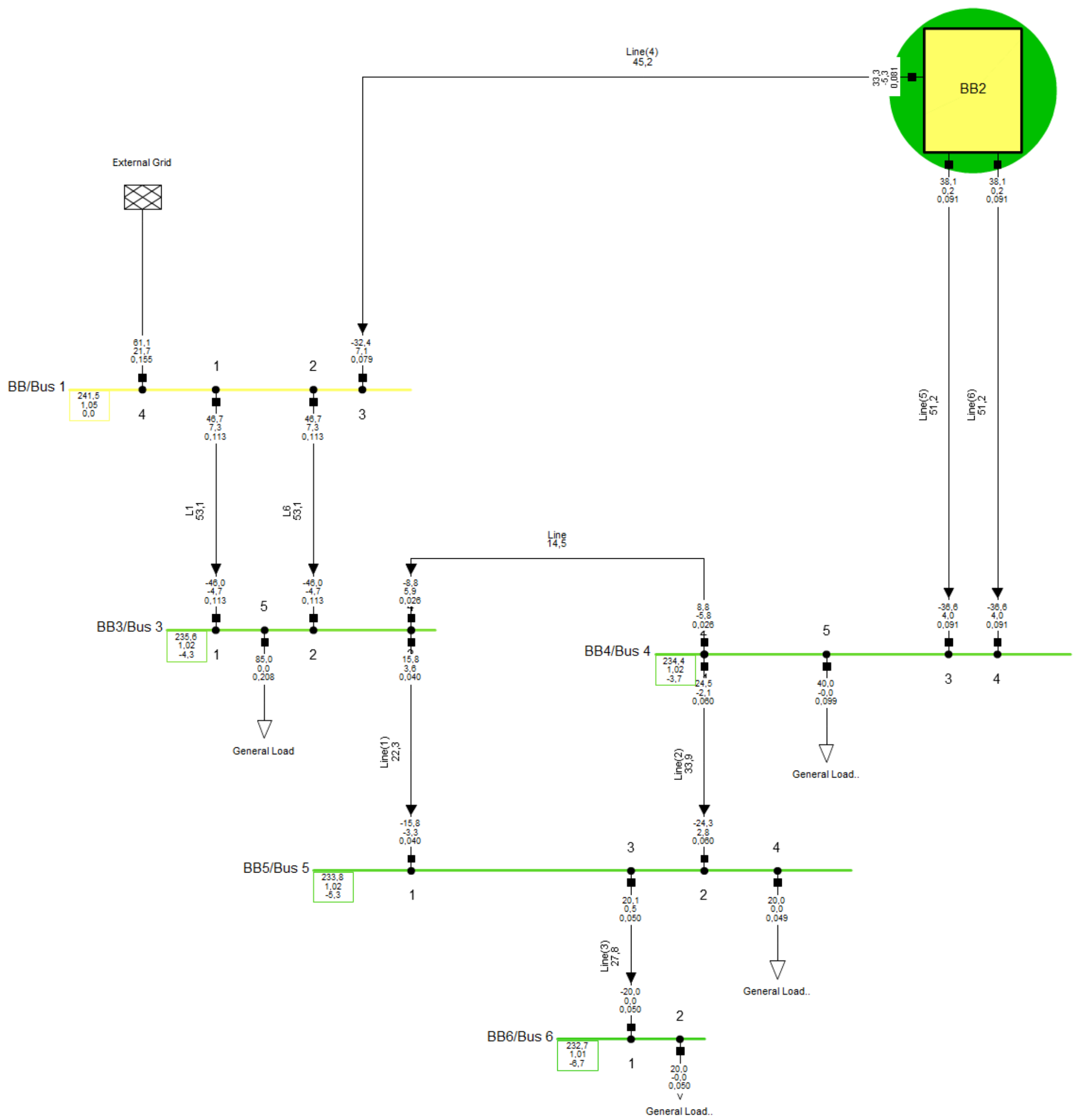

Figure 5.5 Power flow diagram of the transmission system connecting the modified RBTS system.

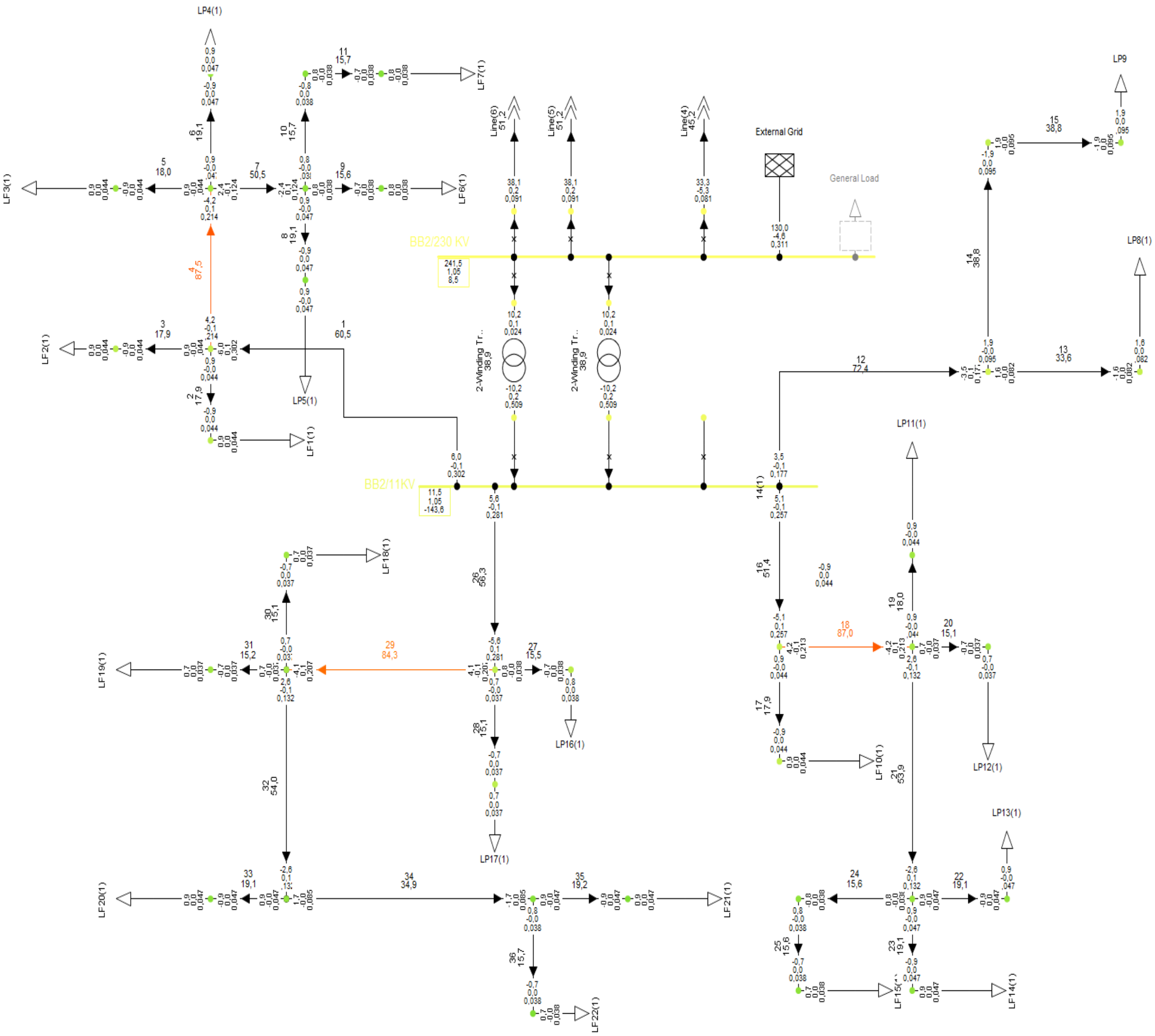

Figure 5.6 Power flow diagram of the RBTS distribution system.

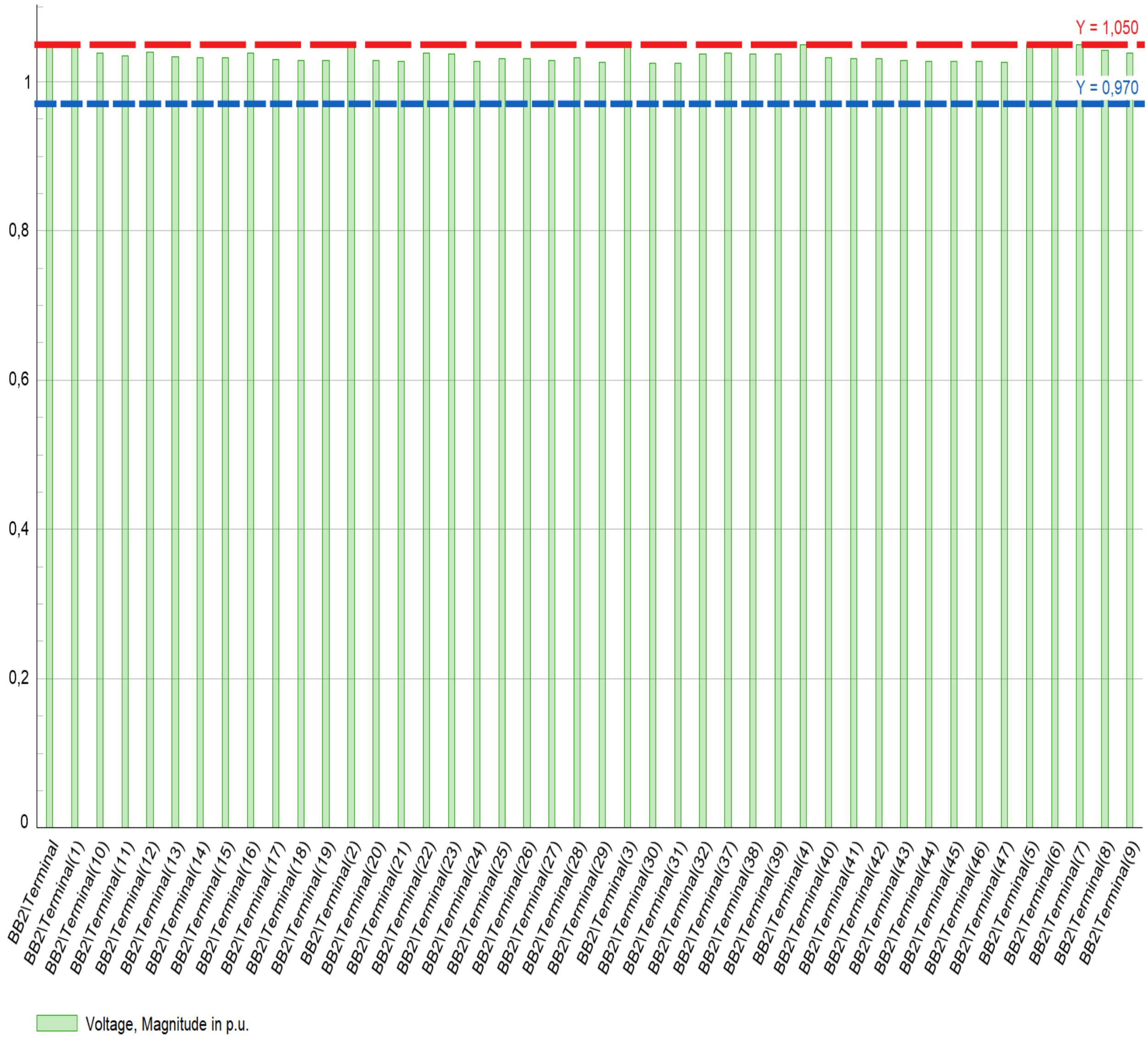

Figure 5.7 Voltage at different terminals in the RBTS distribution system.

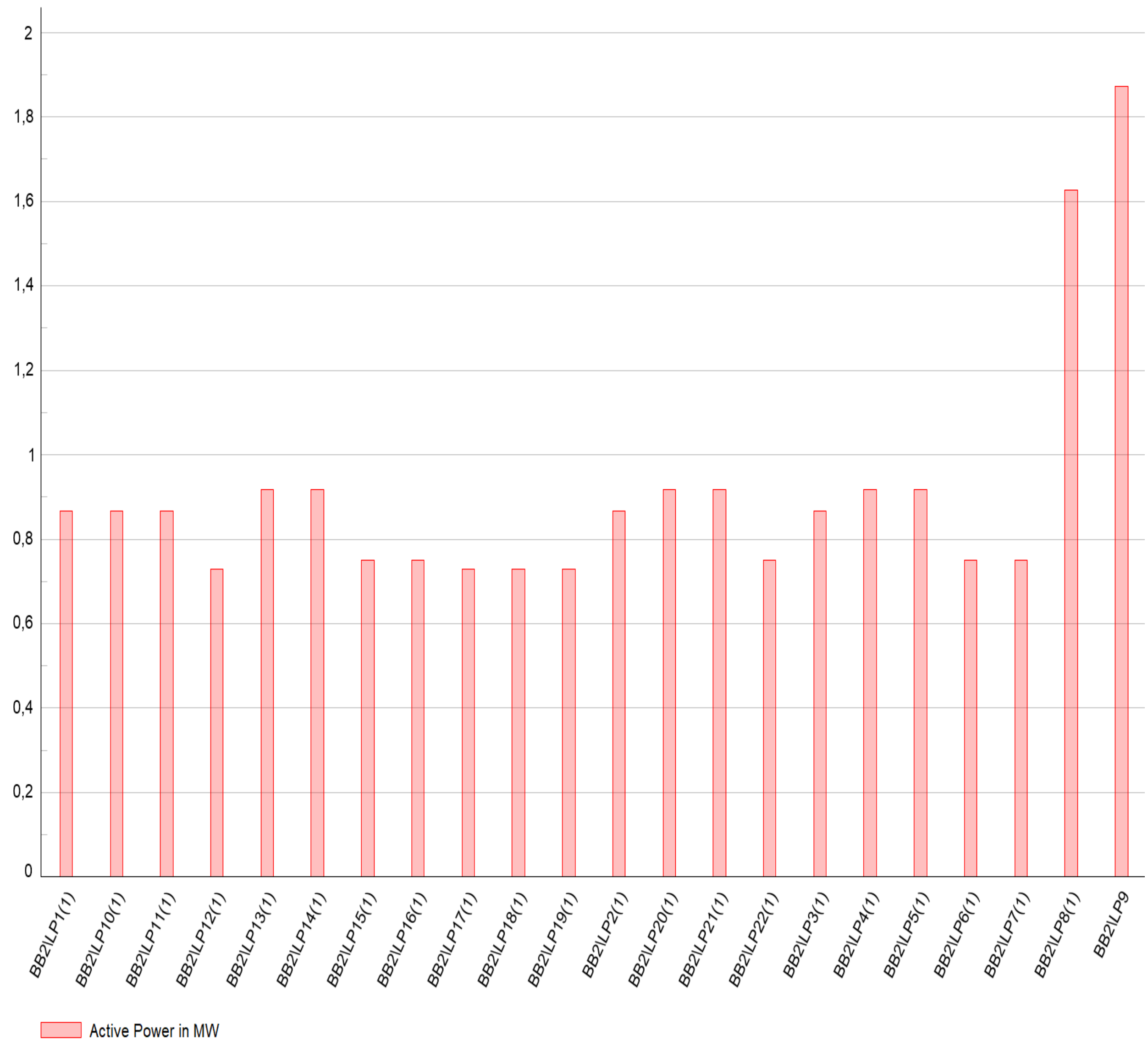

Figure 5.8 Active power at different terminals in the RBTS distribution system.

5.9 Results and discussions

The reliability and economic impacts of integrating RESs into the power system are explored using a modified Roy Billinton system (Figure 5.4).

The power flow of the proposed distribution network was performed using DigSILENT PowerFactory software. Figure 5.5 to 5.8 show the results of the power flow operation.

The system is made up of 26 circuit breakers; 1 transformer each for the solar PV, the wind plant and BESS, and 22 distribution transformers. The repair rates, failure rates, customer and feeder details of the major system components are found in [182]. The system is modeled with a 4 MW diesel generator, 2 MW solar PV, 2 MW wind plant, and 0.3 MW BESS installed capacities. The network performance is measured by utilities using the reliability indices. The integration of RESs using AMPC is necessitated for reliability improvement and cost reduction. Case studies were used to assess the effects of the proposed method. RESs 1, 2, and 3 are solar PV, BESS and wind plant. The case studies are:

i. Power system containing the diesel generator and RES 2.

ii. Power system containing the diesel generator, RESs 1 and 2.

iii. Power system containing the diesel generator, RESs 2 and 3.

iv. Power system containing the diesel generator, RESs 1, 2, and 3.

Table 5.4 shows the impacts on the reliability of the system. Table 5.5 shows the results for the system costs for different case studies. The annual maintenance cost C_{amc}, annual fuel cost C_{afc}, annual emission cost C_{aec}, annual replacement cost C_{arc}, annual capital cost C_{acc}, annual cost of system C_{acs}, net present cost C_{npc}, and cost of energy, C_{coe} were considered for the different case studies. Table 5.6 shows the impacts of incorporating solar PV, wind plant, and BESS on the annual emissions and fuel consumption.

Figures 5.9 to 5.18 show the results of EENS (MWh/yr.), $ECOST$, C_{eens} or K_eEENS, C_{toc},

Table 5.4 Cost impacts on reliability using renewable energy sources integration.

Description	**Case 1**	**Case 2**	**Case 3**	**Case 4**
$EENS$ (MW h/yr)	6 874.4	6 451.4	6 515.2	6 367.5
$ECOST$ (million \$/yr)	8.806	8.269	8.102	8.002
C_{eens} or $K_e EENS$ (million \$/yr)	37.809	35.483	35.834	35.021
C_{toc} (million \$/yr)	37.818	35.491	35.842	35.029
Improvement on $EENS$ (MW h/yr)	-	423.0	359.1	507.0
% improvement on $EENS$	-	6.15	5.22	7.37
Improvement on ECOST (\$/yr)	-	536.9	704.3	804.5
% improvement on $ECOST$	-	6.10	8.00	9.14
Improvement on C_{eens} (million \$/yr)	-	2.326	1.975	2.788
% improvement on C_{eens}	-	6.15	5.22	7.37
Improvement on C_{toc} (million \$/yr)	-	2.327	1.976	2.789
% improvement on C_{toc}	-	3.00	5.23	7.37

Table 5.5 Cost saving impacts of renewable energy sources integration.

Description	Case 1	Case 2	Case 3	Case 4
C_{amc} (million \$/yr)	0.834	0.751	0.687	0.687
C_{afc} (million \$/yr)	6.706	4.895	4.870	4.840
C_{aec} (million \$/yr)	0.510	0.371	0.370	0.368
C_{arc} (million \$/yr)	1.854	1.872	1.872	1.877
C_{acc} (million \$/yr)	2.798	3.005	3.033	3.208
C_{acs} (million \$/yr)	12.694	10.879	10.798	10.979
C_{npc} (million \$/yr)	27.606	23.660	23.483	23.451
C_{coe} ((\$/kW h)	0.075	0.065	0.064	0.064
Improvement in C_{amc} (million \$/yr)	-	0.083	0.147	0.147
% Improvement in C_{amc}	-	9.936	17.591	17.601
Improvement in C_{afc} (million \$/yr)	-	1.811	1.836	1.866
% Improvement in C_{afc}	-	27.011	27.380	27.825
Improvement in C_{aec} (million \$/yr)	-	0.139	0.140	0.142
% Improvement in C_{aec}	-	27.273	27.507	27.909
Increase in C_{arc} (million \$/yr)	-	0.018	0.019	0.024
% Increase in C_{arc}	-	0.971	1.020	1.273
Increase in C_{acc} (million \$/yr)	-	0.208	0.235	0.410
% Increase in C_{acc}	-	7.424	8.397	14.666
Improvement in C_{acs} (million \$/yr)	-	1.815	1.896	1.715
% Improvement in C_{acs}	-	14.298	14.936	13.510
Improvement in C_{npc} ((million \$/yr)	-	3.946	4.123	4.155
% Improvement in C_{npc}	-	14.294	14.935	15.051
Improvement in C_{coe} (\$/yr)	-	0.011	0.011	0.012
% Improvement in C_{coe}	-	14.19	15.12	15.25

Table 5.6 Impacts of incorporating RESs and BESS on the annual emissions and fuel consumption.

Description	Case 1	Case 2	Case 3	Case 4
Fuel (1000 L/yr)	44 036	26 356	20 281	19 610
COx (1000 kg/yr)	57 375	34 425	26 966	25 245
NOx (1000 kg/yr)	584.38	352.38	273.49	256.54
SOx (1000 kg/yr)	31.40	19.12	14.79	13.53

C_{amc}, C_{afc}, C_{aec}, C_{acs}, C_{arc}, C_{acc}, C_{npc}, and C_{coe}, respectively, in the four case studies. Generally, it can be observed that the results in Case 4 supersede the other case studies, thereby demonstrating the benefits of the integration of RES in reliability improvements.

For clarity, the results for cases 2-4 of Figure 5.10 are not the same. The ECOST (million \$/yr) for cases 1-4 are 8.8061, 8.2692, 8.1018 and 8.0016 respectively. The Ceens or KeEENS (million \$/yr) for cases 1-4 are 37.809, 35.483, 35.834 and 35.021 respectively. The Ctoc (million \$/yr) for cases 1-4 are 37.818, 35.491, 35.842 and 35.029 respectively.

Figure 5.9 Change in *EENS*

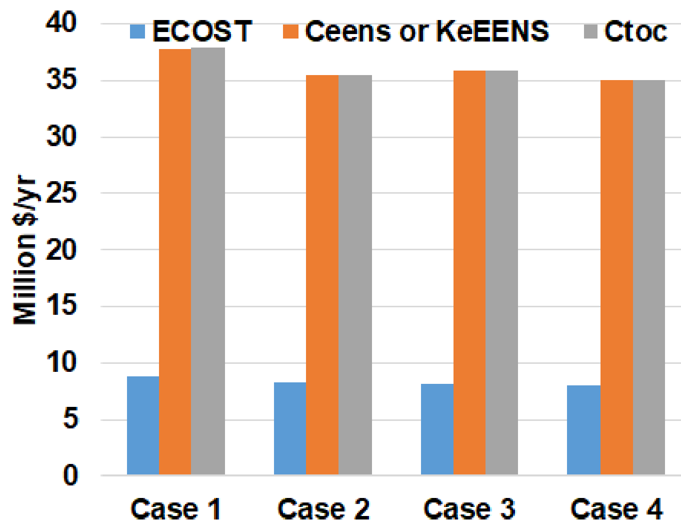

Figure 5.10 Change in $ECOST$, C_{eens} and C_{toc}

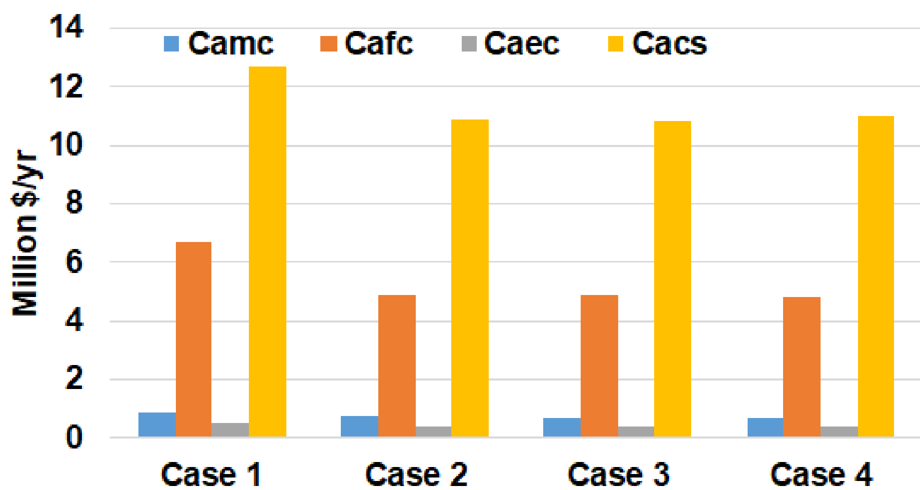

Figure 5.11 Change in C_{amc}, C_{afc}, C_{aec} and C_{acs}

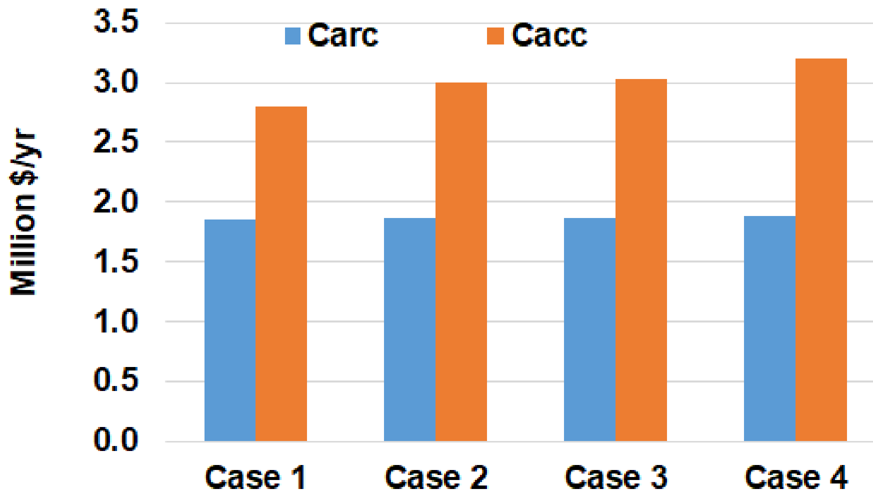

Figure 5.12 Change in C_{arc} and C_{acc}

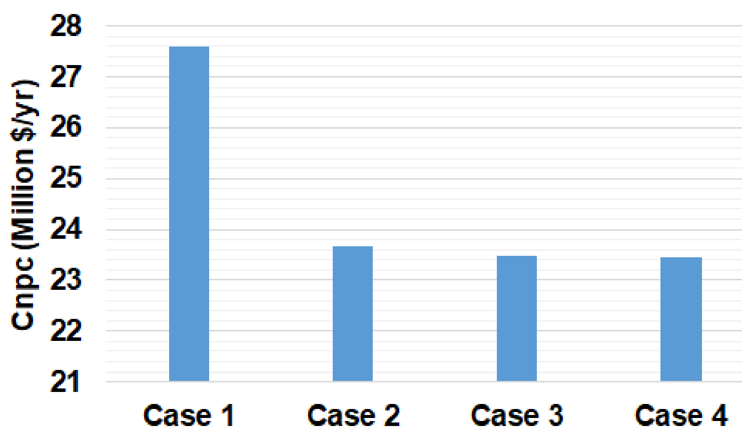

Figure 5.13 Change in C_{npc}

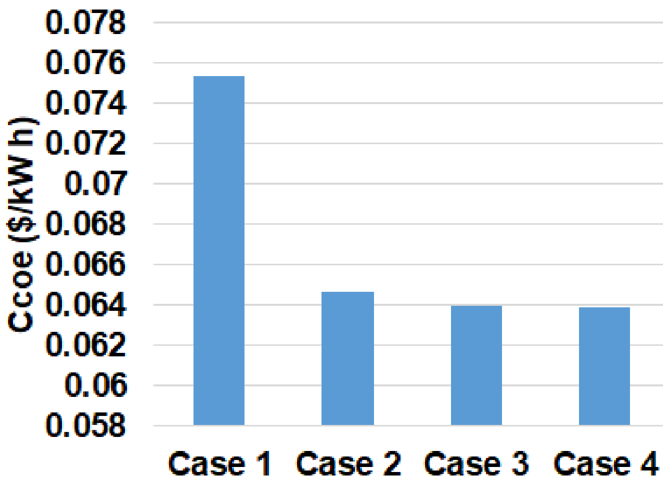

Figure 5.14 Change in C_{coe}

Figure 5.11 shows the improvements in $EENS$ (MWh/yr.), of Cases 2 to 4 from Case 1. Cases 2, 3 and 4 increased by 422.97, 359.14 and 506.89 respectively. In Figures 5.12, Cases 2, 3 and 4 of $ECOST$ ($/yr) improved by 536.9, 704.3 and 804.5 over Case 1; Cases 2, 3 and 4 of C_{eens} (million $/yr) improved by 2.326, 1.975 and 2.788 over Case 1; while for C_{toc} (million $/yr), Cases 2, 3 and 4 improved by 2.327, 1.976 and 2.789 over Case 1 respectively. Figures 5.13 shows that Cases 2, 3 and 4 of C_{amc} (thousand $/yr) improved by 82.83, 146.65 and 146.73 respectively over Case 1 (hence, the integration of RESs results in spending less on maintenance costs); Cases 2, 3 and 4 of C_{afc} (million $/yr) improved by 1.811, 1.836 and 1.866 over Case 1 (resulting in a significant drop in spending on diesel fuel); Cases 2, 3 and 4 of C_{aec} (thousand $/yr) improved by 139.03, 140.22 and 142.27 over Case 1 while Cases 2, 3 and 4 of C_{acs} (million $/yr) improved by 1.815, 1.896 and 1.715 over Case 1 respectively. Figure 5.14 shows that there is an increase in C_{arc} (thousand $/yr) in Cases 2, 3 and 4 by 18.0, 18.9 and 23.6 respectively over Case 1 and an increase in C_{acc} (thousand $/yr) in Cases 2, 3 and 4 by 207.7, 234.9 and 410.3 respectively over Case 1. These two increases are reasonable and understandable. Although there are increases in these two costs in Cases 2 to 4 as compared to Case 1, the overall cost of the system, C_{acs}, shows improvement.

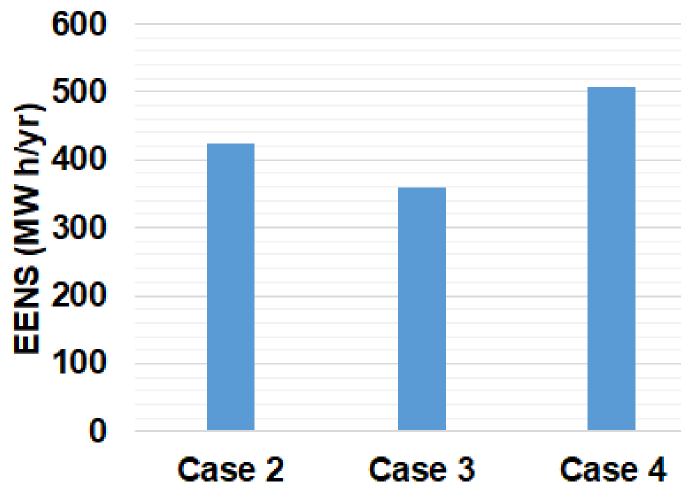

Figure 5.15 Improvements on $EENS$

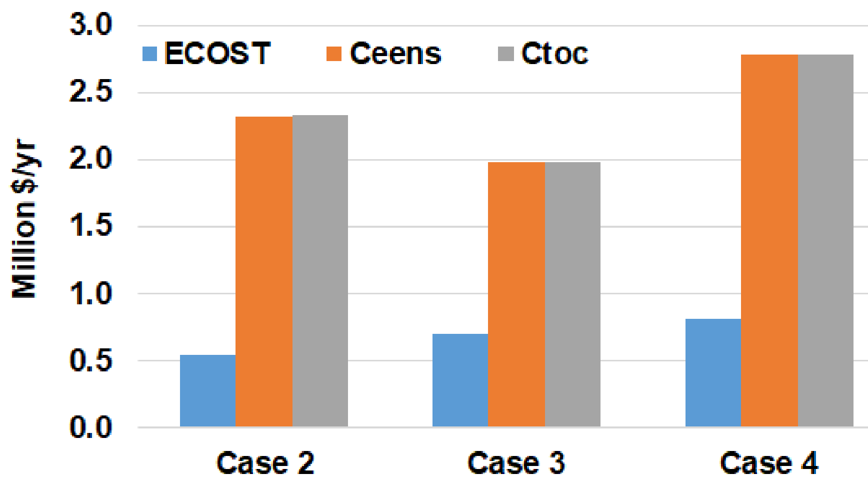

Figure 5.16 Improvements on $ECOST$, C_{eens}, and C_{toc}.

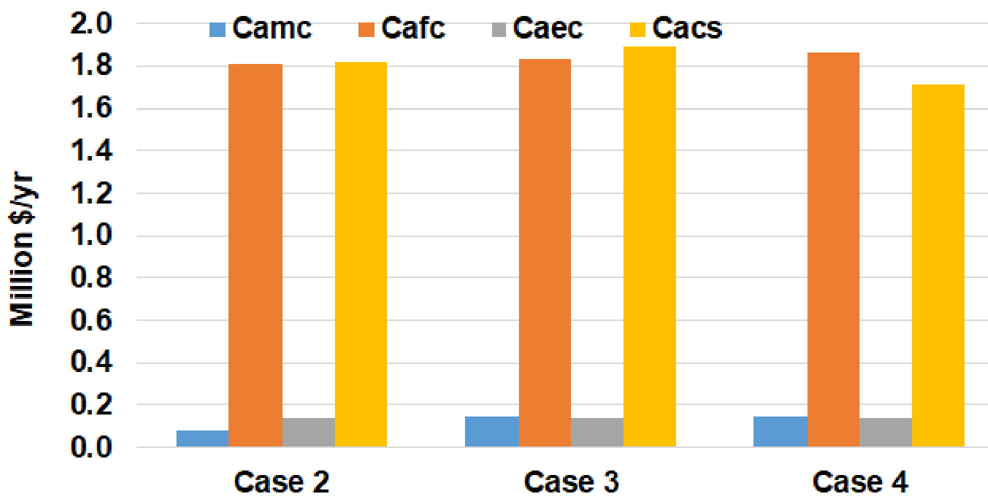

Figure 5.17 Improvements in C_{amc}, C_{afc}, C_{aec}, and C_{acs}.

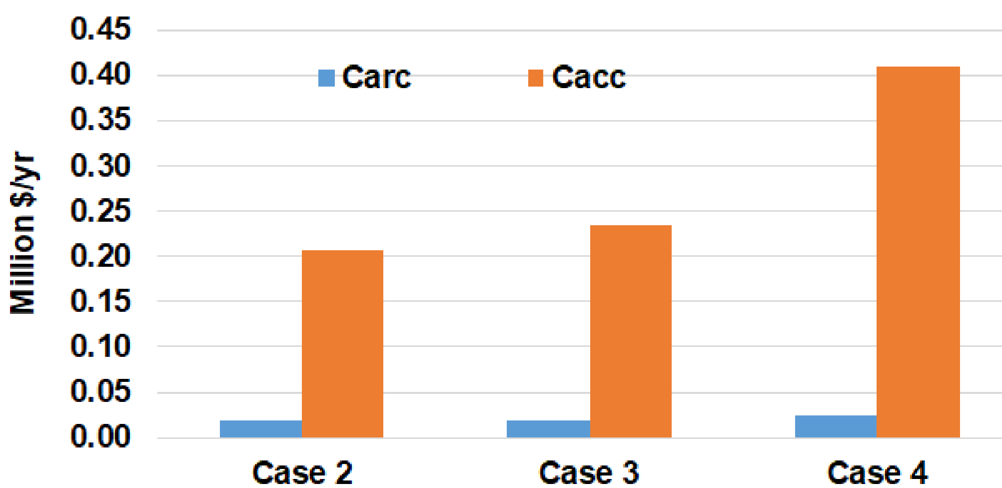

Figure 5.18 Improvements in C_{arc} and C_{acc}.

Figure 5.15 shows C_{npc} (million \$/yr) in Cases 2, 3 and 4 with an improvement of 3.946, 4.123 and 4.155 respectively over Case 1. All these improvements in Figures 5.11-5.15 lead to the improvement in C_{coe} (\$/kWh) in Cases 2, 3 and 4 by 0.0107, 0.0114 and 0.0115 respectively over Case 1, i.e., cheaper costs of electricity units. This is illustrated in Figure. 5.16.

Figure 5.19 Improvement in C_{npc}

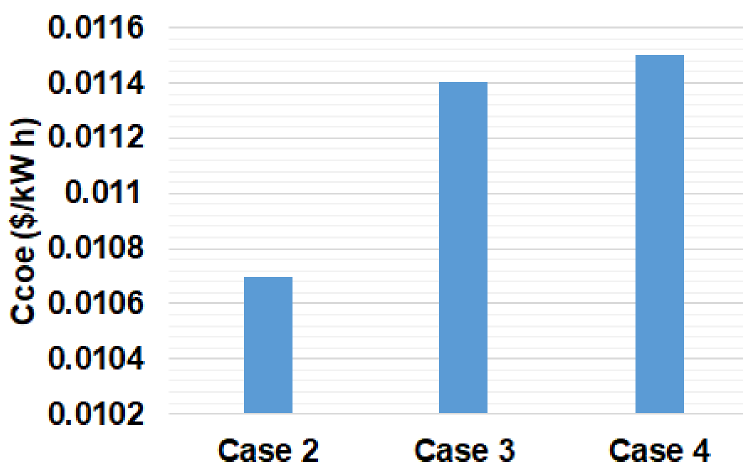

Figure 5.20 Improvements in C_{coe}.

Figures 5.21 to 5.23 illustrate the percentage improvements in Cases 2 to 4 when compared to Case 1. The percentage improvements of $EENS$, C_{npc} and C_{coe} are shown in Figure 17. $EENS$ improved by 6.15 %, 5.22 %, and 7.37 % in Cases 2, 3, and 4, respectively, when compared to Case 1. The percentage improvement in C_{npc} ranges from 14.3 % to 15.0 %, while C_{coe} ranges from 14.2 % to 15.3 %. In Figure 5.22, $ECOST$, C_{eens} and C_{toc} have percentage improvements ranging from 6.1 % to 9.1 %, 6.1 % to 7.4 %, and 2.9 % to 7.4 % respectively. Figure 5.23 shows the C_{amc}, C_{afc}, C_{aec} and C_{acs} with percentage improvements ranging from 9.9 % to 17.6 %, 27.0 % to 27.8 %, 27.3 % to 27.9 % and 13.5 % to 14.9 % respectively. The percentage increase of C_{arc} and C_{acc} in Figure 5.24 range from 0.9 % to 1.2 % and 7.4 % to 14.7 % respectively. These increases in C_{arc} and C_{acc} are projected to reduce overtime as investments in RESs intensify.

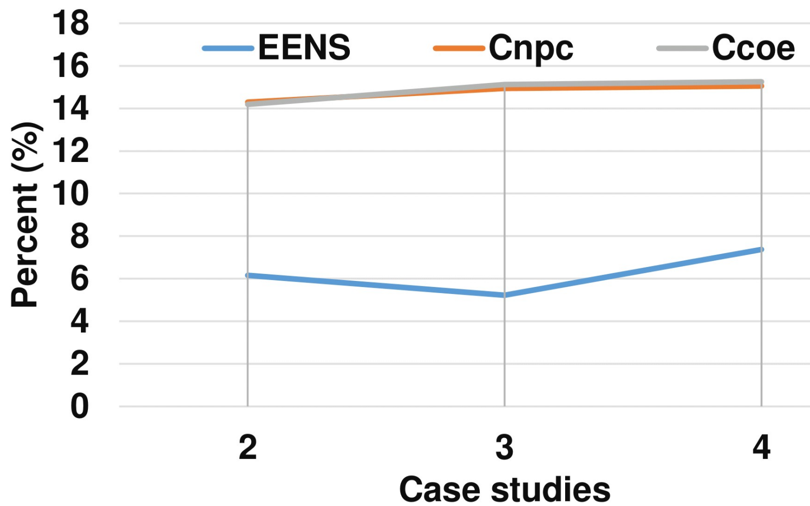

Figure 5.21 Percentage improvement in $EENS$, C_{npc} and C_{coe}.

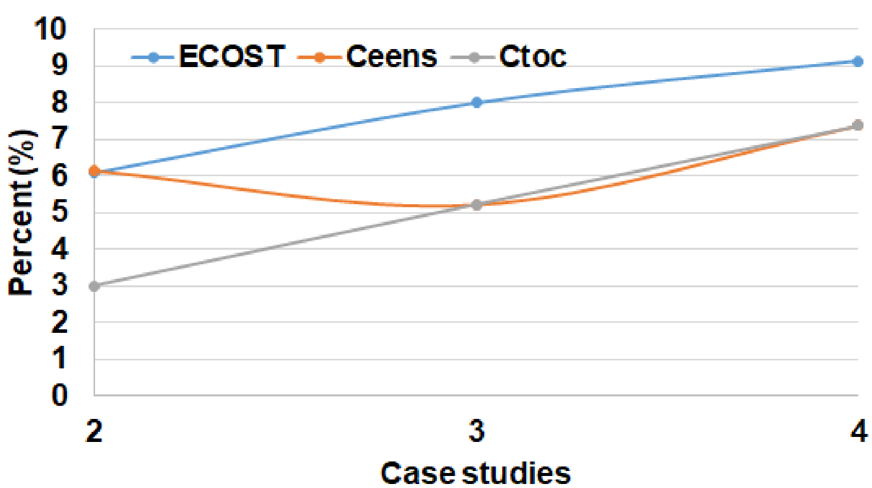

Figure 5.22 Percentage improvements in $ECOST$, C_{eens}, and C_{toc}.

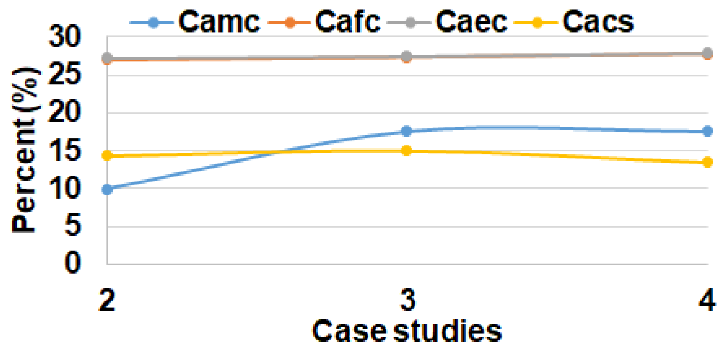

Figure 5.23 Percentage improvement in C_{amc}, C_{afc}, C_{aec}, and C_{acs}.

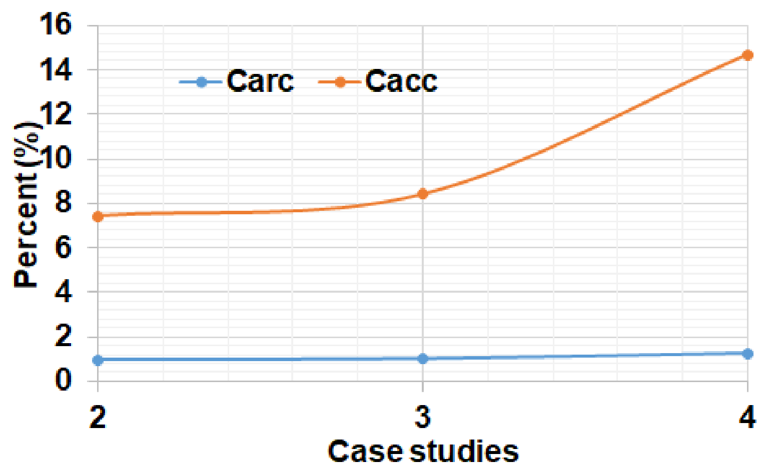

Figure 5.24 Percentage increase in C_{arc} and C_{acc}.

5.10 Impacts of the Annual Real Interest Rate

The effects of the annual real interest rates (ARIRs) on the various economic and emission parameters are presented in this section. The economic parameters considered in this study are C_{acs}, C_{coe}, C_{npc} and C_{toc}. The emission parameters are COx, SOx, and NOx are also addressed.

5.10.1 Relationship Between Annual Real Interest Rate and Annual Cost of System, Net Present Cost and Total Outage Cost.

The plot in Figure 5.25 shows the relationships between the ARIR and C_{acs}, C_{npc}, and C_{toc}. Initially, C_{acs} is approximately \$10.9 million/yr between an ARIR of 2% to 5.2% before increasing to \$11.17 million/yr at 6 % and then steadily increasing to \$11.88 million/yr at 12 %. This shows that higher ARIR means higher C_{acs}. This cost is directly or indirectly borne by the consumers. C_{npc} is shown to be inversely proportional to the ARIR. This illustrates that higher ARIR means lower C_{npc} for RES goods and services. By implication, higher ARIR erodes the present values of RES goods and services. At first, C_{toc} maintains an approximate value of \$35.11 million/yr between an ARIR of 2 % to 4.5 % before increasing to \$35.23 million/yr at 6 %, and then steadily increasing to \$36.33 million/yr at 12 %. By implication, higher ARIR means higher C_{toc} and higher consumer cost burden.

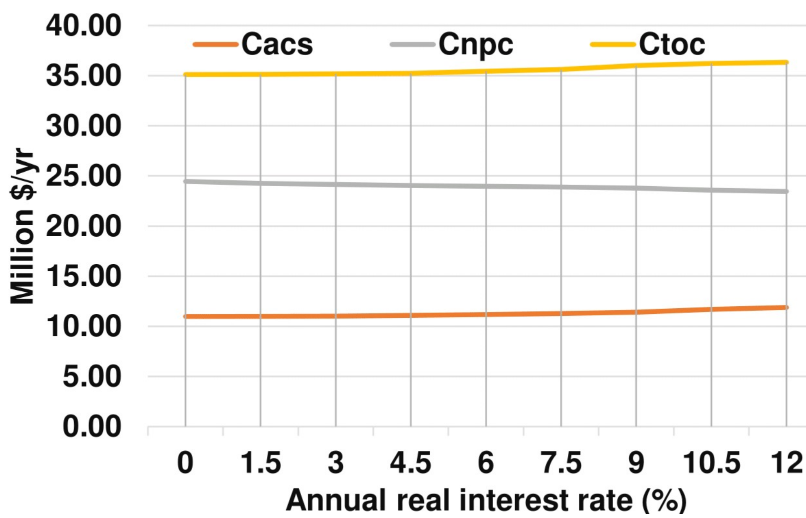

Figure 5.25 Effect of annual real interest rate on C_{acs}, C_{npc} and C_{toc}.

5.10.2 Relationship Between Annual Real Interest Rate and Annual Cost of Energy

Figure 5.26 shows that the relationship between ARIR and the C_{coe} is almost linear and slightly rising. When the ARIR is high, C_{coe} is also high. This implies that policymakers and government should make efforts to reduce the annual real interest rate on RES-related goods and services in order to encourage mass deployment of RESs. This will lead to cheaper electricity for consumers.

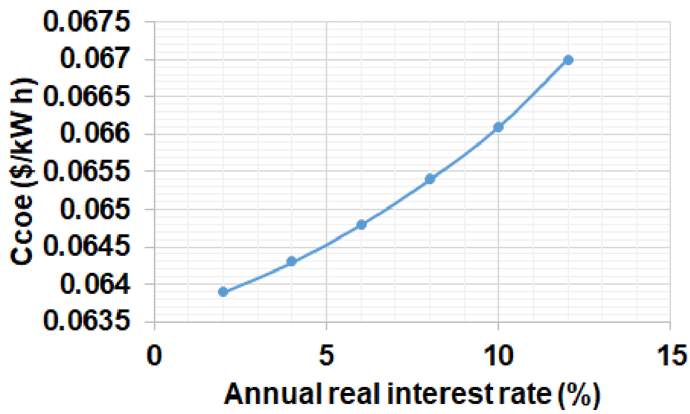

Figure 5.26 Effect of annual real interest rate on C_{coe}.

5.10.3 Relationship Between Annual Real Interest Rate and Emission Parameters

Figures 5.27 to 5.29 show the relationships between the emission oxides (COx, SOx, and NOx), the ARIR, and the RESs. Generally, at lower RES input, the COx, SOx, and NOx emissions were high because the diesel generator operates for more hours. Therefore, the ARIR must be kept low in order to keep the emission low and maintain a high penetration of RESs.

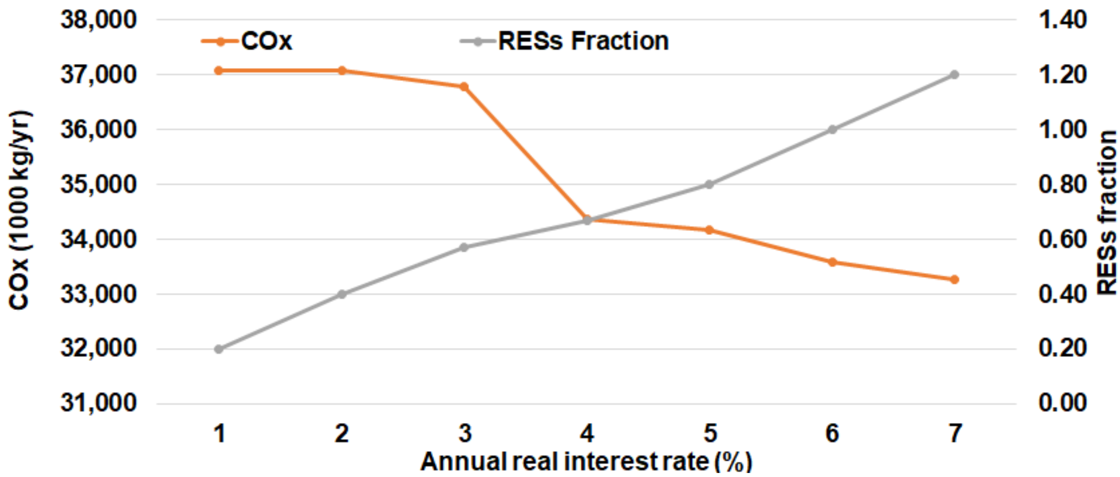

Figure 5.27 Effect of annual real interest rate on COx.

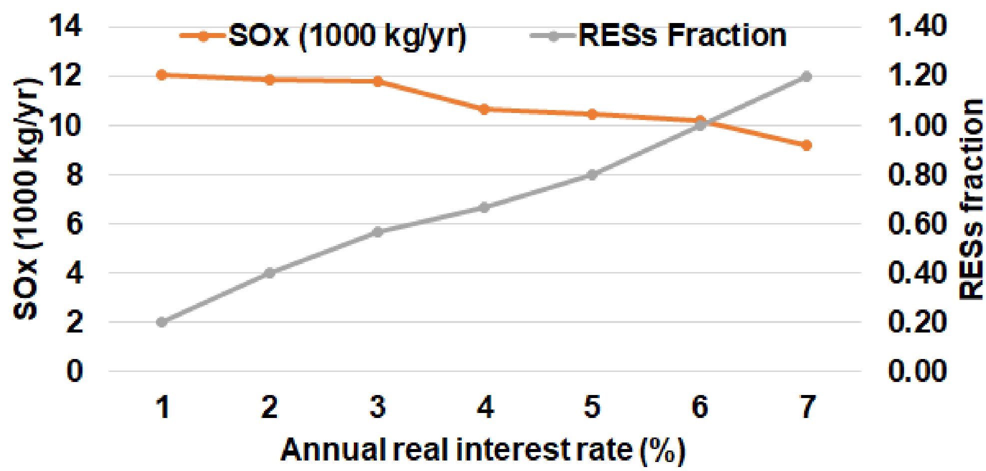

Figure 5.28 Effect of annual real interest rate on SOx.

5.11 Comparison with other Reliability Optimization Methods

Table 5.7 presents the comparison of AMPC with other reliability optimization methods for the cost function formulation of Case 4. The acronymns in Table 5.7 are defined as follows: DS-differential

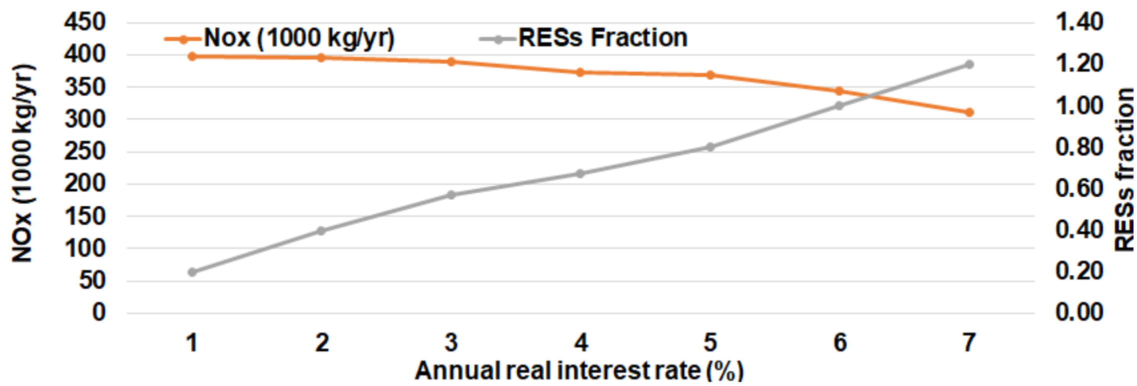

Figure 5.29 Effect of annual real interest rate on NOx.

Table 5.7 Comparison with other reliability optimization methods.

Method	**Simulation Time(s)**	C_{eens} **(million \$/yr)**	$ECOST$ **(million \$/yr)**	COx **(1000 kg/yr)**	C_{acs} **(million \$/yr)**
GSA	83.024	36.105	9.782	36 856	11.605
ACO	87.300	36.559	10.379	36 923	11.947
GA	90.735	37.065	12.010	37 302	13.672
DE	88.121	36.721	10.983	37 018	12.547
PSO	88.981	36.929	11.809	37 275	13.021
DS	85.141	36.093	9.327	36 810	11.103
AMPC	75.424	35.021	8.002	36 777	10.979

search; PSO-particle swarm optimization; DE-differential evolutionary algorithm; GA-genetic algorithm; ACO-ant colony optimization; GSA-gravitational search algorithm; and AMPC-adaptive model predictive control. The results show that the simulation times for AMPC are much less than that of the other methods when calculating C_{eens}, $ECOST$, COx, and C_{acs}. The results also show much smoother characteristics and superior computational efficiency of the AMPC algorithm.

5.12 Conclusions and Future Study

In this study, the economic, environmental, and reliability impacts of fossil fuel generators, Solar PV, WP, and BESS in a micro-grid power system are investigated using the meteorological data of Pietermaritzburg, KZN, South Africa. The objective functions considered are reliability improvement, cost and emission minimization. The variables C_{toc}, C_{amc}, C_{afc}, C_{aec}, C_{arc}, C_{acc}, C_{npc}, and C_{coe} are carefully chosen as operational costs for the network. The oxides selected for emissions are COx, SOx, and NOx. $EENS$ and $ECOST$ are the reliability indices used for the evaluation of the network. The optimization problem is solved using an AMPC algorithm. The verification of the proposed approach is done using a modified RBTS test system. Simulation results show that the integration of a fossil fuel generator, RESs and a BESS using AMPC can improve reliability, reduce emissions and minimize operational costs of the micro-grid. AMPC implementation in a micro-grid system containing a fossil fuel generator, RESs and a BESS decreases the C_{coe} by decreasing the associated operational costs. Decreasing the emissions level is done by reducing the operational hours of the fossil fuel generator. By introducing different sources of renewable energy into the micro-grid, $EENS$ and $ECOST$ are minimized leading to an improvement in the reliability of the system. The results show that for policymakers, government, and investors to embark on a system that makes economic and environmental sense, the ARIR must be kept as low as possible. The economic, environmental, and reliability improvement of the power system is expected to impact the performance of the system. The RESs are projected to dominate power supply worldwide in the future.

However, this study acknowledges the limitation that all the standards, costs and data used in this research are assumed to be accurate at the time this study was conducted. In this study, the physical implementation of the proposed method on the field is not included.

Further research works considering other optimization methods could be conducted to explore further reliability improvement of power systems. While optimal solutions have been determined using AMPC algorithm, similar data and objective functions can be subjected to other algorithms and the output and efficiency compared. Superior results and reduced computation time of the algorithm are possible if a combination of the methods are used.

Chapter 6

Conclusions and Future Work

6.1 Conclusions

The transition to smart grid and sustainable power will create new and complex problems that require appropriate modelling. Such problems find strong examples in the long-term reliability evaluation of the power systems. The integration of RESs into conventional grids or transition to a 100 % RESs can have a significant effect on the reliability of electricity. Hence, modelling appropriately for this type of system is important so that the effects that such transition will have on the reliability and security of supply is evaluated accurately. To evaluate the reliability of power systems, computational intelligent techniques are some of the most appropriate tools. This work investigated the application of computational intelligent techniques in improving the reliability of the power systems with the integration of renewable energy sources. In Chapter 3, an ANN-based predictive model using a back-propagation algorithm of a feed-forward ANN, and the historical outage and meteorological data of Pietermaritzburg, KZN, South Africa were developed to improve the reliability of the power system. The results confirmed that the developed model is robust and appropriate in predicting weather related electricity system failure. The complex relationship between weather events and electricity system failure is demonstrated by the developed model.

In Chapter 4, a CONN-based model was developed to address complex power outage predictive problems using solutions of easier sub-problems to solve the complex problem. The historical outage and meteorological data of Newcastle, KZN, South Africa was used. The CONN model addressed the problems of multiple constraints and non-availability of large outage datasets. An effective optimal power outage forecasting solution is provided by the CONN algorithm according to the various outage events and network constraints. The satisfactory results of the CONN algorithm show that the model is effective in providing power outage forecasting solutions to multi-constrained and complex problems.

Finally, in Chapter 5, an AMPC-based model was developed to investigate the economic, environmental, and reliability impacts of fossil fuel generators, with the integration of RESs, such as solar PV, WP, and BESS in a micro-grid power system using the meteorological data of Pietermaritzburg, KZN, South Africa. The network was evaluated using the EENS and ECOST reliability indices. The approach verified using a modified RBTS test system. The developed AMPC model was able to improve reliability, reduce emissions and minimize operational costs of the micro-grid.

In general, the research work has confirmed that the reliability of the power systems can be improved using computational intelligent techniques and RESs.

6.2 Limitations of the Study

This thesis will like to acknowledge the following limitations:

1. The research work addressed the technical limitations of the various power sources considered, but did not take into consideration the limitations from government policies and other logistics;
2. The historical outage and climatic data of only the cities of PMB and NWC, KwaZulu-Natal, South Africa were considered;
3. The physical implementations of the proposed methods on the field were not included; and
4. All the standards, costs and data used were assumed to be accurate at the time this study was conducted.

6.3 Suggestions for Future Study

The studies considered different reliability problems experienced by power systems and have designed and developed different solutions using different methods. The work is very significant in the field of implementation of intelligent techniques, design and modelling methodologies, smart grid, and RESs. Many technical problems have been addressed and there is the possibility of extending the methods proposed in this thesis to cover different applications. Further work is therefore proposed to cover the following:

1. Practical implementation of the proposed methods could be undertaken to validate the simulation experiments;

2. The integration of more or combination of other algorithms into the proposed methods to increase their scope and applicability;

3. Other optimization methods could be used to investigate the reliability improvement of power systems;

4. Similar data and objective functions can be subjected to other algorithms and the output and efficiency compared;

5. A combination of novel intelligent methods could produce superior results and reduce computation time of the algorithm;

6. Probabilistic models could be developed for home energy management systems (HEMS) and their effects on the reliability of power systems studied; and

7. A user interface program for the integration of the algorithms and techniques could be developed for easier use of the models.

Bibliography

[1] A.K. Onaolapo, R. Pillay Carpanen, D.G. Dorrell, and E.E. Ojo. A comparative assessment of conventional and artificial neural networks methods for electricity outage forecasting. *Energies*, 15(2):511, 2022.

[2] A.K. Onaolapo, R. Pillay Carpanen, D.G. Dorrell, and E.E. Ojo. Event-driven power outage prediction using collaborative neural networks. *IEEE Trans. on Industrial Informatics*, pages 1–10, 2022.

[3] A.K. Onaolapo, R. Pillay Carpanen, D.G. Dorrell, and E.E. Ojo. Reliability evaluation and financial viability of an electricity power micro-grid system with the incorporation of renewable energy sources and energy storage: A case study of KwaZulu-Natal, South Africa. *IEEE Access*, 9:159908 – 159924, 2021.

[4] A.K. Onaolapo, R. Pillay Carpanen, D.G. Dorrell, and E.E. Ojo. Forecasting electricity outage in KZN, South Africa using trend projection and artificial neural networks techniques. pages 1–5. IEEE PES/IAS Power Africa, 2021.

[5] A.K. Onaolapo, R.Pillay Carpanen, D.G. Dorrell, and E.E. Ojo. A comparative evaluation of conventional and computational intelligence techniques for forecasting electricity outage. pages 1–6. Southern African Universities Power Engineering Conference (SAUPEC), 2021.

[6] A.K. Onaolapo, R.Pillay Carpanen, D.G. Dorrell, and E.E. Ojo. Transmission line fault classification and location using multi-layer perceptron artificial neural network. pages 5182–5187. IEEE Industrial Electronics Society Conference (IECON), 2020.

[7] A.K. Onaolapo, R.Pillay Carpanen, D.G. Dorrell, and E.E. Ojo. Assessment of sustainable development: A nexus between reliability, greenhouse gas emissions and renewable energy technologies. pages 1–5. Southern African Universities Power Engineering Conference (SAUPEC), 2022.

[8] A. Alamri, M. Alowaifeer, and A. S. Meliopoulos. Energy storage sizing and probabilistic reliability assessment for power systems based on composite demand. *IEEE Transactions on Power Delivery*, 37(1):1–11, 2021.

[9] M. Memari, A. Karimi, and H. Hashemi-Dezaki. Reliability evaluation of smart grid using various classic and metaheuristic clustering algorithms considering system uncertainties. *International Transactions on Electrical Energy Systems*, 31(6):e12902, 2021.

[10] F. C. Oreke and D. Idoniboyeobu. Reliability assessment of electrical energy distribution system–a case study of port harcourt distribution network. *International Journal for Research in Applied Science Engineering Technology (IJRASET)*, 5(VI):432–441, 2017.

[11] A.K. Onaolapo, K.T. Akindeji, and E. Adetiba. Faults recognition, identification and localization in smart distribution networks–a review. volume 29, page 31. Protection, Automation and Control (PAC) World Conference, Raleigh, North Carolina, USA, 2017.

[12] H. Canton. *International Energy Agency—IEA*. The Europa Directory of International Organizations, Routledge, 2021.

[13] K. R. Naik, B. Rajpathak, A. Mitra, and M. L. Kolhe. Assessment of energy management technique for achieving the sustainable voltage level during grid outage of hydro generator

interfaced dc micro-grid. *Sustainable Energy Technologies and Assessments*, 46:101231, 2021.

[14] V. K. Prajapati and V. Mahajan. Reliability assessment and congestion management of power system with energy storage system and uncertain renewable resources. *Energy*, 215:119134, 2021.

[15] F.S. Kebede, J.C. Olivier, S. Bourguet, and M. Machmoum. Reliability evaluation of renewable power systems through distribution network power outage modelling. *Energies*, 14(11):3225, 2021.

[16] I. Vehvilainen. Joint assessment of generation adequacy with intermittent renewables and hydro storage: A case study in finland. *Electric Power Systems Research*, 199:107385, 2021.

[17] R. Billinton and R. N. Allan. *Reliability Evaluation of Power Systems*. Plenum Press, 1996.

[18] L. de Magalhaes Carvalho. *Advances on the sequential Monte Carlo reliability assessment of generation-transmission systems using cross-entropy and population-based methods*. PhD thesis, Universidade do Porto, Portugal, 2013.

[19] C. Abert. Micromagnetics and spintronics: models and numerical methods. *The European Physical Journal B*, 96(6):1–45, 2019.

[20] A. L. Da Silva, A. Cassula, R. Billinton, and L. Manso. Integrated reliability evaluation of generation, transmission and distribution systems. volume 149, pages 1–6. IEE Proceedings-Generation, Transmission and Distribution, 2002.

[21] M. A. da Rosa. *Agent-based technology applied to power systems reliability*. Phd thesis, Universidade do Porto, Portugal, 2009.

[22] R. Billinton and J. Satish. Predictive assessment of bulk-system-reliability performance indices. volume 141, pages 466–472. IEE Proceedings-Generation, Transmission and Distribution, 1994.

[23] E. Amicarelli. *Control and management strategies of smart grids with high penetration of renewable energy*. Phd thesis, Universite Grenoble Alpes, 2017.

[24] M. Komlanvi. *Computer aided design of 3D of renewable energy platform for Togo's smart grid power system infrastructure*. Phd thesis, University of Derby, Togo, 2018.

[25] W. Ahmed and B. Sarkar. Impact of carbon emissions in a sustainable supply chain management for a second generation biofuel. *Journal of Cleaner Production*, 186:807–820, 2018.

[26] P. Pawar and M. TarunKumar. An iot based intelligent smart energy management system with accurate forecasting and load strategy for renewable generation. *Measurement*, 152:107187, 2020.

[27] M. Hu, J.W. Xiao, S.C. Cui, and Y.W. Wang. Distributed real-time demand response for energy management scheduling in smart grid. *International Journal of Electrical Power & Energy Systems*, 29:233–245, 2018.

[28] W. Wang, H. Huang, L. Zhang, and C. Su. Secure and efficient mutual authentication protocol for smart grid under blockchain. *Peer-to-Peer Networking and Applications*, 14(5):2681–2693, 2021.

[29] O. M. Akinbami, S. R. Oke, and M. O. Bodunrin. The state of renewable energy development in south africa: An overview. *Alexandria Engineering Journal*, 60(6):5077–5093, 2021.

[30] N. A. V. Smith. *Decision support for new and renewable energy systems deployment*. Phd thesis, University of Strathclyde, 2002.

[31] J. A. Gowlett. The discovery of fire by humans: a long and convoluted process. *Philosophical Transactions of the Royal Society B: Biological Sciences*, 371(1696):20150164, 2016.

[32] D. Szalay. Development of biomass and biofuel usage. *International Climate Protection: Springer*, pages 145–153, 2019.

[33] S. Mills. Combining solar power with coal-fired power plants, or cofiring natural gas. *Clean Energy*, 2(1):1–9, 2018.

[34] H. J. Karlsen. Reliability evaluation of energy-limited hydro-electric generation systems. *NTNU*, 2018.

[35] E. Y. Pramono and S. Isnandar. Criteria for integration of intermittent renewable energy to the java bali grid. pages 91–94, 2017.

[36] M. S. Javadi, M. Lotfi, M. Gough, A. E. Nezhad, S. F. Santos, and J. P. Catalao. Optimal spinning reserve allocation in presence of electrical storage and renewable energy sources. pages 1 – 6, 2019.

[37] M. U. Usama, D. Kelle, and T. Baldwin. Utilizing spinning reserves as energy storage for renewable energy integration. pages 1–5, 2014.

[38] A. Banshwar, N. K. Sharma, Y. R. Sood, and R. Shrivastava. Market-based participation of energy storage scheme to support renewable energy sources for the procurement of energy and spinning reserve. *Renewable Energy*, 135:326–344, 2019.

[39] L. He, Z. Lu, J. Zhang, L. Geng, Y. Cai, and X. Li. Economic dispatch of multi-area integrated electricity and natural gas systems considering emission and hourly spinning reserve constraints. *International Journal of Electrical Power Energy Systems*, 132:107177, 2021.

[40] A. García-Olivares, J. Solé, and O. Osychenko. Transportation in a 100% renewable energy system. *Energy Conversion and Management*, 158:266–285, 2018.

[41] J. Z. Thellufsen et al. Smart energy cities in a 100% renewable energy context. *Renewable and Sustainable Energy Reviews*, 129:109922, 2020.

[42] M. Child, C. Kemfert, D. Bogdanov, and C. Breyer. Flexible electricity generation, grid exchange and storage for the transition to a 100% renewable energy system in europe. *Renewable energy*, 139:80–101, 2019.

[43] N. F. Yah, A. N. Oumer, and M. S. Idris. Small scale hydro-power as a source of renewable energy in malaysia: A review. *Renewable and Sustainable Energy Reviews*, 72:228–239, 2017.

[44] J. Jurasz, A. Beluco, and F. A. Canales. The impact of complementarity on power supply reliability of small scale hybrid energy systems. *Energy*, 161:737–743, 2018.

[45] X. Xu, Z. Wei, Q. Ji, C. Wang, and G. Gao. Global renewable energy development: Influencing factors, trend predictions and countermeasures. *Resources Policy*, 63:101470, 2019.

[46] P. A. Østergaard, N. Duic, Y. Noorollahi, H. Mikulcic, and S. Kalogirou. Sustainable development using renewable energy technology. *Elsevier*, 146:2430–2437, 2020.

[47] M. Bagheri, S. H. Delbari, M. Pakzadmanesh, and C. A. Kennedy. City-integrated renewable energy design for low-carbon and climate-resilient communities. *Applied energy*, 239:1212–1225, 2019.

[48] L. Mellouk, M. Ghazi, A. Aaroud, M. Boulmalf, D. Benhaddou, and K. Zine-Dine. Design and energy management optimization for hybrid renewable energy system-case study: Laayoune region. *Renewable Energy*, 139:621–634, 2019.

[49] O. Ogunmodede, K. Anderson, D. Cutler, and A. Newman. Optimizing design and dispatch of a renewable energy system. *Applied Energy*, 287:116527, 2021.

[50] A. Ghaffari and A. Askarzadeh. Design optimization of a hybrid system subject to reliability level and renewable energy penetration. *Energy*, 193:116754, 2020.

[51] R. Selvaggi and F. Valenti. Assessment of fruit and vegetable residues suitable for renewable energy production: Gis-based model for developing new frontiers within the context of circular economy. *Applied System Innovation*, 4(1):10, 2021.

[52] N. Al-Kurdi, B. Pillot, C. Gervet, and L. Linguet. Towards robust scenarios of spatio-temporal renewable energy planning: A gis-ro approach. *International Conference on Principles and Practice of Constraint Programming, Springer.*, pages 729–747, 2019.

[53] M. Z. Jacobson, M. A. Delucchi, M. A. Cameron, and B. V. Mathiesen. Matching demand with supply at low cost in 139 countries among 20 world regions with 100% intermittent wind, water, and sunlight (wws) for all purposes. *Renewable Energy*, 123:236–248, 2018.

[54] A. Sambo. Matching electricity supply with demand in nigeria. *International Association of Energy Economics*, 4:32–36, 2008.

[55] T. Chai and R.R. Draxler. Stochastic, adaptive, and dynamic control of energy storage systems integrated with renewable energy sources for power loss minimization. *Renewable Energy*, 113:1462–1471, 2017.

[56] R. Lamedica, E. Santini, A. Ruvio, L. Palagi, and I. Rossetta. A milp methodology to optimize sizing of pv-wind renewable energy systems. *Energy*, 165:385–398, 2018.

[57] A. Zakaria, F. B. Ismail, M. H. Lipu, and M. A. Hannan. Uncertainty models for stochastic optimization in renewable energy applications. *Renewable Energy*, 145:1543–1571, 2020.

[58] K. Amber, R. Ahmad, M. Aslam, A. Kousar, M. Usman, and M. Khan. Intelligent techniques for forecasting electricity consumption of buildings. *Energy*, 157:886–893, 2018.

[59] A. Fernandez, F. Herrera, O. Cordon, M. J. del Jesus, and F. Marcelloni. Evolutionary fuzzy systems for explainable artificial intelligence: Why, when, what for, and where to? *Computational intelligence magazine*, 14(1):69–81, 2019.

[60] A.K Onaolapo and K.T. Akindeji. Application of artificial neural network for fault recognition and classification in distribution network. In *Southern African Universities Power Engineering Conference/Robotics and Mechatronics/Pattern Recognition Association of South Africa (SAUPEC/RobMech/PRASA)*, pages 299–304. IEEE, 2019.

[61] B. Sathelly. *An Artificial Neural Network Approach to Predict Liver Failure Likelihood*. Journal article, The University of Toledo, 2018.

[62] P. Verpoort, P. MacDonald, and G. J. Conduit. Materials data validation and imputation with an artificial neural network. *Computational Materials Science:*, 147:176–185, 2018.

[63] R. Kruse, C. Borgelt, F. Klawonn, C. Moewes, M. Steinbrecher, and P. Held. Multi-layer perceptrons. *Computational Intelligence:*, pages 47–81, 2013.

[64] C. Simionescu. *Collaborative Artificial Neural Networks*. Phd thesis, Alexandru Ioan Cuza University, 2018.

[65] Guocong Song and Wei Chai. Collaborative learning for deep neural networks. In *32nd Conference on Neural Information Processing Systems (NeurIPS 2018), Montréal, Canada*, pages 1–10. Deep Neural Networks, 2018.

[66] B. T. Lopez. *Adaptive robust model predictive control for nonlinear systems*. Phd thesis, Massachusetts Institute of Technology, 2019.

[67] A. Micallef, M. Apap, C. Spiteri-Staines, J. M. Guerrero, and J. C. Vasquez. Reactive power sharing and voltage harmonic distortion compensation of droop controlled single phase islanded microgrids. *IEEE Transactions on Smart Grid*, 5(3):1149–1158, 2014.

[68] A. Parisio, E. Rikos, and L. Glielmo. A model predictive control approach to microgrid operation optimization. *IEEE Transactions on Control Systems Technology*, 22(5):1813–1827, 2014.

[69] A. Mesbah. Stochastic model predictive control: An overview and perspectives for future research. *IEEE Control Systems Magazine*, 36:30–44, 2016.

[70] A. R. Perez. *Adaptive Model Predictive Control for Offset-Free Setpoint Tracking of Nonlinear Processes*. Phd thesis, California State University, Long Beach, 2020.

[71] F. Behrooz, N. Mariun, M. H. Marhaban, M. A. M. Radzi, and A. R. Ramli. Review of control techniques for hvac systems—nonlinearity approaches based on fuzzy cognitive maps. *Energies*, 11:495, 2018.

[72] D.M. Ward. The effect of weather on grid systems and the reliability of electricity supply. *Climate Change*, 121:103–113, 2013.

[73] Y. Zhou, A. Pahwa, and S. S. Yang. Modeling weather-related failures of overhead distribution lines. *IEEE Trans. Power Syst.*, 21:1683–1690, 2006.

[74] J.R.A Rodriguez and A. Vargas. Fuzzy-heuristic methodology to estimate the load restoration time in mv networks. *IEEE Trans. Power Syst.*, 20:1095–1102, 2005.

[75] K.Zhou, I. Dobson, Z. Wang, A. Roitershtein, and A.P.A Ghosh. Markovian influence graph formed from utility line outage data to mitigate large cascades. *IEEE Trans. Power Syst.*, 35:3224–3235, 2020.

[76] P. Kankanala, S. Das, and A. Pahwa. Adaboost $^+$: An ensemble learning approach for estimating weather-related outages in distribution systems. *IEEE Trans. Power Syst.*, 29:359–367, 2014.

[77] L. Che, X. Liu, Z. Li, and Y. Wen. False data injection attacks induced sequential outages in power systems. *IEEE Trans. Power Syst.*, 34:1513–1523, 2018.

[78] R. Eskandarpour and A. Khodaei. Leveraging accuracy-uncertainty tradeoff in svm to achieve highly accurate outage predictions. *IEEE Trans. Power Syst.*, 33:1139–1141, 2017.

[79] R. Eskandarpourand A. Khodaei. Machine learning based power grid outage prediction in response to extreme events. *IEEE Trans. Power Syst.*, 32:3315–3316, 2016.

[80] A. Jaech, B. Zhang, M. Ostendorf, and D.S. Kirschen. Real-time prediction of the duration of distribution system outages. *IEEE Trans. Power Syst.*, 34:773–781, 2018.

[81] C. F. Ridolfo. Predictive maintenance display system. *Patent: US 6,735,549 B2*, 2004.

[82] D.T Radmer, P.A Kuntz, R.D. Christie, S.S. Venkata, and R.H. Fletcher. Predicting vegetation-related failure rates for overhead distribution feeders. *IEEE Trans. Power Deliv.*, 17:103–113, 2013.

[83] J.R. Aguero, J. Spare, E. Phillips, C. O'Meally, J. Wang, and R.E. Brown. Distribution system reliability improvement using predictive models. pages 1–7. IEEE Power & Energy Society General Meeting, Calgary, AB, Canada, IEEE, 2009.

[84] H.H. Rau, C.Y. Hsu, Y.A. Lin, S. Atique, A. Fuad, L.M. Wei, and M.H. Hsu. Development of a web-based liver cancer prediction model for type ii diabetes patients by using an artificial neural network. *Comput. Methods Programs Biomed.*, 125:58–65, 2016.

[85] A. Pahwa. Effect of environmental factors on failure rate of overhead distribution feeders. pages 691–692. IEEE Power Engineering Society General Meeting, Denver, CO, USA, IEEE, 2004.

[86] S. Yuan, S.M. Quiring, L. Zhu, Y. Huang, and J. Wang. Development of a typhoon power outage model in guangdong, china. *J. Abbr.*, 117:105711, 2020.

[87] B.A Alpay, D. Wanik, P. Watson, D. Cerrai, G. Liang, and E. Anagnostou. Dynamic modeling of power outages caused by thunderstorms. *Forecasting*, 2:151–162, 2020.

[88] D. Pasqualini, K.A. Kaufeld, and M.F. Dorn. Electric power outage forecasting: Model. 34:773–781, 2018.

[89] R. Nateghi, S.D. Guikema, and S.M. Quiring. Forecasting hurricane induced power outage durations. *Nat. Hazards*, 74:1795–1811, 2014.

[90] D. Cerrai, M. Koukoula, P. Watson, and E.N. Anagnostou. Outage prediction models for snow and ice storms. *Sustain. Energy Grids Netw.*, 21:100294, 2020.

[91] D. Cerrai, D.W. Wanik, M.A.E. Bhuiyan, X. Zhang, J. Yang, M.E.B. Frediani, and E.N. Anagnostou. Predicting storm outages through new representations of weather and vegetation. *IEEE Access*, 7, 2019.

[92] T. Dokic and M. Pavlovski. Spatially aware ensemble-based learning to predict weather-related outages in transmission. Hawaii International Conference on System Sciences—HICSS, Maui, HI, USA, 2019.

[93] D.Wanik, E. Anagnostou, B. Hartman, M. Frediani, and M. Astitha. Storm outage modeling for an electric distribution network in northeastern usa. *Nat. Hazards*, 79:1359–1384, 2015.

[94] K.S. Shim, S.J. Ahn, S.Y. Yun, and J.H. Choi. Analysis of low frequency oscillation using the multi-interval parameter estimation method on a rolling blackout in the kepco system. *Energies*, 10:484, 2017.

[95] F.H. Jufri, J.S. Kim, and J. Jung. Analysis of determinants of the impact and the grid capability to evaluate and improve grid resilience from extreme weather event. *Energies*, 10:1779, 2017.

[96] M. Ghorbanzadeh, M. Koloushani, M.B. Ulak, E.E. Ozguven, and R.A. Jouneghani. Statistical and spatial analysis of hurricane-induced roadway closures and power outages. *Energies*, (13):1098, 2020.

[97] R. Lo Frano, S.A. Cancemi, P. Darnowski, R. Ciolini, and S. Paci. Preliminary analysis of an aged rpv subjected to station blackout. *Energies*, 14:4394, 2021.

[98] P.L. Watson, M. Koukoula, and E. Anagnostou. Influence of the characteristics of weather information in a thunderstorm-related power outage prediction system. *Forecasting*, 3:541–560, 2021.

[99] F. Yang, D.W. Wanik, D. Cerrai, M.A.E. Bhuiyan, and E.N. Anagnostou. Quantifying uncertainty in machine learning-based power outage prediction model training: A tool for sustainable storm restoration. *Sustainability*, 12:1525, 2020.

[100] J. Kang and S. Lee. Data-driven prediction of load curtailment in incentive-based demand response system. *Energies*, 11:2905, 2018.

[101] O. Oyebode and D.E. Ighravwe. Urban water demand forecasting: A comparative evaluation of conventional and soft computing techniques. *Resources*, 8:156, 2019.

[102] R. Hyndman, A.B. Koehler, J.K. Ord, and R.D. Snyder. *Forecasting with Exponential Smoothing: The State Space Approach*. Springer Science & Business Media: New York, NY, USA, 2008.

[103] L. Wu, S. You, J. Dong, Y. Liu, and T. Bilke. Multiple linear regression based disturbance magnitude estimations for bulk power systems. In *IEEE Power & Energy Society General Meeting (PESGM), Portland, OR, USA*, pages 1–5. IEEE, 2018.

[104] A.K. Onaolapo, K.T. Akindeji, and E. Adetiba. Simulation experiments for faults location in smart distribution networks using ieee 13 node test feeder and artificial neural network. *J. Phys. Conf. Ser.*, 1378:032021, 2019.

[105] S. Mafi and G. Amirinia. Forecasting hurricane wave height in gulf of mexico using soft computing methods. *Ocean. Eng.*, 142:352–362, 2017.

[106] A. Jarndal and S. Hamdan. Forecasting of peak electricity demand using annga and ann-pso approaches. In *International Conference on Modeling, Simulation, and Applied Optimization (ICMSAO), Sharjah, United Arab Emirates*, pages 1–5, 2017.

[107] S. Hlahla and T.R. Hill. Responses to climate variability in urban poor communities in pietermaritzburg, kwazulu-natal, south africa. *SAGE Open*, 8:2158244018800914, 2017.

[108] T. Aven. Decentralized load frequency control in deregulated environments. *Interpretations of alternative uncertainty representations in a reliability and risk analysis context*, 96:353–360, 2011.

[109] M. Panicker and C. Babu. Challenges and opportunities of load frequency control in conventional, modern and future smart power systems: A comprehensive review. *IOSR J. Eng.*, 22:1352–1356, 2012.

[110] R.J. Hyndman and A.B. Koehler. Another look at measures of forecast accuracy. *int. j. forecast. Int. J. Forecast.*, 22:679–688, 2006.

[111] T. Chai and R.R. Draxler. Root mean square error (rmse) or mean absolute error (mae)?-arguments against avoiding rmse in the literature. *Geosci. Model Development*, 7:1247–1250, 2014.

[112] M. Nitis and Jun. Confidence intervals and point estimators for a normal mean under purely sequential strategies involving gini's mean difference and mean absolute deviation. *Seq. Anal.*, 36:210–239, 2017.

[113] D. Lee and C.S. Park. On the generalized mean square error and its applications. *J. Korean Inst. Ind. Eng.*, 44:102–113, 2018.

[114] F. Shi, H. Zhang, Y. Cao, H. Sun, and Y. Chai. Enhancing event-driven load shedding by corrective switching with transient security and overload constraints. *IEEE Access*, 7:101355–101365, 2019.

[115] A. K. Singh and M. Fozdar. Event-driven frequency and voltage stability predictive assessment and unified load shedding. *IET Generation, Transmission Distribution*, 13:4410–4420, 2019.

[116] K. Mahapatra, S. Lu, A. Sengupta, and N. R. Chaudhuri. Power system disturbance classification with online event-driven neuromorphic computing. *IEEE Transactions on Smart Grid*, 12:2343–2354, 2020.

[117] N. Alemazkoor et. al. Hurricane-induced power outage risk under climate change is primarily driven by the uncertainty in projections of future hurricane frequency. *Scientific reports*, 10(1):1–9, 2020.

[118] D. Wanik et. al. A case study on power outage impacts from future hurricane sandy scenarios. *Journal of Applied Meteorology and Climatology*, 57(1):51–79, 2018.

[119] C. Zhai, T. Y. Chen, A. G. White, and S. D. Guikema. Power outage prediction for natural hazards using synthetic power distribution systems. *Reliability Engineering System Safety*, 208:107348, 2021.

[120] D. Wu et al. An open-source extendable model and corrective measure assessment of the 2021 texas power outage. *Advances in Applied Energy*, 4:100056, 2021.

[121] R. Eskandarpour and A. Khodaei. Component outage estimation based on support vector machine. *IEEE Power & Energy Society General Meeting*, pages 1–5, 2017.

[122] R. Eskandarpour, A. Khodaei, A. Paaso, and N. Abdullah. Artificial intelligence assisted power grid hardening in response to extreme weather events. *CIGRE*, 2018.

[123] S. Mukherjee, R. Nateghi, and M. Hastak. A multi-hazard approach to assess severe weather-induced major power outage risks in the us. *Reliability Engineering & System Safety*, 175:283–305, 2018.

[124] Z. Wang, M. Roman, Q. Sun, A. Molthan, L. Schultz, and V. Kalb. Monitoring disaster-related power outages using nasa black marble nighttime light product. *ISPRS Int. Arch. Photogramm. Remote Sens. Spat. Inf. Sci*, 10:1853–1856, 2018.

[125] S. Oh, J. Kong, M. Choi, and J. Jung. Data-driven prediction method for power grid state subjected to heavy-rain hazards. *Applied Sciences*, 10(14):4693, 2020.

[126] Statistics SA. South african statistics, 2018. Technical report, 2018.

[127] F. Yang, P. Watson, M. Koukoula, and E. N. Anagnostou. Enhancing weather-related power outage prediction by event severity classification. *IEEE Access*, 8:60029–60042, 2020.

[128] A. Abbasian, S. Hatami, A. Afzali-Kusha, M. Nourani, and C. Lucas. Event-driven dynamic power management based on wavelet forecasting theory. *IEEE International Symposium on Circuits and Systems (IEEE Cat. No. 04CH37512)*, 5:V–V, 2004.

[129] T. Ouyang, H. Huang, and Y. He. Ramp events forecasting based on long-term wind power prediction and correction. *IET Renewable Power Generation*, 13(15):2793–2801, 2019.

[130] V. Sultan and B. Hilton. A spatial analytics framework to investigate electric power-failure events and their causes. *ISPRS International journal of geo-information*, 9(1):54, 2020.

[131] M. Doostan and B. Chowdhury. Predicting lightning-related outages in power distribution systems: A statistical approach. *IEEE Access*, 8:84541–84550, 2020.

[132] C. M. Rogerson and J. M. Rogerson. City tourism in south africa: Diversity and change. *Tourism Review International*, 21(2):193–211, 2017.

[133] Y. Zhuang, C. Wu, H. Wu, Z. Zhang, Y. Gao, and L. Li. Collaborative neural network algorithm for event-driven deployment in wireless sensor and robot networks. *Sensors*, 200(10):2779, 2020.

[134] Y. C. Shen, G. T. Lin, K. P. Li, and B. J. Yuan. An assessment of exploiting renewable energy sources with concerns of policy and technology. *Energy Policy*, 38(8):4604–4616, 2010.

[135] Y. Wu, V. K. Lau, D. H. Tsang, L. P. Qian, and L. Meng. Optimal energy scheduling for residential smart grid with centralized renewable energy source. *IEEE Systems Journal*, 8(2):562–576, 2013.

[136] IRENA. Global energy transformation: a roadmap to 2050. Technical report, 2018.

[137] T. Adefarati, G. D. Obikoya, A. K. Onaolapo, and A. Njepu. Design and analysis of a photovoltaic-battery-methanol-diesel power system. *International Transactions on Electrical Energy Systems*, 31:e12800, 2021.

[138] W. Li. Reliability assessment of electric power systems using monte carlo methods. *Springer Science Business Media*, 2013.

[139] D. A. Katsaprakakis and D. G. Christakis. The exploitation of electricity production projects from renewable energy sources for the social and economic development of remote communities. the case of greece: An example to avoid. *Renewable and Sustainable Energy Reviews*, 54(1):341–349, 2016.

[140] H. Ritchie and M. Roser. Access to energy. *Our World in Data*, 2019.

[141] T. Adefarati and R. Bansal. Integration of renewable distributed generators into the distribution system: a review. *IET Renewable Power Generation*, 10(7):873–884, 2016.

[142] A. Ogunjuyigbe, T. Ayodele, and O. Akinola. Optimal allocation and sizing of pv/wind/split-diesel/battery hybrid energy system for minimizing life cycle cost, carbon emission and dump energy of remote residential building. *Applied Energy*, 171:153–171, 2016.

[143] M. D. Keshavarzi and M. H. Ali. Disturbance resilience enhancement of islanded hybrid microgrid under high penetration of renewable energy resources by bess. *IEEE/PES Transmission and Distribution Conference and Exposition (T&D)*, pages 1–5, 2020.

[144] R. Hidalgo-Leon *etal*. A survey of battery energy storage system (bess), applications and environmental impacts in power systems. *ieee second ecuador technical chapters meeting (etcm)*, pages 1–6, 2017.

[145] G. Graditi, R. Ciavarella, and M. Valenti. An innovative bess management for dynamic frequency restoration. *IEEE International Conference on Environment and Electrical Engineering and 2017 IEEE Industrial and Commercial Power Systems Europe (EEEIC/I&CPS Europe)*, pages 1–5, 2017.

[146] H. E. O. Farias and L. N. Canha. Battery energy storage systems (bess) overview of key market technologies. *IEEE PES Transmission & Distribution Conference and Exhibition-Latin America (T&D-LA)*, pages 1–5, 2018.

[147] M. E. Hassanzadeh, M. Nayeripour, S. Hasanvand, and E. Waffenschmidt. Decentralized control strategy to improve dynamic performance of micro-grid and reduce regional interactions using bess in the presence of renewable energy resources. *Journal of Energy Storage*, 31:101520, 2020.

[148] O. D. Montoya, W. Gil-Gonzalez, L. Grisales-Noreña, C. Orozco-Henao, and F. Serra. Economic dispatch of bess and renewable generators in dc microgrids using voltage-dependent load models. *Energies*, 12(23):4494, 2019.

[149] W. Gil-Gonzalez, O. D. Montoya, L. F. Grisales-Noreña, F. Cruz-Peragón, and G. Alcalá. Economic dispatch of renewable generators and bess in dc microgrids using second-order cone optimization. *Energies*, 13(7):1703, 2020.

[150] P. V. Brogan, R. J. Best, D. J. Morrow, K. McKinley, and M. L. Kubik. Effect of bess response on frequency and rocof during under-frequency transients. *IEEE Transactions on power systems*, 34(1):575–583, 2018.

[151] E. Reihani, S. Sepasi, L. R. Roose, and M. Matsuura. Energy management at the distribution grid using a battery energy storage system (bess). *International Journal of Electrical Power Energy Systems*, 77:337–344, 2016.

[152] M. K. Kiptoo, O. B. Adewuyi, M. E. Lotfy, A. M. Ibrahimi, and T. Senjyu. Harnessing demand-side management benefit towards achieving a 100% renewable energy microgrid. *Energy Reports*, 6:680–685, 2020.

[153] S. Ganesan, V. Ramesh, and S. Umashankar. Hybrid control of microgrid with pv, diesel generator and bess. *International Journal of Renewable Energy Research (IJRER)*, 7(3):1317–1323, 2017.

[154] S. M. Alhejaj and F. Gonzalez-Longatt. Investigation on grid-scale bess providing inertial response support. pages 1–6. IEEE, 2016.

[155] S. Ganesan, U. Subramaniam, R. M. Elavarasan A. A. Ghodke, K. Raju, and M. S. Bhaskar. Investigation on sizing of voltage source for a battery energy storage system in microgrid with renewable energy sources. *IEEE Access*, 8:188861–188874, 2020.

[156] B. Marchi, M. Pasetti, and S. Zanoni. Intelligent automatic generation control. *Energy Procedia*, 113:127–134, 2017.

[157] S. K. Sarker F. R. Badal, P. Das and S. K. Das. A survey on control issues in renewable energy integration and microgrid. *Protection and Control of Modern Power Systems*, 4(1):1–27, 2019.

[158] Y. Celikbilek and F. Tüysüz. An integrated grey based multi-criteria decision making approach for the evaluation of renewable energy sources. *Energy*, 115:1246–1258, 2016.

[159] K. Kasturi and M. R. Nayak. Multi-objective mctlbo approach to allocate renewable energy system (pv/bess) in electricity grid: assessing grid benefits. *IEEE Transactions on Power Delivery*, 16(1):1–23, 2020.

[160] S. B. Karanki and D. Xu. Optimal capacity and placement of battery energy storage systems for integrating renewable energy sources in distribution system. pages 1–6, 2016.

[161] S. Tan, X. Wang, and C. Jiang. Optimal scheduling of hydro–pv–wind hybrid system considering chp and bess coordination. *Applied Sciences*, 9(5):892, 2019.

[162] M. Ovaskainen, J. Öörni, and A. Leinonen. Superposed control strategies of a bess for power exchange and microgrid power quality improvement. pages 1–6. IEEE International Conference on Environment and Electrical Engineering and 2019 IEEE Industrial and Commercial Power Systems Europe (EEEIC/I&CPS Europe), IEEE, 2019.

[163] I. Hussain, S. Ranjan, D. C. Das, and N. Sinha. Performance analysis of flower pollination algorithm optimized pid controller for wind-pv-smes-bess-diesel autonomous hybrid power system. *International Journal of Renewable Energy Research (IJRER)*, 7(2):643–651, 2017.

[164] T. Khalili, A. Jafari, S. M. S. Kalajahi, B. Mohammadi-Ivatloo, and A. Bidram. Simultaneous demand response program and conservation voltage reduction for optimal operation of distribution systems. In *IEEE Industry Applications Society Annual Meeting*, pages 1–8. IEEE, 2020.

[165] T. Khalili, S. Nojavan, and K. Zare. Optimal performance of microgrid in the presence of demand response exchange: A stochastic multi-objective model. *Computers & Electrical Engineering*, 74:429–450, 2019.

[166] R. Benabid, D. Merrouche, A. Bourenane, and R. Alzbutas. Reliability assessment of redundant electrical power supply systems using fault tree analysis, reliability block diagram, and monte carlo simulation methods. pages 1–7, 2018.

[167] S. Guner and A. Ozdemir. Reliability improvement of distribution system considering ev parking lots. *Electric Power Systems Research*, (85):106353, 2020.

[168] K. Imayavaramban and R. Karhikeyan. Power system reliability improvement by using

active and passive harmonic filters. *International Journal of Engineering and Techniques*, 3(2):103–111, 2017.

[169] Y. R. Rodrigues, M. M. A. Abdelaziz, L. Wang, and I. Kamwa. Pmu based frequency regulation paradigm for multi-area power systems reliability improvement. *IEEE Transactions on Power Systems*, 36(5):1–13, 2021.

[170] O. M. Babatunde, D. E. Babatunde, T. B. Adedoja I. H. Denwigwe, O. S. Adedoja, and T. E. Okharedia. *Analysis of an optimal hybrid power system for an off-grid community in Nigeria*. International Journal of Energy Sector Management, 2019.

[171] T. Adefarati and R. Bansal. Reliability and economic assessment of a microgrid power system with the integration of renewable energy resources. *Applied Energy*, 206:911–933, 2017.

[172] C. Bordons, G. Teno, J. J. Marquez, and M. A. Ridao. Effect of the integration of disturbances prediction in energy management systems for microgrids. pages 1–6, 2019.

[173] P. A. Gbadega and A. K. Saha. Impact of incorporating disturbance prediction on the performance of energy management systems in micro-grid. *IEEE Access*, 8:162855–162879, 2020.

[174] Y. Zhang, R. Wang, T. Zhang, Y. Liu, and B. Guo. Model predictive control-based operation management for a residential microgrid with considering forecast uncertainties and demand response strategies. *IET Generation, Transmission & Distribution*, 10(10):2367–2378, 2016.

[175] S. Kayalvizhi and D. M. Vinod Kumar. Load frequency control of an isolated micro grid using fuzzy adaptive model predictive control. *IEEE Access*, 5:16241–16251, 2017.

[176] Y. F. Li and E. Zio. A multi-state model for the reliability assessment of a distributed generation system via universal generating function. *Reliability Engineering & System Safety*, 106:28–36, 2012.

[177] D. Y. Leung and Y. Yang. Wind energy development and its environmental impact: A review. *Renewable and Sustainable Energy Reviews*, 16(1):1031–1039, 2012.

[178] A. Zakariazadeh, S. Jadid, and P. Siano. Smart microgrid energy and reserve scheduling with demand response using stochastic optimization. *International Journal of Electrical Power & Energy Systems*, 63:523–533, 2014.

[179] J. M. Nahman and D.M. Peric. Radial distribution network planning under uncertainty by applying different reliability cost models. *Elsevier*, 117:105655, 2020.

[180] B. K. Das, N. Hoque, S. Mandal, T. K. Pal, and M. A. Raihan. A techno-economic feasibility of a stand-alone hybrid power generation for remote area application in bangladesh. *Energy*, (134):775–788, 2017.

[181] L. Valverde, C. Bordons, and F. Rosa. Integration of fuel cell technologies in renewable-energy-based microgrids optimizing operational costs and durability. *IEEE Transactions on Industrial Electronics*, 23(1):167–177, 2015.

[182] R. N. Allan, R. Billinton, I. Sjarief, L. Goel, and K. So. A reliability test system for educational purposes-basic distribution system data and results. *IEEE Transactions on Power systems*, 6(2):813–820, 1991.